Ethylene Trimerization over Supported SNS and PNP Chromium Catalysts

D. R. Venkatesh [a]*, Y. B. Kiran[b], V. Madhu Mohan[b], A.B.V. Kiran Kumar[b]

[a]Department of Humanities and Science, G. Pullaiah College of Engineering & Technologyy, Nandikotkur Rod, Kurnool, India 518 452.

[b]Centre for Applied Sciences, Department of Basic Science and Humanities, Mohan Babu University, A. Rangampet, Sree Sainath Nagar, Tirupati, India 517502.

Received 12 February 2020, revised 11 May 2020, accepted 12 July 2020.

ABSTRACT

Chromium(III) complexes with sulphur, nitrogen and phosphorus tridentate ligands were synthesized and characterized. These complexes were supported on SiO_2 and characterized by BET surface area measurements, XRF, SEM-EDX and FTIR. The complexes were tested for activity and selectivity in the trimerization of ethylene. The substituent's effect and influence on the sulphur on the supported catalysts were studied using the ethyl and the decyl substituted catalysts. The influence of temperature on catalytic performance was evaluated using the PPP supported system. The most active supported catalyst, the decyl substituted SNS catalyst, showed good activity of up to 19 500 g/g Cr h^{-1} and selectivity of 97.3 % to C6 products (98.2 % 1-hexene). This activity and selectivity were comparable to the homogeneous counterpart's performance that achieved 22 000 g/g Cr h^{-1} and 98.2 % C6 products (96.7 % 1-hexene), which surpassed the ethyl substituted catalyst, which was not supported, under the same reaction conditions. The supported PPP catalyst activities showed it was sensitive to higher temperatures, but this depends on the supporting technique.

KEYWORDS

Ethylene trimerization, sulfanyl ligands, phosphine ligands, supported catalysts.

1. Introduction

Supported metal complexes that are well known for ethylene conversions are metallocenes, which are immobilized for ethylene polymerization reactions.[1,2] As a result of the different routes of immobilization and strategies that have been proposed, different catalyst activities and/or polymer properties are obtained. The support alters the supported catalyst activity due to steric and electronic effects attributable to the support itself.[3–8] In many catalytic systems, the trend that has been observed is that the supported complexes exhibit lower catalytic activities than their homogeneous counterparts. This decrease in the activities can be attributed to many factors, *viz*. (i) deactivation of the metal complexes during the grafting reaction, (ii) inaccessibility of the metal complex to the co-catalyst thus hindering the process of catalyst activation, (iii) generation of active sites that have slow propagation rates due to interactions with the support surface and (iv) restrictions of the monomer access to the active site preventing the chain growth.[9] Another complexity that encumbers these kinds of systems is the high levels of heterogeneity of the metal sites formed on, for example, the amorphous silica surface together with the high dilution of the metal. The well-known Cr(II)/SiO_2 Phillips catalyst, though the most successful commercially, is among the least understood at a molecular level.[10]

These challenges have not stopped scientists from studying these kinds of systems. Two of the common ways of recycling the 'homogeneous' catalyst from the product phase are two-phase[11,12] and immobilization catalysis[13–17]. Although studied extensively, the latter has had little commercial success except for the Phillips catalyst.[18–20] The bonding of the silica to the metal complexes can be described in three ways: the metal complexes can be directly adsorbed on the surface of the support[2,21], the

S Afr J Chem, 2022, 76, 14-19
https://journals.co.za/content/journal/chem/

A non-dispersive infrared sensor for real-time detection of cyanogen chloride

D. R. Venkatesh [a]*, Y. B. Kiran[b], V. Madhu Mohan[b], A.B.V. Kiran Kumar[b]

[a]Department of Humanities and Science, G. Pullaiah College of Engineering & Technologyy, Nandikotkur Rod, Kurnool, India 518 452.

[b]Centre for Applied Sciences, Department of Basic Science and Humanities, Mohan Babu University, A. Rangampet, Sree Sainath Nagar, Tirupati, India 517502.

Received 03 March 2021, revised 24 December 2021, accepted 24 December 2021

ABSTRACT

Cyanogen chloride, as a systemic toxic agent, can cause death rapidly. In this paper, a non-dispersive infrared sensor was designed for the infrared absorption detection of cyanogen chloride at 800 cm^{-1}. The roughness of the internal coating material was analyzed by experiments, and the gold-plated gas chamber was selected. The light path propagation of different cross-section gas chambers was simulated, and the circular section gas chamber was selected to increase the infrared detector signal. The effect of flow rate on voltage was studied. The standard curve between voltage and concentration was obtained under the optimal condition of 0.4 L min^{-1}. The maximum response time was 19 s, and RSD was less than 2%. The interference experiment results showed that common gases entering the gas chamber do not cause interference. The non-dispersive infrared sensor for cyanogen chloride has good stability and detects cyanogen chloride in real-time.

KEYWORDS

cyanogen chloride, NDIR, real-time, qualitative analysis, quantitative analysis

INTRODUCTION

Cyanogen chloride (CNCl) is an important chemical intermediate, widely used in pesticides, medicine, and chemical additives and was used as a systemic toxic agent in World War II. For example, CNCl is used to produce cyanuric chloride and the synthesis of tetramethyl guanidine.[1,2] CNCl has the characteristics of low boiling point and volatility and usually exists as a gas.[3,4] Cyanogen in CNCl has strong coordination ability. It can combine with the trivalent iron ion in cells, affecting normal respiration and causing asphyxia. After poisoning, people will have dizziness, nausea and vomiting; in severe cases, the body muscles will be paralyzed, and the reflex will be lost, resulting in death within a few minutes.[5-7] With the increase of storage capacity and types of hazardous chemicals year by year, safety issues should not be underestimated. The rapid and accurate detection of CNCl has become an indispensable requirement. Generally, gas detection methods mainly include ion chromatography,[8–10] catalytic combustion,[11,12] electrochemical methods,[13,14] and gas chromatography.[15–17] However, most detection devices on which these methods are based are expensive, inconvenient to carry and cannot detect CNCl in real-time.

Non-dispersive infrared (NDIR), as a real-time gas detection method, selects the specific infrared absorption as the basis of qualitative recognition and quantitative analysis. At present, NDIR sensors play an important role in coal mine safety, air detection, environmental management, and other fields,18-20 since they can detect CO_2, CO, NO, NO_2, SO_2, CH_4 C_2H_5OH, C_2H_4 and other inorganic and organic gases.[21-23] Barritault et al. report the fabrication and characterization of an NDIR sensor based on a micro-bolometer detector and a Micro-Electro-Mechanical System (MEMS) IR-source, which has a very low power consumption.[24] Gibson and Macgregor developed a new type of carbon dioxide NDIR sensor combined with a mid-infrared light-emitting diode light source and a photodiode detector.[25] The sensor has the advantages of fast stabilization time, low power consumption and low cost.[25] Tan et al. designed an NDIR device with a parabolic gas chamber where environmental temperature, humidity, and pressure changes are reduced through linear compensation.[26] Therefore, NDIR sensor detection methods have good poison detection and analysis prospects.

*To whom correspondence should be addressed
Email: liugh01@163.com

ISSN 1996-840X Online / South African Chemical Institute / http://saci.co.za/journal
https://doi.org/10.17159/0379-4350/2022/v76a03

American Journal of Heterocyclic Chemistry

ISSN: 2575-7059 (Print); ISSN: 2575-5722 (Online)

Evaluation of Ethyl Acetate, Chloroform and Toluene Fractions of *Thevetia peruviana* K. Schum Methanolic Leaf Extract for Uterotonic Activity

M Ravi[1], P Malathi[2], R Pradeep[3]

[1] G.Pullaiah college of Engineering & Technology(A), Kurnool, AP, India

[2] G.Pullaiah college of Engineering & Technology(A), Kurnool, AP, India

[3]Institute of Pharmaceutical Sciences, K L University, Vijayawada, AP, India

Email address:
Ravim5148@gmail.com

Received: November 22, 2021; **Accepted**: December 10, 2021; **Published**: June 12, 2022

Abstract: *Thevetia peruviana* (Pers.) K. Schum (Apocynacae) leaves have a reputation of abortifacient activity. We investigated traditional claim and found that methanolic leaf extract produce antifertility activity by lowering the progesterone level in rat model. Aim of the present study was to find out the chemical constituent (s) responsible for antifertility activity of methanolic leaf extract of *Thevetia peruviana* (Pers.). The ethyl acetate, chloroform and toluene fractions of methanolic extract of *T. peruviana* leaves freed from cardiac glycosides [TPL-Me-G] were selected for phytochemical investigation and *in-vitro* uterotonic activity. The methanolic extract of *T. peruviana* leaves (1.103g) was fractionated with toluene (100ml, n=20); chloroform (100ml, n=20); and ethyl acetate (100ml, n=20) in the successive order. These fractions were examined for phytoconstituents and evaluated for *in-vitro* uterotonic activity. The toluene fraction (TPL-T) was found to have triterpenes, flavonoids and phytosterols. Quercetin (0.8904%) is present in TPL-T. The chloroform fraction (TPL-Ch) was found to contain flavonoids, triterpenes and phytosterols. Presence of alkaloids and flavonoids (quercetin 0.1606%) were observed in ethyl acetate fraction (TPL-Et-Ac). In contrast to TPL-Et-Ac, the TPL-T and TPL-Ch induced dose dependent uterine contraction in the isolated estrogenized rat uterus model. Highest uterotonic activity was found with TPL-Me-G which has kaempferol as phyto-constituent additionally. The *in-vitro* uterotonic activity is not influenced by quercetin and primary contributor is kaempferol though some unknown phytoconstituent/s also contributes to uterotonic activity and synergizes the action of kaempferol too. So, further research is needed to identify other contributory unknown phytoconstituent/s for antifertility activity of methanolic leaf extract of *Thevetia peruviana* (Pers.).

Keywords: *Thevetia peruviana* (Pers.) Leaves, Methanolic Extract, Fractionation, Kaempferol, Unknown Phytoconstituent/s, Uterotonic Activity

1. Introduction

To meet the ever increasing need of safe and economic antifertility agents, plants with ethno-pharmacological or ethno-botanical reputation are now focused [1], Exhaustive literature survey revealed that *Thevetia peruviana* (Pers.) K. Schum (Apocyanaceae) is one of the 577 plants used traditionally for regulation of female fertility [2]. *T. peruviana* is a rich source of secondary metabolite like flavonoids and terpenoids [3-5]. Different parts of *T. peruviana* plant (fruits, leaves, seeds) have been found to possess cardiac glycosides such as thevetin A, thevetin B, neriifolin, peruvoside, thevetoxin and ruvoside etc [5] Researches on *T. peruviana* proved that it exhibits several pharmacological effect in life threatening diseases like cancer,AIDS as well as some common patho-physiological conditions like inflammation, pain, microbial and fungal infections.

First synthesis of 6,7-diaminoindole and 1,2,5-selenadiazolo[3,4-*g*]indole

M Ravi* and A Uma Ravi Shankar*

Department of Chemistry, G.Pullaaih college of Engineering & Technology, Nandikotkur road, Kurnool-518452.
E-mail: ravim5148@gmail.com

Abstract

5-Methyl-4-nitro-2,1,3-benzoselenadiazole (**1**) was converted into 1,2,5-selenadiazolo[3,4-*g*]indole (**3**) by the Batcho-Leimgruber indole synthesis. Subsequent deselenation afforded 6,7-diaminoindole (**4**) which on treatment with biacetyl afforded 2,3-dimethylpyrrolo[2,3-*f*]quinoxaline (**5**) in 80% yield from **3**.

Keywords: Benzoselenadiazole, diaminoindole, deselenation, quinoxaline

Introduction

Aromatic amines represent an important class of compounds for a wide variety of pharmaceuticals, pesticides, additives and dyes. In recent years, mutagenic aminoimidazo- quinoxalines, -quinolines and -naphthyridines have been prepared[1] for analytical purposes andfor structure-biological activity studies related to food carcinogens.[2] Retrosynthetic analysis of some needed bioisosteric pyrroloquinoxalines led to 6,7-diaminoindole (**4**). Surprisingly, although derivatives of **4** are known,[3] the unsubstituted indole **4** has not been reported. Moreover, neither has the possible precursor 6,7-dinitroindole nor any suitable amino- nitro(so)indole. On the other hand, deselenation of 2,1,3-benzoselenadiazoles (bsd) has previously afforded *ortho*-benzenediamines which have then been conveniently converted into, *eg*, less accessible 4-nitrobenzimidazoles[4] and elusive 5-nitroquinoxalines.[5] Thus, we thoughtthat the unsubstituted indole **4** might be obtained from the readily available **1**[6] via the novel 1,2,5-selenadiazolo[3,4-*g*]indole (**3**).

This paper communicates the first preparation of selenadiazoloindole **3** and diaminoindole **4**, together with an illustration of their synthetic use en route to nitrogen heterocycles.

Regular Article

Highlighted Paper selected by Editor-in-Chief

Synthesis and Evaluation of Quinone Derivatives for Activity against *Trypanosome cruzi*

Yutaka Suto,*[a] Tatiana Ascencio,[b] Tomoya Nobuta,[a] Noriyuki Yamagiwa,[a] Yoko Onizuka,[b] Mayumi Ishii,[c] Kayoko Kanemitsu,[c] and Junko Nakajima-Shimada*[b]

[a] *Faculty of Pharmacy, Takasaki University of Health and Welfare; Takasaki, Gumma 370–0033, Japan:* [b] *Department of Molecular and Cellular Parasitology, Graduate School of Health Sciences, Gunma University; Maebashi, Gumma 371–8514, Japan: and* [c] *Drug Discovery Initiative, The University of Tokyo; Bunkyo-ku, Tokyo 113–0033, Japan.*
Received August 26, 2021; accepted September 28, 2021

A series of quinone derivatives with a variety of side chains were synthesized. These synthetic quinone compounds were evaluated for *in vitro* antitrypanosomal activity against trypomastigotes and amastigotes of *Trypanosoma cruzi*, the causative agent of Chagas disease. Measurement of solubility of quinones and their ability to permeate cell membranes were assessed to address their possible use as oral drugs. Some synthesized compounds exhibited potent antitrypanosomal activity. However, most compounds with a promising activity showed poor solubility that did not seem suitable for oral usage. Meanwhile, compound 5a, an *N-tert*-butoxycarbonylpiperidine derivative, exhibited good antitrypanosomal activity, ability to permeate membranes, and good solubility.

Key words *Trypanosoma cryzi*; Chagas disease; quinone

Introduction

Chagas disease is a neglected tropical disease caused by the protozoan parasite, *Trypanosoma cruzi* (*T. cruzi*).[1] The parasite is primarily transmitted *via* bites of the carrier vector, the blood-sucking "kissing bug." Blood transfusion, organ transplants, congenital transmission, and ingestion of contaminated food have been documented as other routes of infection.[2–4] In rural areas of 21 Latin American countries where *T. cruzi* is endemic, Chagas disease is an important health problem. The disease affects 5–8 million people and causes approximately 10000 deaths per year. Almost 70 million people are at risk of infection.[5] Recently, the disease has become a public health concern in nonendemic countries in North America, Europe, Australia, and Japan as a result of immigration from Latin America.[6–9]

Chagas disease has two distinct phases. The acute phase is often asymptomatic, or patients develop nonspecific symptoms, such as fever and general malaise. In most cases, these symptoms decline spontaneously after 1–2 months.[10,11] After activation of the host immune system, parasitemia fades and becomes undetectable. This indeterminate state can last for years and even decades. The majority of infected individuals will continue their life unaffected. However, between 30 and 40% of infected individuals will progress to chronic disease. Such patients may develop severe cardiac and digestive pathologies leading to severe disability or death.[12]

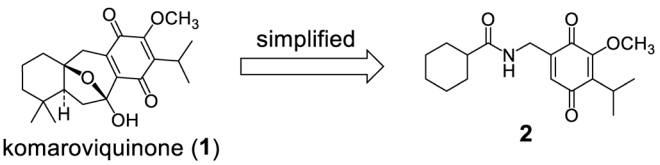

Fig. 1. Chemical Structure of Komaroviquinone (**1**) and Related Compound **2**

Only two drugs, benznidazole and nifurtimox developed more than 40 years ago, are currently in use.[13,14] Both drugs cause significant side effects, require long courses of treatment—up to 60 d, and are effective only in the acute phase of infection. Efficacy is limited in the chronic phase. The emergence of drug resistance is also problematic. CYP51 inhibitors, such as posaconazole and E1224 (prodrug of ravuconazole), recently demonstrated encouraging results in *in vitro* and *in vivo* models and were tested in clinical trials.[15,16] Unfortunately, these azoles were ineffective as compared with benznidazole. Thus, an urgent need exists for safe drugs with high clinical efficacy in both phases of the disease.

Komaroviquinone, a quinone-type diterpene isolated from *Dracocephalum komarovii*, inhibits the growth of trypomastigotes of *T. cruzi*.[17,18] We developed an asymmetric total synthesis of komaroviquinone and studied the importance of the quinone moiety and fused cyclic structure for activity against *T. cruzi*. We thus evaluated the antitrypanosomal activity of synthetic intermediates of komaroviquinone and related quinone compounds.[19,20] The quinone moiety of komaroviquinone was crucial for expression of antitrypanosomal activity but the complex structure with chiral centers was not. Further, we identified that some quinones with simplified organic syntheses showed antitrypanosomal activity similar to komaroviquinone. A representative is compound **2** in Fig. 1. We present a structure–activity relationship study of compound **2**. We synthesized compound **2**-related quinone compounds and evaluated their *in vitro* antitrypanosomal activity and assessed their solubility and ability to permeate cell membranes.

Chemistry

An overview of analogs is provided in Fig. 2. We synthesized compounds **3a**–**k** where the other substituent was replaced by an isopropyl group in compound **2**. These analogs were used to examine whether lipophilicity, size, and electron-

* To whom correspondence should be addressed. e-mail: ysuto@takasaki-u.ac.jp; jshimada@gunma-u.ac.jp

Imbuing an Old Heterocycle with the Power of Modern Catalysis: An Isoxazolidin-5-one Story

E. Swarna Gowri [a]*, Y. B. Kiran[b], V. Madhu Mohan[b], A.B.V. Kiran Kumar[b]

[a]Department of Humanities and Science, G. Pullaiah College of Engineering & Technologyy, Nandikotkur Rod, Kurnool, India 518 452.

[b]Centre for Applied Sciences, Department of Basic Science and Humanities, Mohan Babu University, A. Rangampet, Sree Sainath Nagar, Tirupati, India 517502.

Isoxazolidin-5-ones have been regarded as *β*-amino acid surrogates owing to their labile N–O bond. While many efforts have been devoted to the catalytic enantioselective synthesis of the core of this heterocycle, its further transformation has been less explored, especially in the context of catalysis. This review summarizes the author's research on the development of catalytic reactions using isoxazolidin-5-ones as substrates. Asymmetric catalysis has proven effective for C–C bond formation at the carbonyl *α*-carbon. Catalytic asymmetric allylation and direct Mannich-type reactions have been developed. Further, the resulting products have been readily converted into the corresponding quaternary *β*^{2,2}-amino acids. Moreover, isoxazolidin-5-ones have been identified as alkyl nitrene precursors in the presence of a suitable metal catalyst. The generated metallonitrene undergoes either the electrophilic amination of the aromatic ring or aliphatic C–H insertion, affording a series of cyclic *β*-amino acids. A remarkable difference in chemoselectivity between rhodium and copper alkyl nitrenes has also been demonstrated, highlighting the unique nature of the underexplored reactive intermediates. The various linear and cyclic *β*-amino acids obtained through the study are likely to find great utility in a broad range of chemical sciences.

Key words catalysis; *β*-amino acid; N-heterocycle; nitrene

1. Introduction

Over the past decades, the evolution of catalysis has revolutionized the way chemists synthesize molecules. Catalysts have provided a new mode of activation that enables the transformation of otherwise inert compounds.[1] They have also been sophisticated in orchestrating a highly ordered transition state to realize various selectivities including enantioselectivity.[2] Given the incredible feats accomplished, it is unsurprising that three Nobel prizes have been awarded for catalysis-related research in the 21st century.

Isoxazolidin-5-ones are isoxazol-derived, five-membered heterocycles,[3,4] whose preparation was documented as early as in 1909.[5] Since their characteristic N–O bond is readily cleaved under reductive conditions, isoxazolidin-5-ones have been considered as *β*-amino acid equivalents upon ring opening.[6] The prevalence of *β*-amino acids and their derivatives in biologically active compounds[7] such as *β*-lactams has led to the development of several cyclization approaches for the synthesis of functionalized isoxazolidin-5-ones. In some studies, asymmetric syntheses relying on either chiral auxiliary[8–13] or asymmetric catalysis[14–16] have been achieved. The catalytic asymmetric synthesis of isoxazolidin-5-ones has been summarized in a recent review.[17]

In contrast to the catalytic construction of the five-mem- bered ring, the use of the heterocycle itself as a substrate in

This review of the author's work was written by the author upon receiving the 2021 Pharmaceutical Society of Japan Award for Young Scientists.

South African Journal of Botany 139 (2021) 386—398

Contents lists available at ScienceDirect

South African Journal of Botany

journal homepage: www.elsevier.com/locate/sajb

Review

Natural product remedies for COVID-19: A focus on safety

P.Malathi [a]*, , V. Madhu Mohan[b], Y. B. Kiran[b] ,A.B.V. Kiran Kumar[b]

[a]Department of Humanities and Science, G. Pullaiah College of Engineering & Technologyy, Nandikotkur Rod, Kurnool, India 518 452.

[b]Centre for Applied Sciences, Department of Basic Science and Humanities, Mohan Babu University, A. Rangampet, Sree Sainath Nagar, Tirupati, India 517502.

ARTICLE INFO

Article History:
Received 26 November 2020
Revised 23 January 2021
Accepted 3 March 2021
Available online 18 March 2021

Edited by S Gupta

Keywords:
Coronavirus
COVID-19 treatment
Natural products
Safety
Self-medication
Toxicity

ABSTRACT

Infection by the novel coronavirus SARS-CoV-2 causing the coronavirus disease (COVID-19), is currently a global pandemic with more than two million deaths to date. Though a number of vaccines have recently been approved against the virus, availability remains a big challenge, and also acceptance by most people has become a big debate. This review discusses possible/proposed natural product remedies and some major conventional treatment options used to manage the infection and, safety concerns on the use of unproven or unapproved health products against COVID-19. An extensive literature review indicated that the influx of unproven and unapproved health products in the global market are on the rise, leading to various forms of self- medication. To this effect, there have been warnings by the United States Food and Drug Administration and the World Health Organisation against the use of such products. Conventional drugs such as remdesivir, chloroquine/hydroxychloroquine and dexamethasone are the major proposed drugs that are currently undergoing clinical trials for the management of this disease. Efforts are being made globally in the search for possible therapeutics which may be the best way to eradicating this disease. Some countries have approved the use of natural products in the management of COVID-19, despite little or no clinical evidence on their efficacy and safety. Natural products may hold a great potential in the fight against COVID-19 but without detailed clinical trials, their potency against the virus and their safe use cannot be established. To attain this goal, extensive research followed by clinical studies are needed. Collaborative efforts between researchers, clinicians, governments and traditional medicinal practitioners in the search and development of safe and effective therapeutics from natural products for the treatment of COVID-19 could be a potential option.

1. Introduction

Coronaviruses are a large group of viruses belonging to the family Coronaviridaea that cause upper-respiratory tract illnesses, ranging from common colds to more severe diseases (WHO, 2020a). Coronaviruses are zoonotic with many varieties common in animal species (WHO, 2020a). From these animal origins, they can undergo mutation, recombination and adaptation and be passed on to humans (Health24, 2020; Lau et al., 2020; WHO, 2020a). The first coronavirus was characterised and identified in humans in the mid-1960s (Kahn and McIntosh, 2005; Andersen et al., 2020; Jaiswal and Saxena, 2020). To date, seven coronaviruses have been recorded in humans and are classified as a-coronaviruses (NL63 and 229E) and b-coronaviruses (OC43 and HKU1) (Andersen et al., 2020; Jaiswal and Saxena, 2020). The b-coronavirus SARS-CoV, which causes severe acute respiratory syndrome (SARS) was first recorded in humans in 2002 (Lau et al., 2020). This was followed by the b-MERS-CoV, known as the Middle East respiratory syndrome

* Corresponding author.
E-mail address: rcpgd@ukzn.ac.za (J. Van Staden).

https://doi.org/10.1016/j.sajb.2021.03.012
0254-6299/

South African Journal of Botany 139 (2021) 192–196

Contents lists available at ScienceDirect

South African Journal of Botany

journal homepage: www.elsevier.com/locate/sajb

Survival strategy of *Watsonia fourcadei* (Iridaceae); allocation of resources to sexual reproduction and vegetative survival of the parent plant

P.Malathi [a]*, Y. B. Kiran[b] ,A.B.V. Kiran Kumar[b]

[a]Department of Humanities and Science, G. Pullaiah College of Engineering & Technologyy, Nandikotkur Rod, Kurnool, India 518 452.

[b]Centre for Applied Sciences, Department of Basic Science and Humanities, Mohan Babu University, A. Rangampet, Sree Sainath Nagar, Tirupati, India 517502.

ARTICLE INFO

Article History:
Received 8 May 2020
Revised 9 February 2021
Accepted 15 February 2021
Available online 9 March 2021

Edited by K Balkwill

Keywords:
Geophytes
Fynbos
Reproductive effort
Resource partitioning
Sexual reproduction

ABSTRACT

Geophytes are abundant in the Cape fynbos vegetation and many of the Cape geophytes, such as *Watsonia* species, flower mostly only in the first year after a fire. This study investigates the question if these plants have a resource allocation strategy which limits sexual reproduction to the post-fire environment and that they favor resource allocation to the storage organ for the survival of the parent plant at a cost to sexual reproduction. To test the hypothesis that the Cape geophyte *Watsonia fourcadei* represses sexual reproduction in favor of the survival of the parent plant, three levels of defoliation (20, 50 and 100%) were applied during a phenological stage when resources were least in the parent corms. Resource allocation to different plant parts was investigated when plants were in the seeding phase. Dry mass and nutrient (N, P. K, Ca, Mg and Ca) content were used as indicators of the resource allocation pattern. Dry mass and nutrient allocation patterns were similar, with significantly higher percentages of resources allocated to vegetative survival of the parent plant than to sexual reproductive organs (inflorescence and seeds) after complete defoliation, than after 20 and 50% defoliation. The *W. fourcadei* plants were able to accumulate adequate resources in the post-fire growth season to support sexual reproduction after up to 50% defoliation, albeit to a lesser extent than in control plants, but sexual reproduction was poorly supported after complete defoliation. Results indicate that *W. fourcadei* plants must be able to accumulate at least 3.5 g of dry mass in the new developing corm before resources are allocated to sexual reproductive plant parts. Replenishment of nutrient content after defoliation was not a limiting factor for resources allocation to sexual reproduction, except in the case of phosphate. *W. fourcadei* plants acted as a functional unit and resources allocation to sexual reproduction was controlled and depended on the availability of resources. None of the current resource allocation models are applicable to *W. fourcadei* and factors that could have selected for the apparent '*K*' survival strategy in this and other Cape geophyte species are discussed.

1. Introduction

Geophytes are abundant and unusually rich in species in the fynbos vegetation of South Africa, where they exhibit great variability in the type and size of their storage organs (Proches et al., 2005; 2006). The success of geophytes in the fynbos environment has been ascribed to their ability to accumulate nutrients in their storage organs from the generally nutrient-poor soils which enable them to survive the dry summers of this Mediterranean-type ecosystem (Ruiters et al., 1995; 1992; 1993). The accumulated nutrient and carbohydrate resources in the belowground storage organs also enable these plants to exploit an opened post-fire environment rapidly, with most Cape fynbos geophyte species flowering in the first year after a fire (Ruiters, 1995; Manning and Goldblatt, 2012; Vlok, 2020). Cape geophytes are not only abundant in their natural environment, many

Editor: Dr K. Balkwill
E-mail address: janvlok@mweb.co.za

https://doi.org/10.1016/j.sajb.2021.02.024
0254-6299/

ISSN: 2249-6661
Vol-43, No.-04 (IV) July-September (2021)

Analyzing the physical characteristics of lithium boreate glass with silver doping

.**B.Suneetha[1], A.Prabhakar Reddy[2], Shaik Rasool Saheb[3]**
[1]Department of H&S, G.Pullaiah College of Engineering &Technology, Kurnool, India
[2]Department of H&S, Sreyas Institute of Engineering and Technology, Hyderabad, India
[3]H&S Department, CMR Engineering College, Kandlakoya, Medchal, Hyderabad-501401,

Abstract

present paper explains the preparation and characterization methods of lithium borate glasses doped with Ag ions with the chemical composition $40Li_2O$-$(60-x)B_2O_3$-xAg_2O (with x = 0, 0.5, and 1 mol%). Three glasses have been prepared by doping of Ag_2O. The experimental techniques like XRD discussed in detail. This paper also explains determination of different physical properties like density, refractive index, molar volume, oxygen packing density, silver ion concentration, inter ionic distance and polaran radius.

Keywords: Physical Properties, Lithium Borate Glasses, Refractive index

Introduction

A study of the physical properties of the glasses is of considerable importance because of the insight it gives into the fundamental process taking place in them. Such a study paved the way for the application of some of these glasses in technology. In fact, the physical properties of the glasses are to a large extent controlled by the structure, composition, and the nature of the bonds of the glasses. The investigation of the changes in the physical properties of glasses with controlled variation of chemical composition, doping etc., is of considerable interest from the application point of view [1-4].

Borate glasses are an important class of oxide glasses, whose anionic structure consists of diverse structural and superstructural units represented by different boro-oxygen groupings and complicated anionic complexes [5, 6]. It has been determined that when the framework of alkali borate glasses undergoes polymerization bridge bonds of the type – B – O – B – as well as non-bridge bonds M – O – B – coordinated by alkali metal ions (M = Cs, Rb, K, Na, Li) can form. The fraction of the nonbridge bonds is related with the ratio of boron in ternary and quaternary coordination, depends on the alkali-metal fraction, and has a large effect on the physical properties of glass [7, 8].

The covalent radii of the elements decrease from left to right across a row in the transition series (Sc, Ti, V, Cr, Mn, Fe, Ag, Co, Ni, Cu, Zn) until near the end when the size increases slightly. On passing from left to right, extra protons are placed in the nucleus and extra orbital electrons are added. The orbital electrons shield the nuclear charge incompletely (d electrons shield less efficiently than p electrons, which in turn shield less effectively than s electrons). Because of this poor screening by d electrons, the nuclear charge attracts all of the electrons more strongly: hence a contraction in size occurs [9-12].

Due to their potential applications in various domains of modern technology, glasses containing transition-metal oxides have been the subject of intensive investigations. For example, the glasses containing transition metal ion such as Ag_2O is used in electrochemical, electronic and electro-optic devices. The addition of silver oxide to borate glass makes it electrically ionic. Borate glasses are also of academic interest because of the boron anomaly and also B_2O_3 is one of the best glass formers [11].

In view of the importance of the alkali borate glasses and the role played by Ag metal ion, present glass system is chosen as: Li_2O-B_2O_3-xAg_2O

The glasses used for the present studies are $40Li_2O$ –$(60-x)B2O_3$:-xAg_2O (with x = 0, 0.5 and 1.0 mol.%) From the approximate glass forming regions, $40Li_2O$-$(60-x)B_2O_3$-xAg_2O glass systems was prepared. The details of the glasses used for the present studies are:

SERIES 1: $40Li_2O$-$(60-x)B_2O_3$-xAg_2O
(with x = 0, 0.5, 0.1 mol%)

For x=0 mol%, LB 1: 40 Li_2O –60 B_2O_3
x = 0.5 mol%, LB 2: 40 Li_2O –59.5 B_2O_3-0.5 Ag_2O
x = 0.1 mol%, LB 3: 40 Li_2O –59 B_2O_3-1.0 Ag_2O

Preparation of Glasses

The glasses used for the present study are prepared by the melting and quenching techniques [46-48]. The starting materials used for the preparation of the present glasses were Analytical grade reagents Li_2O, B_2O_3, Ag_2O: the appropriate amounts of these compounds were thoroughly mixed in an agate mortar and melted in a porcelain crucible. PID temperature controlled furnace was used in present study. The glasses were melted in the temperature range 900-950 ºC for an ½ hour till a bubble free liquid was formed. The glass samples were obtained by pouring the melt into a preheated brass mould shown in figure 1. The samples were subsequently annealed at lower temperatures and then sliced and polished. The approximate final dimensions of the glasses used for studying the of XRD and Evaluation of Physical parameters are 1 cm x 1 cm x 0.2 cm.

INSTITUTE OF PHYSICS PUBLISHING JOURNAL OF PHYSICS D: APPLIED PHYSICS
J. Phys. D: Appl. Phys. **36** (2021) 994–1000 PII: S0022-37217(03)519455-4

Effect of Te doping and electron irradiation on thermal diffusivity of Bi_2Se_3 thin films by photo-thermal technique

B.Suneetha[1], **S.Loka Raghavendra**[2],
G.Pullaiah College of Engineering&Technology,Kurnool

Received 11 February 2021, in final form 6 March 2021
Published 2 April 2021

Abstract
Photo-thermal beam deflection technique has been employed for the measurement of thermal diffusivity of undoped, Te doped and electron irradiated Bi_2Se_3 thin films. Slope from the tangential component of deflection signal with the pump-probe offset is used to evaluate the numerical value of thermal diffusivity *(α)*. Doped and electron irradiated samples show a substantial reduction in the value of α compared to undoped sample. The variations in the thermal diffusivity of doped and electron irradiated samples are explained in terms of phonon assisted heat transfer mechanism. It is seen that α is very sensitive to structural variations arising from doping and electron irradiation. The experimentally observed results are correlated with x-ray diffraction studies.

1. Introduction

In recent years, thermal wave physics has become an active area of research, particularly in characterizing and analysing the material parameters [1–3]. The non-intrusive and non-destructive laser induced photo-thermal techniques like probe beam deflection (PBD), photo-acoustic (PA) methods etc are widely used for investigating the thermal, transport and optical properties of semiconductors, ceramics, liquid crystals etc [4–6]. Photo-thermal techniques are based on the detection, by one means or other, of periodic thermal waves generated due to non-radiative de-excitations in the sample following a chopped or pulsed optical excitation. The PBD technique or mirage technique is very useful in determining the thermal diffusivity of thin films compared to the other. The application of PA technique requires the knowledge of exact thickness of the thin film for the determination of thermal diffusivity. Moreover, the sample under study must be optically opaque and thermally thick to make the analysis of the PA signal for thermal diffusivity evaluation simple. However, the PBD technique can be employed irrespective of the sample being thermally thick or thermally thin, optically opaque or optically transparent. Above all no knowledge of the thickness of the sample is required for the thermal diffusivity evaluation using the mirage technique. The structural variations in thin films could have a direct bearing on their thermal diffusivity values, which can be accurately measured using this technique. Hence PBD method is one of the ideal methods for the thermal diffusivity measurements of Bi_2Se_3 thin films coated on glass substrates.

Thermal diffusivity is an important thermo-physical parameter which determines the distribution of temperature in systems where heat flow occurs while the reciprocal of thermal diffusivity is a measure of the time required to heat up a conducting material to a specific temperature level. This parameter is closely dependent on the micro structural variation and composition as well as on the processing conditions of

The effects of fracture and fatigue on Graphene Nanocomposites

*S Loka Raghavendra,B Lavanya**

Graphene, a single-atom-thick sheet of sp^2-bonded carbon atoms, has generated much interest due to its high specific area and novel mechanical, electrical, and thermal properties.[1–7] Recent advances[8–10] in the production of bulk quantities of exfoliated graphene sheets from graphite have enabled the fabrication of graphene–polymer composites. Such composites show tremendous potential for mechanical-property enhancement due to their combination[11–12] of high specific surface area, strong nanofiller–matrix adhesion and the outstanding mechanical properties of the sp^2 carbon bonding network in graphene. Graphene fillers have been successfully dispersed in poly(styrene), poly(acrylonitrile) and poly(methyl methacrylate) matrices and the responses of their Young's modulus, ultimate tensile strength, and glass-transition temperature have been characterized.[11–12] However, to the best of our knowledge there is no report on the fracture toughness and fatigue properties of graphene–polymer composites. Fracture toughness describes the ability of a material containing a crack to resist fracture and it is a critically important material property for design applications. Fatigue involves dynamic propagation of cracks under cyclic loading and it is one of the primary causes of catastrophic failure in structural materials. Consequently, the material's resistance to fracture and fatigue crack propagation are of paramount importance to prevent failure.

Herein we report the fracture toughness, fracture energy, and fatigue properties of an epoxy polymer reinforced with various weight fractions of functionalized graphene sheets. Remarkably, only 0.125% weight of functionalized graphene sheets was observed to increase the fracture toughness of the pristine (unfilled) epoxy by ≈65% and the fracture energy by ≈115%. Toachievecomparable enhancement, carbonnanotube (CNT) and nanoparticle epoxy composites[13–15] require one to two orders of magnitude larger weight fraction of nanofillers. Under fatigue conditions, incorporation of 0.125% weight of functionalized graphene sheets drastically reduced the rate of crack propagation in the epoxy ≈25-fold. Fractography analysis revealed that the extraordinary effectiveness of graphene to resist fracture and fatigue is related to deflection processes associated with the planar (two-dimensional) structure of graphene, which enables it to deflect cracks far more effectively than one-dimensional CNTs or low-aspect-ratio nanoparticles. Given the widespread use of epoxies in structural applications, these results are expected to translate into significant practical applications for such nanocomposite epoxies.

In order to synthesize bulk quantities of exfoliated graphene sheets and to effectively disperse these sheets in polymer composites we utilized a technique pioneered by Aksay and coworkers.[8,9] This method generates bulk quantities of functionalized (i.e., partially oxygenated) graphene sheets (FGS) by the rapid thermal expansion ($>2000\,^{8}C\ min^{-1}$) of completely oxidized graphite oxide. The oxygen functionalities on the graphene sheetsfacilitate theirdispersion[10,16] inpolarsolvents, whichmakes thisprocess convenientforcomposite applications. The protocols used to oxidize graphite to graphite oxide and then generate FGS by the thermal exfoliation of graphite oxide are provided in the Experimental Section and the Supporting Information (we used the same protocols as described in References [8,9]). The procedures used to disperse FGS in a bisphenol-A based thermosetting epoxy[17–19] are also described in the Experimental Section. Both compact tension samples for crack propagation study and dog-bone-shaped coupons (samples) for uniaxial tensile testing were fabricated and tested.

Figure 1a shows a scanning electron microscopy (SEM) image of a typical FGS flake synthesized by the above approach and deposited on a silicon wafer for imaging. The flake dimensions are ≈4.4 mm × 2.4 mm; note the wrinkled surface texture of the FGS, which could play an important role in enhancing mechanical interlocking and load transfer with the matrix.[11,12] Figure 1b is a high-resolution transmission electron microscopy (HRTEM) image of the edge of a typical FGS flake, indicating that each flake is composed of ≈2–3 individual graphene sheets. The electron diffraction pattern (shown in the inset of Figure 1b) confirms the signature of few-layered graphene.[11] Figure 1c shows an SEM image of a freeze-fractured nanocomposite sample with ≈5% weight of FGS. The image clearly indicates epoxy-coated FGS flakes on the fracture surface of the sample. The inset in Figure 1c depicts a high-resolution SEM image, indicating the wavy edge structure of the FGS sheets that are protruding out of the fracture surface. At low weight fractions of FGS (below 0.5%), it was quite challenging to study the FGS dispersion by SEM analysis due to the planer sheet geometry of the FGS and the epoxy coating on the FGS, which allows only the exposed sheet edges to be discerned.

DOI: 10.1002/smll.2019901480

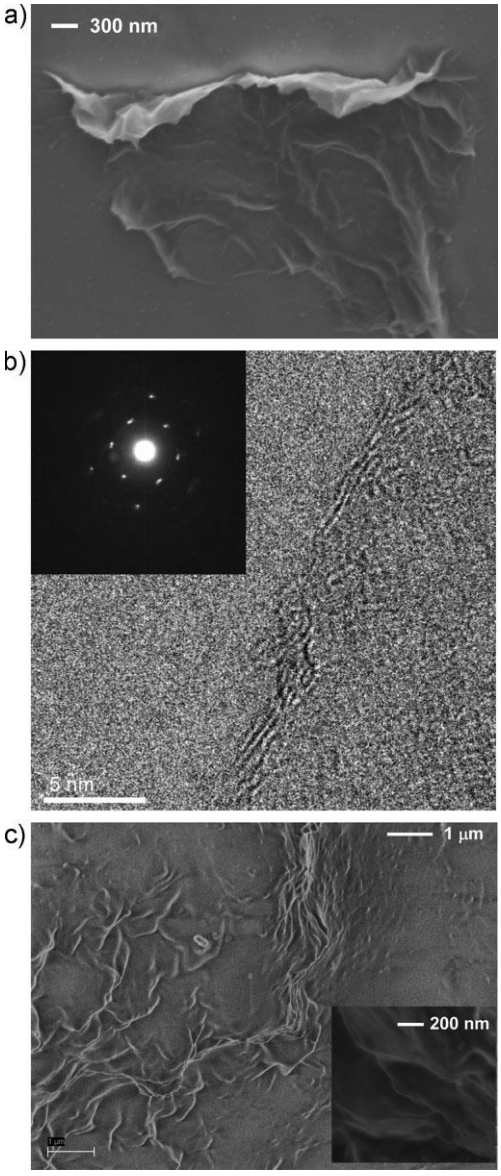

Figure 1. a) SEM image of a typical functionalized graphene flake depositedon asiliconwaferforimaging. b) HRTEMimageof theedgesof a typical graphene flake showing 2–3 graphene layers. The inset shows the measuredelectron diffraction pattern, which is typical for few-layered graphene. c) SEM analysis of the freeze-fractured surface of the nanocomposite indicating epoxy-coated FGS on the fracture surface. The inset shows the wavy edges of the FGS sheets protruding out of the fracture surface.

Crack-opening tests on compact tension samples were performed to measure the Mode I fracture toughness (K_{Ic}) of the pure epoxy matrix and the FGS–epoxy nanocomposites at various weight fractions of FGS. The tests were conducted using a MTS-858 material testing system following ASTM standard D5045 (Supporting Information). An initial pre-crack was created in the compact tension samples by gently tapping a fresh razor blade over a molded starter notch. The radius at the tip of the pre-crack was similar for all the samples tested, which was confirmed by opticalmicroscopy prior to testing. Ateach weight fraction of FGS additives, we tested 4–6 different samples to check for reproducibility of the results. Figure 2a shows that the Mode I fracture toughness (K_{Ic}) of the baseline epoxy (without FGS) is ≈0.93 MPa $\sqrt{m}$, which correlates well with published literature[17–19] for epoxy materials. The addition of FGS into the epoxy matrix causes a sharp increase in the nanocomposite K_{Ic} value to ≈1.75 MPa $\sqrt{m}$ at 0.125% weight fraction of FGS, which corresponds to a ≈65% increase in fracture toughness. For higher loading fractions, the enhancement in K_{Ic} diminishes (Figure 2a) and finally begins to approach the pure epoxy value at a FGS weight fraction of ≈0.5%. This might be a result of degradation in the dispersion of the FGS additives above a weight fraction of 0.125%. We have observed similar degradation[17–19] in the dispersion quality of CNTs in epoxy composites but at significantly larger nanotube weight fractions (>0.5%). Therefore, dispersion of two-dimensional FGS appears to be more challenging as compared to one-dimensional CNTs or Al_2O_3/TiO_2/SiO_2 nanoparticles, which have been successfully dispersed in epoxies at very high loading fractions (up to 20%).[14,15] This is not an unexpected result given that the two-dimensional FGS(several micrometers in dimension; Figure 1a) are more easily entangled and therefore show a greater tendency to agglomerate as compared to nanoparticles or nanotubes. In spite of this, the maximum enhancement in K_{Ic} (≈65% at 0.125% weight fraction of FGS) is impressive. To achieve comparable increase (≈62%) in K_{Ic}, the required weight fraction[14] (≈14.8%) of SiO_2 nanoparticles in epoxy is ≈120-fold larger than FGS. Similarly, to obtain a 65% increase in K_{Ic}, the volume fraction of Al_2O_3 (≈5%) and TiO_2 (≈10%) nanoparticles[15] in epoxy is ≈30- to 60-fold larger than FGS.

Intercalated nanoclays[20–22] have also proven to be effective in toughening epoxy systems. For example, Zerda et al.[20] obtained ≈61% increase in fracture toughness for 3.5% nanoclay weight fraction. Wang et al.[21] obtained similar levels of K_{Ic} enhancement (≈78%) at 2.5% weight fraction of nanoclay fillers. Liu et al.[22] demonstrated ≈110% increase in K_{Ic} for an epoxy system with ≈3% weight of nanoclay additives. These weight fractions are 20–30 times higher than the FGS weight fraction of 0.125% in our study. Moreover, in the case of nanoclay epoxy composites addition of nanoclays (in the 2.5–3.5% weight fraction range) causes degradation in the tensile strength. For example, the tensile strength of the matrix[21] was reduced by 17% due to incorporation of 2.5% weight of nanoclay. Similarly the tensile strength decreased by 7.5% for 3.5% weight fraction of nanoclays in the epoxy matrix[20]. By contrast, the FGS additives were found to enhance the tensile strength by up to 45% in the 0.1–0.125% weight fraction range (Figure 2b).

For CNT–epoxy composites, the best reported enhancement[13] in K_{Ic} is ≈43%, which occurs at ≈fourfold-higher nanofiller weight fraction (≈0.5% weight of amine-functionalized double-walled CNTs). Our recent work[17] with CNT–epoxy composites indicated ≈11% improvement in fracture toughness with 0.25% weight of multi-walled CNT additives. These results indicate that FGS are highly effective in suppressing crack propagation in polymer materials. However, there is a clear need to develop improved techniques for FGS dispersion in polymer matrices in order to realize their full potential. For example, pre-modifying FGS by the use of specially designed surfactants may enable enhanced dispersion at higher FGS loading fractions (>0.125%).

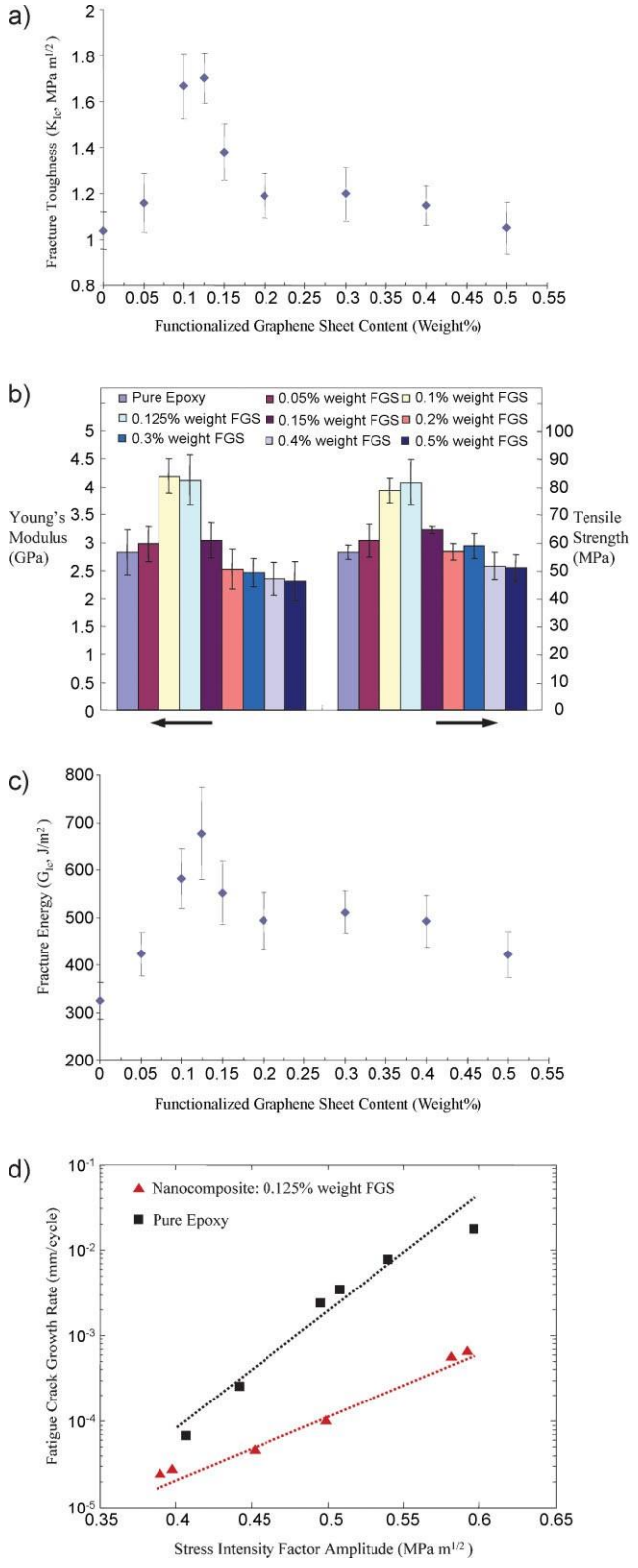

Figure 2. a) Mode I fracture toughness (K_{Ic}) plotted as a function of the weight fraction of FGS in the epoxy matrix. b) Young's modulus and ultimate tensile strength of pure epoxy and nanocomposite samples with various weight fractions of FGS. c) Variation of fracture energy (G_{Ic}) as a function of the weight fraction of FGS in the epoxy matrix. d) Fatigue crack-propagationtesting; crackgrowthrate(d*a*/d*N*) plottedasafunctionofthe stress intensity factor amplitude (D*K*) for the pristine epoxy and nanocomposite samples with 0.125% weight fraction of FGS.

We characterized the nanocomposite's Young's modulus and ultimate strength by performing tensile loading tests on dog-bone-shaped coupons. Figure 2b depicts the measured modulus for the pristine epoxy and FGS/epoxy nanocomposites. At 0.125% FGS weight fraction, the Young's modulus of the nanocomposite is ≈50% greater than the baseline epoxy. Figure 2b also shows the ultimate tensile strength measurements; we observe ≈45% enhancement in the ultimate tensile strength at 0.125% weight fraction of FGS. In contrast, CNTs show ≈30% increase in modulus and ≈15% increase in strength for 1% weight of functionalized single-walled CNTs in epoxy.[23] Therefore, compared to CNTs, FGS imparts superior tensile strength and stiffness properties to the epoxy matrix at nearly an order of magnitude lower nanofiller weight fraction. This is indicative of improved mechanical interlocking and adhesion between the FGS and the polymer matrix, which may result from the rough and wrinkled texture of FGS (Figure 1a). Distortions caused by oxygen functionalization and the resultant defects during thermal exfoliation of graphite oxide, as well as the extremely small thickness of FGS, lead to a wrinkled topology at the nanoscale.[12] This nanoscale surface roughness likely results in enhanced mechanical interlocking with the polymer chains and, consequently, better adhesion. Such an effect has also been suggested by recent molecular dynamics studies.[24-25] The glass-transition temperature of the FGS–epoxy nanocomposite was also significantly elevated in comparison to the pristine epoxy (Supporting Information); this could result from enhanced adhesion[11,12] at the FGS–matrix interface as well as conformational changes[26,27] to the epoxy polymer in the vicinity of the FGS.

The measurement of modulus (E) and fracture toughness (K_{Ic}) enables us to compute the critical energy release rate, $G_{Ic} = K_{Ic}^2\left(\frac{1-\nu^2}{E}\right)$, where ν is the Poisson ratio. The fracture energy (G_{Ic}) quantifies the energy required to propagate the crack in the material. Figure 2c indicates that the G_{Ic} of the baseline epoxy (without FGS) is ≈225 J m^{-2}, which correlates well with published literature[28] for brittle polymers, which typically show G_{Ic} less than 500 J m^{-2}. Incorporation of FGS into the epoxy causes a large increase in the nanocomposite's G_{Ic} to ≈700 J m^{-2} at 0.125% weight fraction of FGS, which corresponds to a ≈115% increase. The critical energy release rate for the FGS–epoxy nanocomposite is comparable to brittle metals, which typically display G_{Ic} in the range of 800–2000 J m^{-2}.

To evaluate the nanocomposite's performance in fatigue environments, dynamic crack-propagation tests were performed on compact tension samples using ASTM standard E647 (details provided in the Supporting Information). Figure 2d shows the measured crack-propagation rate (da/dN) versus the applied stress intensity factor amplitude (DK) for the baseline epoxy and the nanocomposite with 0.125% weight fraction of FGS. The weight fraction was not increased beyond 0.125% since it is challenging to maintain FGS dispersion at higher loading fractions. The results indicate a significant reduction in crack growth rate for the nanocomposite compared to the pristine epoxy over the full range of stress intensity factor amplitudes that were tested. Forexample, at DK = 0.5 MPa $\sqrt{m}$, the da/dN for the nanocomposite (1.0165×10^{-4} mm/cycle) is ≈25 times lower than the baseline

epoxy (2.49 × 10−3 mm/cycle). We fitted the crack growth results (Figure 2d) to the Paris–Erdogan law: $\frac{da}{dN} = C(\Delta K)^n$. We find a significant reduction in the exponent n (from ≈17.33 to ≈7.94) and the constant C (from ≈394.26 to ≈0.0358) for the nanocomposite compared to the baseline epoxy.

Todevelop an understanding of the enhanced ability of FGS to resist fracture and fatigue, we performed fractography analysis of the fracture surface of the compact tension samples tested in the study. SEM analysis of the fracture surface (Supporting Information) did not reveal any direct evidence of crack pinning or crack bridging by the FGS additives. However, we observed a significant increase in average surface roughness of the fracture surface with FGS content, as indicated in Figure 3a. The average surface roughness (R_a) of the fracture surfaces was measured using a Dektak Surface Profiler (from VEECO); at least 6 separate measurements were performed for each sample for statistics. The data indicates a doubling in the average surface roughness with increase in FGS content from 0 to 0.125% weight. This roughening effect begins to saturate with furtherincrease inthe FGScontent. Theincreasingroughness of the fracture surface with FGS content suggests that crack deflection appears to play a significant role in the observed toughening. Crack deflection is the process by which an initial crack tilts and twists when it encounters a rigid inclusion. This generates an increase in the total fracture surface area, resulting in greater energy absorption as compared to the unfilled polymer material. The tilting and twisting of the crack front as it is forced to move out of the initial propagation plane also forces the crack to grow locally under mixed-mode (tensile/in-plane shear and tensile/anti-plane shear) conditions. Crack propagation under mixed-mode conditions requires a higher driving force than in Mode I (tension), which also results in higher fracture toughness of the material. If such crack deflection processes playa major role then we expect a linear increase[28,29] in the fracture surface roughness (R_a) as the fracture energy (G_{Ic}) is increased. This indeed appears to be the case in the 0–0.125% FGS weight fraction range, as indicated in Figure 3b. However, for higher weight fractions the trend reverses, which suggests that a competing mechanism (probably agglomeration of FGS) that decreases the fracture toughness comes into play.

To understand why crack deflection may be more effective for high-aspect-ratio FGS sheets as compared to conventional fillers, we used the classical Faber and Evans model[30] for crack deflection. In the Supporting Information we show the normalized toughening increment generated by crack tilting versus the particle aspect ratio (as predicted by the Faber and Evans model) for particles with rod, sphere, and plate geometries. The results (Supporting Information) indicate that for plates with large aspect ratio (such as an FGS sheet), the tilting of the crack front acts as a significant source of toughening. It is also evident that neither the sphere nor the rod-shaped particles derive noticeable toughening from the crack tilting process. Furthermore, the aspect ratio of the rod has little effect on the toughening during the crack tilt process. This indicates that the FGS sheet geometry with its very large aspect ratio is expected to be highly effective in toughening the matrix, which is consistent with our experimental observations.

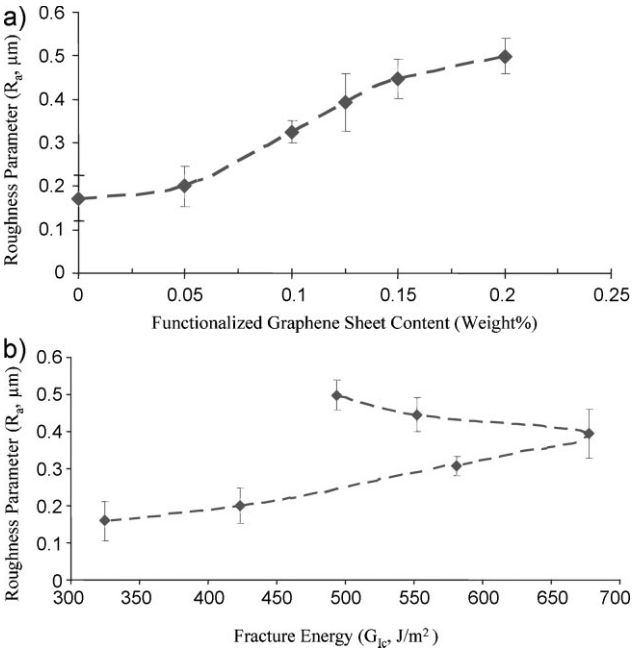

Figure 3. a) Fracture surface roughness parameter (R_a) plotted as a functionof the weightfraction of FGS in the epoxy matrix. b) Variation in R_a as a function of the fracture energy (G_{Ic}). The linear increase of R_a with G_{Ic} (in the 0–0.125% FGS weight fraction range) indicates that crack deflection processes appear to play a significant role in the toughening of the FGS/epoxy nanocomposite.

In summary, functionalized graphene sheets are remarkably effective at enhancing the fracture toughness, fracture energy, stiffness, strength, and fatigue resistance of epoxy polymers at significantly lower nanofiller loading fractions in comparison to CNTs, nanoparticles, and nanoclay additives. This can be attributed to their enhanced specific surface area, two-dimensional geometry, and strong nanofiller-matrix adhesion. However, improved techniques to quantify the dispersion of graphene in polymer matrices and enhanced dispersion of graphene sheets at high nanofiller loading fractions are necessary to realize the full potential of graphene-based composite materials.

Experimental Section

Natural graphite flakes with an average diameter of 48 mm were supplied from Huadong Graphite Factory (Pingdu, China). Concentrated sulfuric acid (95–98%), concentrated nitric acid (68%) and hydrochloric acid (36–38%) were purchased from Beijing Chemical Factory, China. Potassium chlorate (99.5%) was obtained from Fuchen Chemical Reagents (Tianjin, China). The epoxy used in the present study was a Bisphenol-A-based epoxy (Epoxy 2000 from Fibreglast, USA) and the curing agent used was 2120 Epoxy Hardener from Fibreglast, USA.

FGS fabrication: Graphite oxide was prepared by oxidizing graphite in a solution of sulfuric acid, nitric acid, and potassium chlorate for 96 hours based on the work of Aksay and coworkers.[8,9] X-ray diffraction patterns of natural graphite and graphite oxide are provided in the Supporting Information. Thermal exfoliation of graphite oxide was achieved by placing the graphite oxide powder (200 mg) in a 200-mm-inner-diameter, 1-m-long quartz tube that was sealed at one end. The other end of

the quartz tube was closed using a rubber stopper. An argon inlet was then inserted through the rubber stopper. The sample was flushed with argon for 10 min, and the quartz tube was quickly inserted into a tube furnace (Thermolyne 79300, Thermo Fisher Scientific Inc., USA) preheated to 1050 °C and held in the furnace for 30 s. Rapid heating (>2000 °C min^{-1}) splits the graphite oxide into functionalized graphene sheets (FGS) through the evolution of CO_2 gas as demonstrated in References [8, 9].

Dispersion of FGS in epoxy matrix: The desired amount of FGS was first weighed and dispersed in acetone (ratio of 100 mL of acetone to 0.1 g of FGS) using an ultrasonic probe sonicator at high amplitude (Sonics Vibracell VC 750, Sonics and Materials Inc., USA) for 1.5 h in an ice bath. The epoxy (System 2000 Epoxy Resin, Fibreglast Inc, USA) was added to the mixture and sonicated following the same procedure for another 1.5 h. Next, the acetone was evaporated off by heating the mixture on a magnetic stir plate using a Teflon-coated magnetic bar for 3 h at 70 °C. Subsequently, the mixture is placed in a vacuum chamber for 12 h at 70 °C to ensure that all of the acetone had been removed. After allowing the FGS/epoxy slurry to cool down to room temperature to prevent any premature curing, a low-viscosity curing agent (2120 Epoxy Hardener, Fibreglast Inc, USA) was added and mixed using a high-speed shear mixer (ARE-250, Thinky, Japan) for 4 min at 2000 rpm. The mixture was again placed in a vacuum chamber to degas the epoxy for approximately 30 min. Finally, the mixture was poured into Silicon moulds and the nanocomposite was cured at room temperature and 90 psi pressure for 24 h, followed by 4 h of post cure at 90 °C.

Acknowledgements

N.K. acknowledges funding support from the US Office of Naval Research (Award Number: N000140910928) and the US National Science Foundation (Award Number: 0900188).

Keywords:

graphene · nanocomposites · fractures · fatigue

[1] D. Li, R. B. Kaner, *Science* 2008, *320*, 1170.
[2] K. N. Kudin, B. Ozbas, H. C. Schniepp, R. K. Prud'homme, I. A. Aksay, *Nano Lett.* 2008, *8*, 36.
[3] A. K. Geim, K. S. Novoselov, *Nat. Mater.* 2007, *6*, 183.
[4] F. Schedin, A. K. Geim, S. V. Morozov, E. W. Hill, P. Blake, M. I. Katsnelson, K. S. Novoselov, *Nat. Mater.* 2007, *6*, 652.
[5] D. C. Elias, R. R. Nair, T. H. G. Mohiuddin, S. V. Morozov, P. Blake, M. P. Halsall, A. C. Ferrari, D. W. Boukhvalov, M. I. Katsnelson, A. K. Geim, K. S. Novoselov, *Science* 2009, *323*, 610.
[6] S. Y. Zhou, G.-H. Gweon, A. V. Fedorov, P. N. First, W. A. De Heer, D.-H. Lee, F. Guinea, A. H. Castro Neto, A. Lanzara, *Nat. Mater.* 2007, *6*, 770.
[7] C. Lee, X. Wei, J. W. Kysar, J. Hone, *Science* 2008, *321*, 385.
[8] H. C. Schniepp, J.-L. Li, M. J. McAllister, H. Sai, M. Herrera-Alonso, D. H. Adamson, R. K. Prud'homme, R. Car, D. A. Saville, I. A. Aksay, *J. Phys. Chem. B* 2006, *110*, 8535.
[9] M. J. McAllister, J.-L. Li, D. H. Adamson, H. C. Schniepp, A. A. Abdala, J. Liu, M. Herrera-Alonso, D. L. Milius, R. Car, R. K. Prud'homme, I. A. Aksay, *Chem. Mater.* 2007, *19*, 4396.
[10] S. Stankovich, R. D. Piner, S.-T. Nguyen, R. S. Ruoff, *Carbon* 2006, *44*, 3342.
[11] S. Stankovich, D. A. Dikin, D. Dommett, K. Kohlhaas, E. J. Zimney, E. A. Stach, R. D. Piner, S. T. Nguyen, R. S. Ruoff, *Nature* 2006, *442*, 282.
[12] T. Ramanathan, A. A. Abdala, S. Stankovich, D. A. Dikin, M. Herrera-Alonso, R. D. Piner, D. H. Adamson, H. C. Schniepp, X. Chen, R. S. Ruoff, S. T. Nguyen, I. A. Aksay, R. K. Prud'homme, L. C. Brinson, *Nat. Nanotechnol.* 2008, *3*, 327.
[13] F. H. Gojny, M. H. G. Wichmann, B. K. Fiedler, K. Schulte, *Comp. Sci. Technol.* 2005, *65*, 2300.
[14] B. R. K. Blackman, A. J. Kinloch, J. Sohn Lee, A. C. Taylor, R. Agarwal, G. Schueneman, S. Sprenger, *J. Mater. Sci.* 2007, *42*, 7049.
[15] B. Wetzel, P. Rosso, F. Haupert, K. Friedrich, *Eng. Fract. Mech.* 2006, *73*, 2375.
[16] S. Park, J. A. An, I. Jung, R. D. Piner, S. J. An, X. Li, A. Velamakanni, R. S. Ruoff, *Nano Lett.* 2009, *9*, 1593.
[17] W. Zhang, I. Srivastava, Y.-F. Zhu, C. R. Picu, N. Koratkar, *Small* 2009, *5*, 1403.
[18] W. Zhang, C. R. Picu, N. Koratkar, *Appl. Phys. Lett.* 2007, *91*, 193109.
[19] W. Zhang, C. R. Picu, N. Koratkar, *Nanotechnology* 2008, *19*, 285709.
[20] A. S. Zerda, A. J. Lesser, *J. Polym. Sci. Pol. Phys.* 2001, *39*, 1137.
[21] K. Wang, L. Chen, J. Wu, M. L. Toh, C. He, A. F. Yee, *Macromolecules* 2005, *38*, 788.
[22] W. Liu, S. V. Hoa, M. Pugh, *Compos. Sci. Technol.* 2005, *65*, 2364.
[23] J. Zhu, J. Kim, H. Peng, J. L. Margrave, V. N. Khabashesku, E. V. Barrera, *Nano Lett.* 2003, *3*, 1107.
[24] F. W. Starr, T. B. Schroder, S. C. Glotzer, *Macromolecules* 2002, *35*, 4481.
[25] G. D. Smith, D. Bedrov, L. W. Li, O. Byutner, *J. Chem. Phys.* 2002, *117*, 9478.
[26] V. A. Harmandaris, K. C. Daoulas, V. G. Mavrantzas, *Macromolecules* 2005, *38*, 5796.
[27] T. Desai, P. Keblinski, S. K. Kumar, *J. Chem. Phys.* 2005, *122*, 134910.
[28] D. Hull, *Fractography: observing, measuring, and interpreting fracture surface topography*, Cambridge University Press, Cambridge 1999.
[29] K. Arakawa, K. Takahashi, *Int. J. Fract.* 1991, *48*, 103.
[30] K. T. Faber, A. G. Evans, *Acta. Metall. Mater.* 1983, *31*, 565.

Received: August 10, 2009
Revised: October 12, 2009
Published online: November 18, 2009

The synthesis of graphene nanocomposites can be highly efficient

S Loka Raghavendra, B Lavanya*,

† ‡

Department of Sciences G Pullaiah College Of Engineering and Technology, Kurnool,India

ABSTRACT: Graphene consists of a monolayer of sp^2 bonded carbon atoms and has attracted considerable interest over recent years due to its extreme mechanical, electrical, and thermal properties. Graphene nanocomposites have naturally begun to be studied to capitalize upon these properties. A range of complex chemical and physical processing methods have been devised that achieve isolated graphene sheets that attempt to prevent aggregation. Here we demonstrate that the simple casting of a polymer solution containing dispersed graphene oxide, followed by thermal reduction, can produce well-isolated monolayer reducedgraphene oxide. The presence of single layer reduced-graphene oxide is quantitatively demonstrated through transmission electron microscopy and selected area electron diffraction studies and the reduction is verified by thermogravimetric, X-ray photoelectron spectroscopy, infrared spectrum, and electrical conductivity studies. These findings provide a simple, environmentally benign and commercially viable process to produce reduced-graphene oxide reinforced polymers without complex manufacturing, dispersion or reduction processes

KEYWORDS: Graphene oxide, nanocomposite, dielectrics, electrical conductivity, TEM, thermal reduction

The inclusion of nanoscale particles into a matrix material can lead to orders of magnitude enhancement in the mechanical, electrical, optical, and thermal properties relative to the neat polymer. These significant improvements can be achieved with a relatively low loading of the nanofiller due to the high surface area to volume ratio. Graphene has drawn significant interest in recent years for polymer nanocomposites due its high specific surface area (2600 m^2/g) and enormous mechanical, electrical, and thermal properties.[1−4] The modulus and fracture strength of single layer graphene membranes have shown values of ∼1 TPa and ∼130 Gpa, respectively, with 25% strain at failure.[2] The thermal conductivity has been estimated to be 4840−5300 W/mK through analysis of the shift in the Raman G peak with increasing incident laser power.[3] Graphene has also been shown to have ballistic electron transport with electron mobility as high as 15 000 $cm^2/(V\ sec)$.[4] The results of these studies have clearly demonstrated the potential for graphene to result in materials and devices with extraordinary properties.

Various processing methods have been investigated for producing graphene-reinforced nanocomposites; however the majority rely on graphene oxide as the starting material due to

challenges associated with producing large scale quantities of isolated pristine graphene sheets. Recent results have shown the direct exfoliation in highly polar organic solvents such as dimethylformamide (DMF)[5] and N-methyl-pyrrolidone (NMP)[6] by sonication or in chlorosulfonic acid[7] through simple dissolution, but these methods are not currently suited for polymers since the colloidal suspensions cannot support high graphene concentrations and the stability of the mixture strongly depends on the surface energy of the solvent.[6] The highly oxidized nature of GO interrupts the electrical properties of the material and thus significant research has been performed to investigate methods to produce polymers with reducedgraphene oxide (RGO) sheets.[8]

The majority of the research in the field has focused on GO[9−11] or performed reduction of the GO prior to its dispersion into the polymer, which yields nanocomposites with multilayer platelets rather than single layer sheets.[12−18] Three primary methods are used for the synthesis of reduced

Received: August 31, 2021
Revised: November 4, 2021
Published: November 22, 2021

dx.doi.org/10.1021/nl203023k | Nano Lett. 2021, 12, 84−90

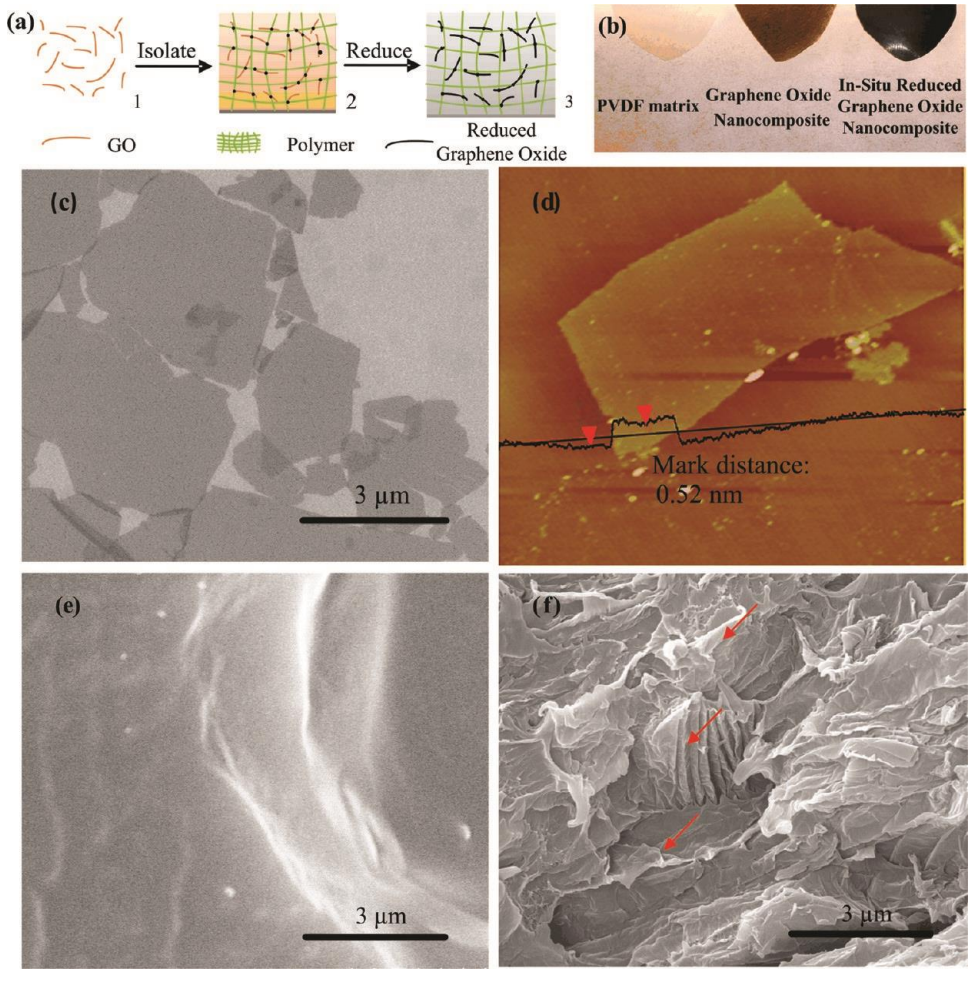

Figure 1. Image of the graphene oxide and nanocomposite: (a) the in situ reduced process for the single layer reduced-graphene oxide nanocomposite, (b) digital image of graphene oxide and in situ reduced-graphene oxide nanocomposite, (c) SEM image of graphene oxide, (d) AFM scan of the graphene oxide, (e) SEM images obtained from a fracture surface of PVDF, and (f) SEM images obtained from a fracture surface of composite samples of in situ reduced-graphene oxide nanocomposites.

graphene oxide nanocomposites, in situ polymerization, grafting, and solution or melt processing.[8] In situ polymerization intercalates the graphene oxide with a hydrophilic polymer[19−21] or polar monomers,[22] then polymerizes the intercalent to isolate the single layer sheets. Grafting utilizes the functional groups present on the GO to covalently attach reactive species to incorporate the graphene element into the polymerization reaction.[9,23−27] Solution casting or melt processing can produce nanocomposites[28−31] from a variety of polymers in a highly scalable manner. While this is a simple approach, it has not yet been demonstrated to produce single layer graphene sheets without the use of stabilizers or surfactants that may negatively affect the composite, specifically the interface.

Here we provide the first quantitative demonstration that the simple casting of a polymer solution of dispersed GO in a highly polar organic solvent can result in well isolated monolayer sheets that can be reduced after removal of the solvent to create monolayer RGO nanocomposites. By performing the reduction of the graphene oxide once it is dispersed in a rigid polymer, the sheets become immobilized and cannot aggregate (Figure 1a). The polymer solution or blended resin forms indefinitely stable suspensions that do not require aggressive sonication or high shear mixing prior to polymerization because the GO is readily dispersed in the solvent. Existing methods, which are limited to specific polymer systems, employ hazardous reducing agents, for example, dimethylhydrazine, and complex processes to achieve isolated graphene sheet are unnecessary.[8,9] Transmission electron microscopy (TEM) and selected area electron diffraction (SAED) results provide quantitative evidence of isolated monolayer RGO, which has not been previously shown for polymer nanocomposites. The results offer a highly scalable, environmentally benign process that is compatible with the commercial production of RGO-reinforced polymers.

dx.doi.org/10.1021/nl203023k | Nano Lett. 2021, 12, 84−90

The in situ reduction process is demonstrated here on a polyvinylidene fluoride (PVDF) polymer matrix, although any polymer with high-temperature stability could be used. The morphology and thickness of the graphene oxide were characterized by field emission scanning electron microscopy (FE-SEM) and atomic force microscopy (AFM) in Figure 1c,d. These results demonstrate a high level of exfoliation of the GO with a typical sheet thickness less than 1 nm. The GO was first dispersed in N,N-dimethylformamide (DMF) through vortex mixing and mild sonication to form a colloidal suspension of single layer GO sheets (Figure 1a1). PVDF was then dissolved into the pressure. The resulting film has a light brown color as shown in Figure 1b. Once the solvent is entirely removed from the polymer matrix, the graphene oxide sheets become immobilized in the rigid polymer matrix (Figure 1a2). The in situ reduction process is then carried out by hot pressing the PVDF/GO film at 200 °C for 2 h, yielding nanocomposites with isolated single layers of reduced-graphene oxide (Figure 1a3). The color of the film changes during heat treatment from light brown to black as shown in Figure 1b, which indicates removal of the oxygen functionalities and the partial restoration of the graphitic structure during thermal treatment. Figure 1e,f shows the

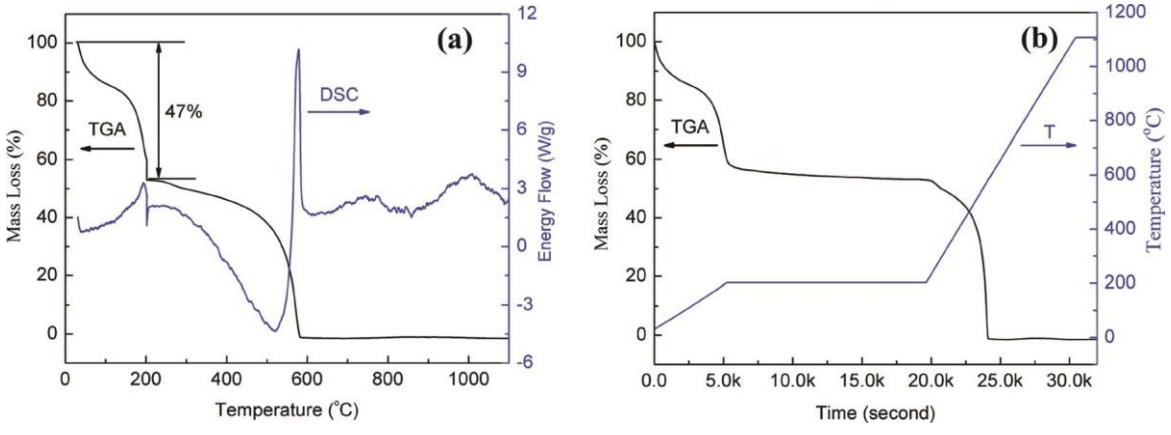

Figure 2. Thermal analysis of GO powder: (a) TGA and DSC plot of graphene oxide and (b) the heating process in the TGA.

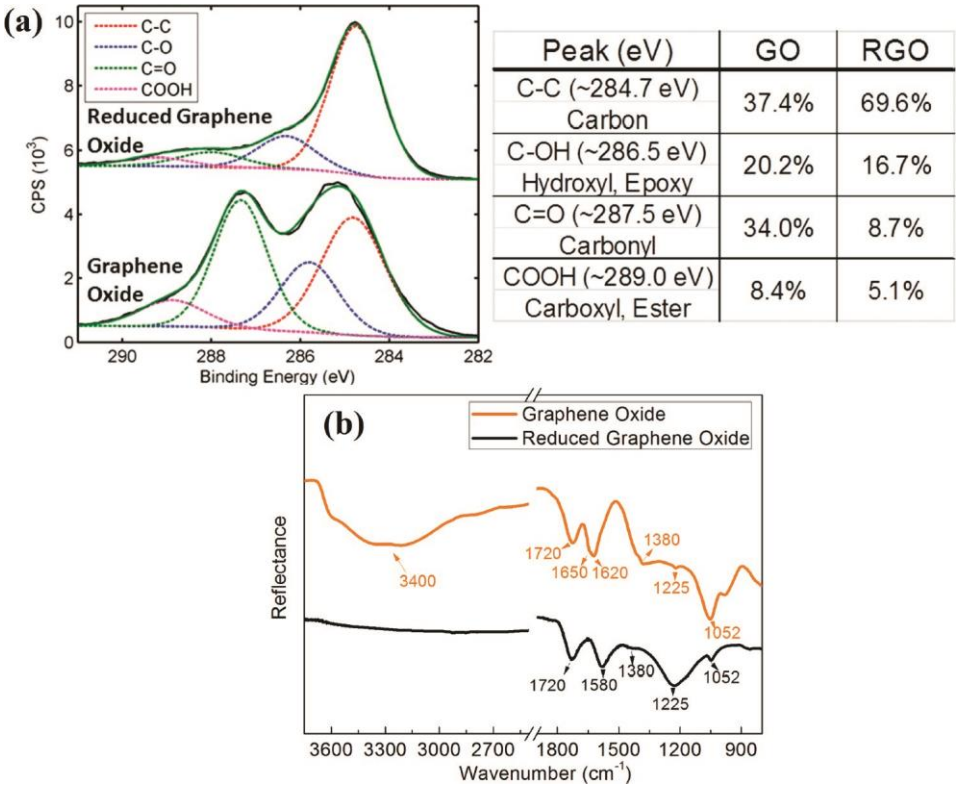

Peak (eV)	GO	RGO
C-C (~284.7 eV) Carbon	37.4%	69.6%
C-OH (~286.5 eV) Hydroxyl, Epoxy	20.2%	16.7%
C=O (~287.5 eV) Carbonyl	34.0%	8.7%
COOH (~289.0 eV) Carboxyl, Ester	8.4%	5.1%

Figure 3. (a) X-ray photoelectron spectroscopy analysis (b) IR analysis spectra indicating a substantial reduction in oxygen containing groups.

DMF/GO solution, cast onto a Telfon substrate, and then allowed to dry overnight at 60 °C under atmospheric fracture surface of virgin PVDF and PVDF with reducedgraphene oxide, respectively. The nanocomposites

dx.doi.org/10.1021/nl203023k | Nano Lett. 2021, 12, 84–90

with reduced-graphene oxide become rough compared to the cross section of PVDF. The wrinkled surface indicates the reduced graphene oxide in the polymer as shown in arrow of Figure 1f.

Thermogravimetric analysis (TGA) and differential scanning calorimetry (DSC) are used to characterize the reaction progress during thermal reduction of the graphene oxide. Figure 2 shows the mass loss of the graphene oxide filler during reduction together with the heat flow and the temperature profile used. There is a mass loss below 100 °C that can be attributed to the removal of adsorbed water. At 200 °C, there is a dramatic mass loss accompanied by an exothermic peak, which is ascribed to the decomposition of oxygen functional groups present on the GO surface. Samples were prepared by reducing the graphene oxide in the nanocomposite at 200 °C for two hours and thus the temperature profile used in the TGA analysis held the materials at 200 °C to capture the reduction process and determine if longer holding times could benefit the material. The GO is primarily reduced simply by heating to 200 °C, where it lost 41% of the original mass. The GO continued to reduce during the temperature-holding period, losing an addition 5% of the original mass after 2 h and 1% after another 2 h. Two hours is an appropriate holding time and longer reductions appear largely ineffective for further restoring the conductivity of the graphene oxide. The reduction process continues with increasing temperature, indicating that some oxygen-containing groups still remain on the sample and that the graphene sheets are only partially reduced at 200 °C. Finally, there is a sharp exothermic spike around 500 °C, indicating that oxidation of graphene occurs and formation of CO_2. Thermal analysis of the material demonstrates that 200 °C is sufficient to remove a large portion of the oxygen containing functional groups and shows that higher temperatures are effective in further reducing the materials but not mandatory to achieving filler conductivity. The mild reduction temperature enables the use of a range of common polymers, both thermosets and thermoplastics.

X-ray photoelectron spectroscopy (XPS) was also used to assess the degree of reduction produced by the simple thermal treatment. Two samples of the filler were produced on copper substrates, one of GO drop cast from DMF at room temperature and another drop cast and reduced at 200 °C for two hours in air. The samples were mounted underneath a copper mask and through the lens charge cancelation ensured that no charge shifting occurred in the data and thus the data were not shifted to compensate for this. High-resolution C1s scans provide a good assessment of the state of carbon atoms in graphene oxide and reduced graphene oxide because the data can distinguish between different numbers of carbon−oxygen bonds (zero, one, two, or three carbon−oxygen bonds). The data are fitted by an error minimization routine in CASA-XPS, as consistent

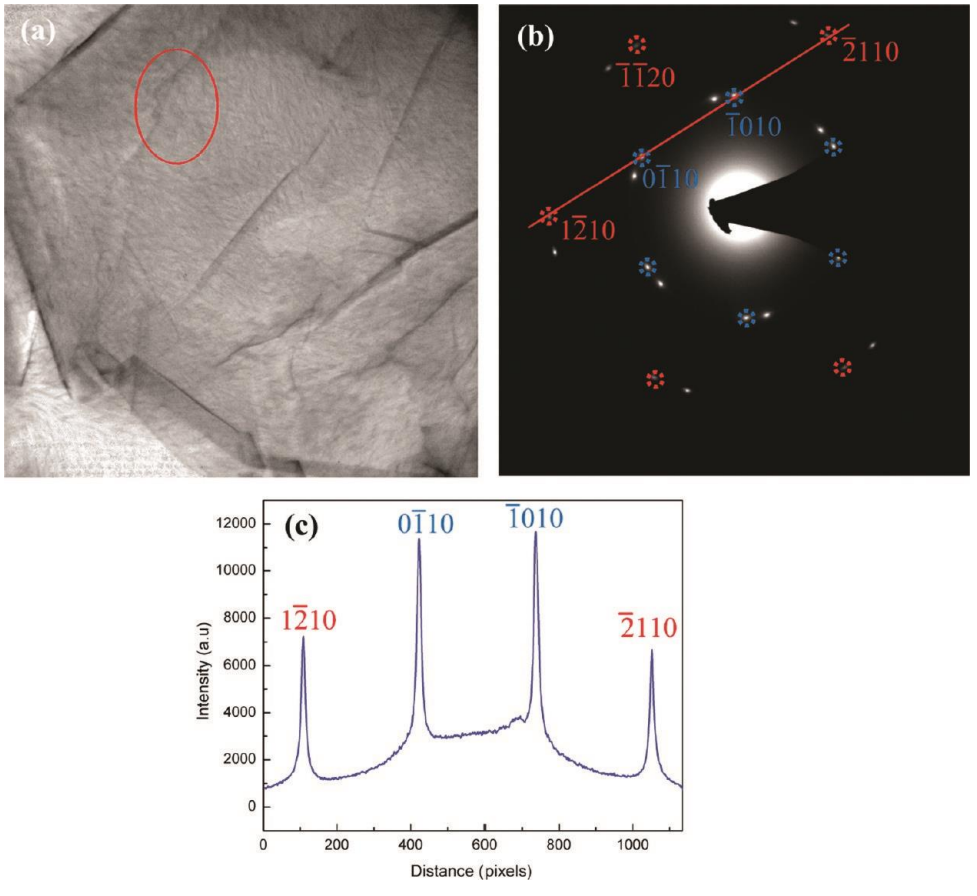

Figure 4. TEM of nanocomposite: (a) TEM image of two overlapping reduced-graphene oxide sheet in nanocomposite, (b) SAED pattern of reduced-graphene oxide in matrix, and (c) intensity profile through the diffraction spots labeled in panel b.

dx.doi.org/10.1021/nl203023k | Nano Lett. 2021, 12, 84–90

with previously published literature,[32] to quantify the relative surface fraction of each level of oxidation. The highresolution C1s scan for the as-synthesized GO and following reduction at 200 °C for 2 h is shown in Figure 3, illustrating the reduction in oxygen groups bound to carbon. The fraction of carbon−carbon bonding increases from 37.4 to 69.6% and the fraction of all other oxygen levels significantly decreases. The substantial reduction indicated by the XPS data is consistent with the mass loss observed with TGA and changes in the infrared spectrum (IR, Figure 3b) and can be attributed specifically to the removal of oxygen functional groups from the material.

The infrared absorbance spectrum of the graphene oxide before and after reduction is presented in Figure 3b. Several significant changes occur after thermal reduction, owing to removal and reactions of various functional groups. The studies by Bagri et al.[33] and Acik et al.[34,35] specifically track the desorption, evolution, and reaction of the various functional groups during reduction and closely match the results in these experiments. The thermal reduction removes many of the hydroxyl groups (~3400, 1380, 1052 cm^{-1}) through desorption.[33−38] Thermal reduction at 200 °C is incapable of removing all carbonyl moieties, thus a significant peak at 1720 cm^{-1}, attributed to C=O stretching, remains after reduction of the graphene oxide.[33−35] Two closely overlapping peaks are observed at ~1650 and ~1620 cm^{-1}, attributed to COOH and aromatic C=C stretching, respectively. After reduction, the unstable COOH groups are removed from the material while the conjugated network of aromatic groups increases substantially.[34] The reduced graphene oxide shows no peak at 1650 cm^{-1} and the increased sp^2 hybridization pushes the C=C peak from 1620 to 1580 cm^{-1}.[34,35] The peak at 1225 cm^{-1} corresponds to cyclic ether moieties, such as furan or pyran.[35] Graphene oxide has relatively few of these groups and thus a relatively small peak; however, after reduction some of the hydroxyl groups convert into ethers and appear as defects in the graphene structure. The variety of substituents and sizes of the rings which contain oxygen leads to a broad peak that remains well above the reduction temperatures employed in these experiments (350 °C).[35] The infrared analysis of these samples clearly demonstrates that thermal reduction can remove many of the oxygen moieties from graphene oxide and partially restore the sp^2 hybridized structure and properties; however, the relatively low temperatures used in this experiment do not completely

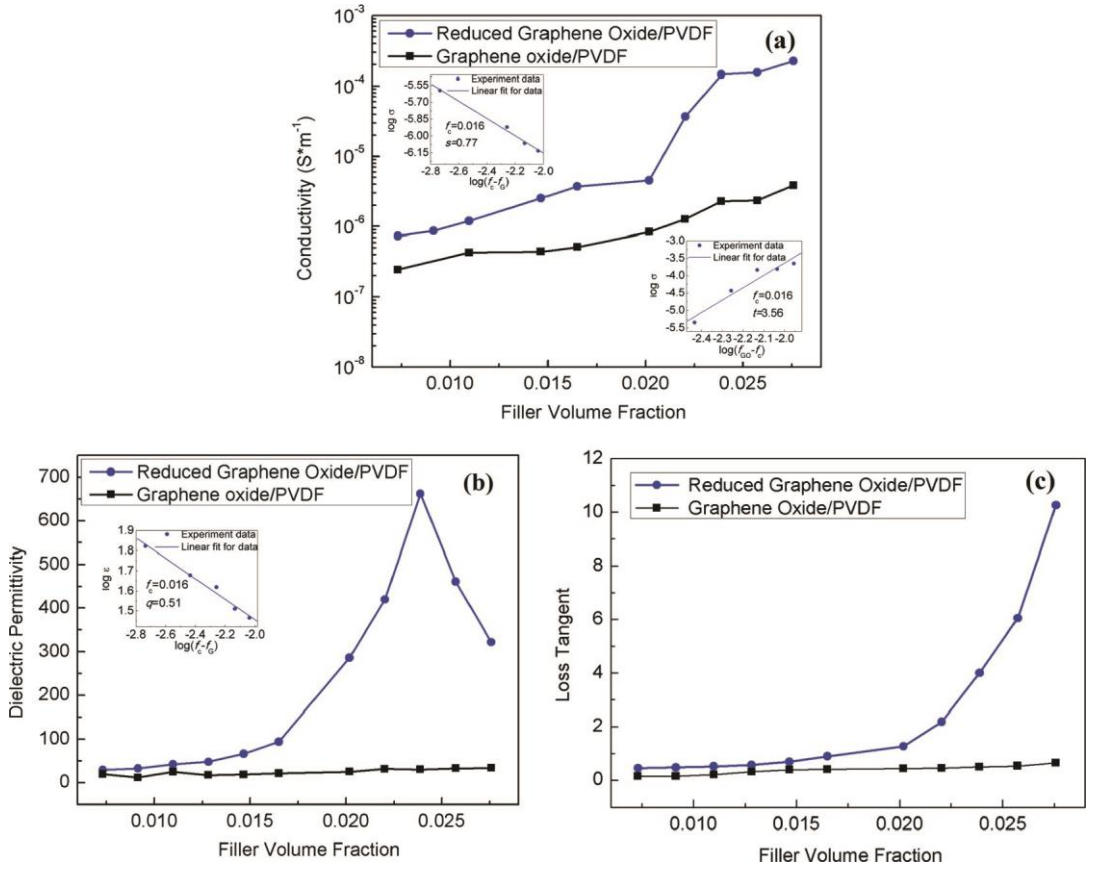

Figure 5. Dependence of (a) the conductivity, (b) relative dielectric permittivity, and (c) loss tangent of the graphene oxide/PVDF and reduced graphene oxide/PVDF nanocomposites on the reduced graphene volume fraction, f_{GO}, measured at room temperature and 10^3 Hz. The inset in (a) and (b) show the best fits of the conductivity and the dielectric permittivity, respectively.

dx.doi.org/10.1021/nl203023k | Nano Lett. 2021, 12, 84–90

remove all oxygen groups or completely restore a defect free graphene structure.

The X-ray diffraction (XRD) data presented in Figure S1 in the Supporting Information demonstrates the absence of a regular crystalline structure in the nanocomposite implying isolation of single layer RGO sheets in the polymer, however it cannot prove the presence of monolayer RGO. Unlike XRD, TEM can be used to directly identify the presence of the single layer graphene crystal structure in the nanocomposite without dissolving the surrounding polymer.[6,7,39−41] TEM samples were prepared by spin coating the solution of GO dispersed in DMF and PVDF onto a copper grid and followed by thermal reduction of the sample at 200 °C for 2 h, using the same process as the nanocomposites. Figure 4a shows a representative image of the RGO sheets in the PVDF matrix obtained by the TEM. The RGO sheet in Figure 4a shows a wrinkled surface, which is consistent with the morphology of RGO in Figure 1f. The presence of monolayer RGO can be confirmed using SAED of the nanocomposites. The SAED pattern of the region marked in Figure 4a is shown in Figure 4b and demonstrates the crystalline filler in the amorphous polymer has a hexagonal pattern consistent with graphene. The SAED pattern actually shows two concentric hexagonal patterns rotated by 10.6°. The two patterns are attributed to the polymer containing two sheets of RGO or one sheet folded arbitrarily with the angle corresponding to the misorientation between two individual RGO sheets.[39] The spots of one of the two hexagonal patterns are labeled in Figure 4b using MillerBravais hkil notation and shows the pattern is consistent with those obtained from the single layer graphene.[6,7,39−41] In order to quantify the number of layers, the relative intensities between the $(0\bar{1}10)$ type and $(1\bar{2}10)$ type reflections can be used to distinguish between single-sheet graphene and few-layer graphene.[6,7,39−41] A−B stacked graphene-like structure thicker than one monolayer will give higher diffracted intensities for $(1\bar{2}10)$ type spots than $(0\bar{1}10)$ type spots because of interference between electrons scattered from the A-type and B-type layers.[6,7,39−41] The intensity of a line section through the $(1\bar{2}10)$−$(0\bar{1}10)$−$(\bar{1}010)$−$(\bar{2}110)$ spots is shown in Figure 4c. The inner $(0\bar{1}10)$ type reflections are more intense than the outer $(1\bar{2}10)$ type reflections, which indicate that the sample is consistent with isolated single layer graphene. The TEM images demonstrate that the polymer prevents aggregation of the sheets during the reduction process.

The removal of the functional groups from the surface of the graphene oxide sheets leads to the restoration of the πconjugation and therefore renders the sheets electrically conductive. An evaluation of the dielectric and conductivity of the nanocomposites has been performed to assess the percolation and the processing methods use for creating conductive polymers. As a reference, the relative dielectric constant and conductivity of PVDF composites containing unreduced graphene oxide sheets are also measured and are shown in Figure 5a,b. It can be seen that the samples with graphene oxide are not electrically conductive ($\sigma \leq 10^{-6}$ S/m), while those that have been reduced clearly demonstrate an insulator−conductor transition at a percolation threshold of approximately 0.016 volume fraction identified through power laws. The electrical conductivity of GO composite is 3 orders of magnitude lower than that of samples with reduced graphene because the GO sheets have very little conductivity. The conductivity of the nanocomposites following reduction at 200 °C reach values consistent with carbon nanotube composites,[42] however this technique offers significant advantages in preparation because it provides uniform dispersion without the use of surfactants or harsh mixing methods such as high shear mixing or high intensity sonication.[8,9] Graphene also offers advantages in cost over carbon nanotubes; both the raw materials and processing are less expensive than typical production of single-walled carbon nanotubes. The mild heat treatment at 200 °C sufficiently increases the conductivity to benefit the composite without requiring inert atmospheres or high-temperature furnaces and is compatible with many commercial polymers potentially allowing it to be integrated in the cure cycle of thermosetting resins. Furthermore, with an appropriate solvent the GO-polymer dispersion is indefinitely stable allowing for the production of commercial resins with long shelf life. While PVDF cannot reach the temperatures required for the full reduction, it is expected that a polymer with higher temperature stability would allow further reduction of the graphene and enhance the conductivity of the filler and composite even further.

In addition to the high conductivity of the nancomposite, a sharp increase in the relative dielectric constant occurs near the percolation threshold, as shown in Figure 5b. This increase is predicted by the percolation theory, indicating that the filler is conductive and matches standard models.[42−44] The relative dielectric permittivity of the GO-PVDF nanocomposite is between 20 and 40 within the range of GO fillers volume fractions tested. After the reduction treatment, the relative dielectric constant improves dramatically to 100 at the percolation threshold, which is 10 times larger than that of pure PVDF ($\varepsilon \approx 10$). As the volume fraction of filler increases beyond the percolation threshold, the relative dielectric constant of reduced graphene/PVDF nanocomposites continues to rise to 662 at 2.4% filler volume fraction, twice that of similar multiwalled carbon nanotube/PVDF nanocomposites that exhibited a maximum relative dielectric constant of 300.[42] It is noted that the loss tangent undergoes a large change near the percolation threshold due to significantly increased conductivity in the nanocomposite (Figure 5c).[44−47] The in situ reduction process demonstrates the possibility for making next generation high dielectric constant nanocomposite and electrically conductive nanocomposites.

Nanocomposites with isolated monolayer reduced-graphene oxide sheets have been successfully fabricated through the in situ thermal reduction of graphene oxide. The reduction process uses the rigid polymer matrix to

dx.doi.org/10.1021/nl203023k | Nano Lett. 2021, 12, 84−90

prevent aggregation of the GO during its reduction and conversion to graphene. This simple process has been shown for the first time to produce isolated single layers of RGO using TEM and SAED analysis. The homogeneous dispersion of single layer RGO in the PVDF matrix was shown to significantly improve the dielectric constant and conductivity of a polymer, demonstrating in this model system that simple processes can effectively translate some of the extraordinary properties of graphene to a polymer nanocomposite. The conductivity of the RGO nanocomposite is comparable to that achieved with a MWCNT/PVDF nanocomposite, and the dielectric permittivity is twice that of a MWCNT/PVDF nanocomposite.[42] The in situ reduction process reported here is compatible with a wide range of polymer matrix materials including both thermosets and thermoplastics because GO has been shown to reduce at temperatures as low as 200 °C[48] and the GO material does not require high intensity ultrasonic or shear mixing for dispersion.[8,9] With this demonstration that the dispersion and subsequent reduction of graphene oxide in a polymer matrix provides isolated single layer RGO, manufacturing processes for industrial production of polymers that capture some of the incredible properties of graphene reinforcement may soon be possible.

ASSOCIATED CONTENT

* Supporting Information

Additional details on fabrication of nanocomposites, characterization method, X-ray diffraction analysis, and percolation and conductivity theory. This material is available free of charge via the Internet at http://pubs.acs.org.

AUTHOR INFORMATION

Corresponding Author

*E-mail: hsodano@ufl.edu.

ACKNOWLEDGMENTS

The authors gratefully acknowledge support from the National Science Foundation (Grant CMMI-0826159) and the use of the LeRoy Eyring Center for Solid State Science at Arizona
State University.

REFERENCES

(1) Geim, A. K.; Novoselov, K. S. Nat. Mater. 2007, 3, 183−191.

(2) Lee, C.; Wei, X.; Kysar, J. W.; Hone, J. Science 2008, 5887, 385− 388.

(3) Balandin, A. A.; Ghosh, S.; Bao, W.; Calizo, I.; Teweldebrhan, D.; Miao, F.; Lau, C. N. Nano Lett. 2008, 8, 902−907.

(4) Novoselov, K. S.; Geim, A. K.; Morozov, S. V.; Jiang, D.; Zhang, Y.; Dubonos, S. V.; Grigorieva, I. V.; Firsov, A. A. Science 2004, 5696, 666−669.

(5) Blake, P.; Brimicombe, P. D.; Nair, R. R.; Booth, T. J.; Jiang, D.; Schedin, F.; Ponomarenko, L. A.; Morozov, S. V.; Gleeson, H. F.; Hill, E. W.; Geim, A. K.; Novoselov, K. S. Nano Lett. 2008, 8, 1704−1708.

(6) Hernandez, Y.; Nicolosi, V.; Lotya, M.; Blighe, F. M.; Sun, Z.; De, S.; McGovernI., T.; Holland, B.; Byrne, M.; Gun'Ko, Y. K.; Boland, J. J.; Niraj, P.; Duesberg, G.; Krishnamurthy, S.; Goodhue, R.; Hutchison, J.; Scardaci, V.; Ferrari, A. C.; Coleman, J. N. Nat. Nanotechnol. 2008, 9, 563−568.

(7) Behabtu, N.; Lomeda, J. R.; Green, M. J.; Higginbotham, A. L.;
Sinitskii, A.; Kosynkin, D. V.; Tsentalovich, D.; Parra-Vasquez, A.; Schmidt, J.; Kesselman, E.; Cohen, Y.; Talmon, Y.; Tour, J. M.; Pasquali, M. Nat. Nanotechnol. 2010, 6, 406−411.

(8) Potts, J. R.; Dreyer, D. R.; Bielawski, C. W.; Ruoff, R. S. Polymer 2011, 1, 5−25.

(9) Stankovich, S.; Dikin, D. A.; Dommett, G. H. B.; Kohlhaas, K. M.; Zimney, E. J.; Stach, E. A.; Piner, R. D.; Nguyen, S. T.; Ruoff, R. S. Nature 2006, 7100, 282−286.

(10) Ramanathan, T.; Abdala, A. A.; Stankovich, S.; DikinD., A.; Herrera-Alonso, M.; Piner, R. D.; Adamson, D. H.; Schniepp, H. C.; Chen, X.; Ruoff, R. S.; Nguyen, S. T.; Aksay, I. A.; Prud'Homme, R. K.; Brinson, L. C. Nat. Nanotechnol. 2008, 6, 327−331.

(11) Liang, J.; Huang, Y.; Zhang, L.; Wang, Y.; Ma, Y.; Guo, T.; Chen, Y. Adv. Funct. Mater. 2009, 14, 2297−2302.

(12) Ansari, S.; Giannelis, E. P. J. Polym. Sci., Part B: Polym. Phys. 2009, 9, 888−897.

(13) Kim, H.; Miura, Y.; Macosko, C. W. Chem. Mater. 2010, 11, 3441−3450.

(14) Liang, J.; Wang, Y.; Huang, Y.; Ma, Y.; Liu, Z.; Cai, J.; Zhang, C.; Gao, H.; Chen, Y. Carbon 2009, 3, 922−925.

(15) Kim, H.; Macosko, C. W. Polymer 2009, 15, 3797−3809.

(16) Steurer, P.; Wissert, R.; Thomann, R.; Mülhaupt, R. Macromol. Rapid Commun. 2009, 4−5, 316−327.

(17) Kim, H.; Macosko, C. W. Macromolecules 2008, 9, 3317−3327. (18) Das, B.; Prasad, K. E.; Ramamurty, U.; Rao, C. N. R.
Nanotechnology 2009, 12, 125705.

(19) Jang, J. Y.; Kim, M. S.; Jeong, H. M.; Shin, C. M. Compos. Sci. Technol. 2009, 2, 186−191.

(20) Gu, Z.; Zhang, L. J. Polym. Sci., Part B: Polym. Phys. 2009, 6, 1093−1102.

(21) Gu, Z.; Li, C.; Wang, G.; Zhang, L.; Li, X.; Wang, W.; Jin, S. J. Polym. Sci., Part B: Polym. Phy.s 2010, 12, 1329−1335.
(22) Wen, P. W.; Cai, Y. P. Polym. Eng. Sci. 2004, 12, 2335−2339.
(23) Fang, M.; Wang, K.; Lu, H.; Yang, Y.; Nutt, S. J. Mater. Chem. 2009, 38, 7098−7105.
(24) Lee, S. H.; Dreyer, D. R.; An, J.; Velamakanni, A.; Piner, R. D.; Park, S.; Zhu, Y.; Kim, S. O.; Bielawski, C. W.; Ruoff, R. S. Macromol. Rapid Commun. 2010, 3, 281−288.
(25) Zhang, B.; Chen, Y.; Zhuang, X.; Liu, G.; Yu, B.; Kang, E.; Zhu,
J.; Li, Y. J. Polym. Sci., Part A: Polym. Chem. 2010, 12, 2642−2649.
(26) Li, G. L.; Liu, G.; Li, M.; Wan, D.; Neoh, K. G.; Kang, E. T. J. Phys. Chem. C 2010, 29, 12742−12748.
(27) Zhuang, X.; Chen, Y.; Liu, G.; Li, P.; Zhu, C.; Kang, E.; Noeh,
K.; Zhang, B.; Zhu, J.; Li, Y. Adv. Mater. 2010, 15, 1731−1735.
(28) Chen, D.; Zhu, H.; Liu, T. ACS Appl. Mater. Interfaces 2010, 12, 3702−3708.
(29) Zhao, X.; Zhang, Q.; Chen, D.; Lu, P. Macromolecules 2010, 5, 2357−2363.
(30) Xu, Y.; Hong, W.; Bai, H.; Li, C.; Shi, G. Carbon 2009, 15, 3538−3543.
(31) Jiang, L.; Shen, X.; Wu, J.; Shen, K. J. Appl. Polym. Sci. 2010, 1, 275−279.
(32) Ehlert, G. J.; Lin, Y.; Sodano, H. A. Carbon 2011, 13, 4246−
4255.
(33) Bagri, A.; Mattevi, C.; Acik, M.; Chabal, Y. J.; Chhowalla, M.; Shenoy, V. B. Nature Chem. 2010, 7, 581−587.
(34) Acik, M.; Mattevi, C.; Gong, C.; Lee, G.; Cho, K.; Chhowalla,
M.; Chabal, Y. J. ACS Nano 2010, 10, 5861−5868.
(35) Acik, M.; Lee, G.; Mattevi, C.; Chhowalla, M.; Cho, K.; Chabal,
Y. J. Nat. Mater. 2010, 10, 840−845.
(36) Dreyer, D. R.; Murali, S.; Zhu, Y.; Ruoff, R. S.; Bielawski, C. W.
J. Mater. Chem. 2011, 10, 3443−3447.
(37) Dreyer, D. R.; Park, S.; Bielawski, C. W.; Ruoff, R. S. Chem. Soc. Rev. 2010, 1, 228−240.
(38) Si, Y.; Samulski, E. T. Nano Lett. 2008, 6, 1679−1682.
(39) Wilson, N. R.; Pandey, P. A.; Beanland, R.; Young, R. J.; Kinloch, I. A.; Gong, L.; Liu, Z.; Suenaga, K.; Rourke, J. P.; York, S. J.; Sloan, J. ACS Nano 2009, 9, 2547−2556.
(40) Meyer, J. C.; Geim, A. K.; Katsnelson, M. I.; Novoselov, K. S.; Obergfell, D.; Roth, S.; Girit, C.; Zettl, A. Solid State Commun. 2007, 1−2, 101−109.
(41) Meyer, J. C.; Geim, A. K.; Katsnelson, M. I.; Novoselov, K. S.; Booth, T. J.; Roth, S. Nature 2007, 7131, 60−63.
(42) Wang, L.; Dang, Z. Appl. Phys. Lett. 2005, 4, 042903.
(43) He, F.; Lau, S.; Chan, H. L.; Fan, J. Adv. Mater. 2009, 6, 710− 715.
(44) Dang, Z.; Wang, L.; Yin, Y.; Zhang, Q.; Lei, Q. Adv. Mater. 2007, 6, 852−857.
(45) Li, Y.; Xu, M.; Feng, J. Q.; Dang, Z. M. Appl. Phys. Lett. 2006, 7, 072902−3.
(46) Li, Q.; Xue, Q; HaO, L.; Gao, X.; Zheng, Q. Compos. Sci. Technol. 2008, 68, 2290−2296.
(47) Ahmad, K.; Pan, W.; Shi, S. L. Appl. Phys. Lett. 2006, 13, 133122−3.
(48) Chen, W.; Yan, L. Nanoscale 2010, 4, 559−563.

dx.doi.org/10.1021/nl203023k | Nano Lett. 2021, 12, 84–90

Assessing the Mechanical and Physical Characteristics of Natural Hybrid Composites

B Lavanya,‘S Loka Raghavendra,’B Suneetha, ‘
‘Dept. of Humanities & Sciences,G Pullaiah College of Engineering & Technology,Kurnool

***Abstract*—Brake lining is one of the components in the braking system that directly rub against the rotating drum or disk. The ability of brake lining can be seen from several things including being able to absorb the amount of kinetic energy when braking, having good hardness, low water absorption. Previously, brake lining was made of asbestos material which has resistance to high temperatures reaching 800˚C, but asbestos material has a negative impact on the environment and human health. This research was developed to overcome these problems, namely finding alternative brake lining materialsthat have good impact strength, good hardness and do notinterfere with the health of the driver of the vehicle and are environmentally friendly. This paper describes the mechanical and physical properties of the developed brake lining material. This brake lining material is made from basalt powder, shellfish powder, alumina powder and phenolic resin polymer as a binder with five variations of weight fraction. This material wasmade through a sintering process at a temperature of 150°C with a pressure of 2000 kg for 30 minutes, then each specimen was tested for impact strength using a Charpy impact testaccording to ASTM D 6110 standard, hardness was tested usingVickers test according to ASTM E384-99, and water absorption based on ASTM D 570-98 standards. The average impact strength of brake lining specimens was obtained at 0.0003327 J/mm², better than the average impact strength of brake liningsfrom asbestos material. While the hardness obtained was the lowest 24.72 VHN and the highest was 26.55 VHN, still better than the asbestos brake lining of 24.75 VHN, and the highest water absorption of the brake lining specimens obtained was 0.041558 still lower than the water absorption of asbestos brakelining.**

***Index Terms*—Natural hybrid composite, hardness, impact strength, water absorption.**

I. Introduction

One component of the braking system is the brake lining, which this component serves to reduce speed or stop the vehicle. This component rubs directly against the rotating drum or disk [1]. In general, brake pads are asbestos, which have a high temperature resistance of 800°C [2], and they also have low water absorption [3]. However, asbestos brake linings have been discontinued because they have a negative impact on the environment and human health [4], [5].

Then other researchers also developed clamshell brake pads with a grit size of 600 μm which were tested at speeds below 100 km/h [6]. Morphological testing of shellfish granules is very possible to use as a friction plate for asbestos substitutes [7], and thermal test of shellfish material for friction material has also been carried out and has good properties [8]. However, the results achieved at this time have not been able to maintain mechanical properties, especially for wear resistance, temperature resistance, and high water absorption.

This paper discusses brake linings made from hybrid composites by mixing basalt powder, shellfish powder, alumina powder and phenolic polymer resin (PR-51510i) as a binder. Basalt is a rock from a volcanic eruption crushed into powder of a specific size. This material has heat resistance up to 1500˚C [9], has excellent corrosion resistance properties, low water absorption and is non-toxic [10]. Besides this material has excellent physical and mechanical properties, good ductility, high wear resistance [11], and this fiber can replace glass fibers [12]. Besides that, the main characteristic of this material is that it has low thermal conductivity.

Manuscript received September 6, 2021; revised November 12, 2021.

IK. Adi Atmika is with the Udayana University, Indonesia (e-mail: tutadi2001@yahoo.com).

II. Material and Method

A. Materials

This research was carried out by hybridizing three materials as reinforcement and one material as binding matrix in specific compositions. The reinforcing material consists of basalt powder, shellfish powder and alumina powder which are all in the form of solid particles with a size of 0.0074 millimeters, then as a matrix material is a phenolic resin (PR-51510i). Basalt characteristics are shown in Table I.Shellfish powder used consisted of several elements, namely 0.03% Fe_2O_3, 1.25% Al_2O_3, 7.88% SiO_2, 22.28% MgO, and 66.70% CaO.

TABLE I: Properties of Basalt Material

Properties of basalt	Value (unity)
Tensile strength	500k-550k (psi)
Density	2600-2630 (kg/m^3)
Operation temperature	-265 - 700 (ºC)
Sintering temperature	1050 (ºC)
Modulus of elastisitas	9100 - 1100 (kg/mm^3)
Elongation at break	3.15 (%)
Heat resistance	700-1000 (ºC)
Melting point	1170 (ºC)
Mohs Hardness @20ºC	5-9

B. Method

This brake lining material is made by mixing, compacting, and sintering at a temperature of 150°C. The sintering process of this brake lining material specimen was carried outwith emphasis for approximately 30 minutes and a compressive load of 2000 N. The size and shape of the test specimen were made according to ASTM D 3171-09 standard, as shown in Fig. 1 and Fig. 2.

doi: 10.18278/ijmmm.2021.7.6.467

Research into grip clamps for expanded diameter half-hard aluminum conductors with a c **involves experiments and finite element simulations**

B. Lavanya, B.Suneetha
Department of Sciences, G Pullaiah College Of Engineering and Technology, Kurnool,India

***Abstract*—The cross-sectional area and outer diameter of the wire that have been put into use in the project are similar to those of the newly designed JLZX1K/F2A-530(630)/55 sparse-twisted carbon fiber expanded wire. The finite element analysis and the compatibility test of the stranded carbon fiber expanded diameter wire were carried out, and the combination of test and simulation was used to judge the radial pressure resistance of the composite mandrel and the force of the aluminum strand of the profile. It is concluded that the newly designed JLZX1K/F2A-530(630)/55 sparse-twisted carbon fiber expanded conductor can be used with the SKLT-60 grip clamps; the aluminum strand stress concentrates from the inner layer to the outer when the wire clamp clamps the wire.**

***Index Terms*—Grip clamps, expanded diameter half -hard aluminum conductors composite core reinforced, force transfer finite element, test.**

I. Introduction

Carbon fiber composite conductor has been widely used in transmission line engineering due to its advantages of high strength, large capacity, high temperature resistance, light weight, low linear expansion coefficient, low sag, non-magnetic, high temperature resistance and corrosion resistance [1], [2]. With the promotion of the theme of energy conservation and environmental protection, a new type of sparsely twisted carbon fiber diameter enlargement (reducing the material cost but ensuring the cross-sectional area of the conductor) conductor JLZX1K/F2A-530(630)/55 (below "530k630 carbon fiber diameter enlargement conductor") was born [3]. During the construction of all kinds of temporary anchor and tight wire for erecting wires, the force transmission between the wire and the anchor force system should be completed through the clamping of the clamping device.

Compatibility finite element analysis is carried out on 530k630 expanded diameter half-hard aluminum conductors composite core reinforced with grip clamps of three conductors with equal outer diameter that has been put into use in the project in this paper, and according to the results are related with test and analysis, finally got 530k630 expanded diameter half-hard aluminum conductors composite core reinforced can be used with SKLT-60 type grip clamps.

Manuscript received May 14, 2019; revised July 21, 2019. This work was supported in part by the State grid corporation of China (WBS: 52110417000T).

Jiancheng Wan is with the China Electric Power Research Institute, 100085, No. 15 Xiaoying East Road, Qinghe, Haidian District, Beijing (e-mail: wjc1971@163.com).

Yaao Zhou is with the China Electric Power Research Institutemale, 100085, No. 15 Xiaoying East Road, Qinghe, Haidian District, Beijing (e-mail: zhouyaao2016@163.com).

Min Wang is with the Zhejiang Electric Power Corporation, 310007, No. Huanglong Road, Hangzhou City, Zhejiang, China (e-mail: wang_min@zj.sgcc.com.cn).

II. Analysis of Force Principle of Card Wire Device

The parallel movable grip clamps is A four-link structure, as shown in Fig. 1. The pull plate and the press-plate are hinged at point A, and the press-plate and the upper press-plate are hinged at point C.The distance between hinge point A and the far end point B of the slideway is the length of the drawplate LAB, and the distance between hinge point A and O is the length of the clamping plate LOA.The pull ring of the cable clamping device can beopened by parallel movement to the left. The wire is put in from the side, and the upper and lower clamping nozzles hold the wire after tightening the pull ring.TAB under transverse tensile F_0, the tension through four bar linkage pass and translated into positive pressure toward a wire clip mouth F_N, pulling through the TAB to the grip clamps of the fuselage.

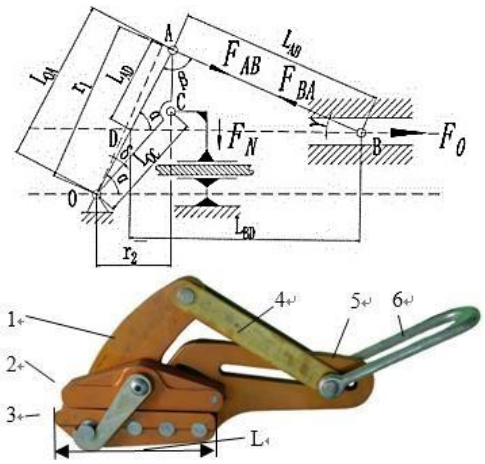

1—Pressing plate; 2— Clip on the mouth;
3—Under the mouth; 4—Pull a board;
5— Ontology; 6—Pull tab

Fig. 1. Clamping force and structure diagram of clamping device.

The main force type of connecting rod is axial tension or pressure.When the clamping device clamps the wire, it shall ensure that the wire is stable and not loose when it is clamped [5]:

doi: 10.11178/ijmmm.2021.7.6.473

Current Physical Chemistry Vols. 38-21 (2022) pp 551-556 *Online: 2022-08-07*
© (2022) ,ISSN:3825-5845
doi:10.4028/www.scientific.net/CPC.38-21.551

Crystallographic axis of Induction-welded and Heat Pipeline Steel

Palle Divya[1,a], Ö. E. Güngör[2,b] , and H. K. D. H. Bhadeshia[2]
[1]Department of Humanities and sciences, G. Pullaiah college of engineering and technology,Kurnool, A.P. INDIA-518452.
[2]ArcelorMittal R&D Gent, OCAS NV, Pres. J. F. Kennedylaan 3, BE-9060 Zelzate, Belgium
[a]pdivya@gmail.com, [b]ozlem.esma.gungor@arcelormittal.com,

Keywords: crystallographic texture; pipeline steel; induction welding; induction heat-treatment.

Abstract. Large-diameter steel pipes are produced by induction seam-welding followed by induction-assisted heat treatment. The microstructure and distribution of crystal orientations have been studied and related to the mechanical properties of the welded regions. The welding and heat-treatment process leads to a microstructure, a simple observation of which can not explain the observed variations in toughness in the vicinity of the welding joint, because the crystallographic grain size, which represents the scale of similarly oriented adjacent grains, is much coarser than the ordinary grain size. Furthermore, heating the affected zone into the austenite phase field followed by cooling does not completely eliminate the coarse regions of similarly oriented grains. The consequences of this on mechanical properties are discussed.

Introduction

Pipes for oil and gas transmission are made from low-alloy steels designated X60, X65, X70 etc. depending on the strength and toughness required and the intended application [1–3]. One method of fabricating pipes from these materials is by high–frequency induction seam–welding. Pipes some 18 m in length, 500 mm in diameter and 12.7 mm in thickness are routinely manufactured in this way [4]. The toughness of line pipes is paramount in their suitability for application [5–7]. The joint resulting from induction welding is quite narrow, with a central 2 mm wide region, but it represents a source of weakness, so the welding process is immediately followed by induction heat treatment. The intention of the latter is to refine the microstructure by reaustenisation at a lower temperature than the peak temperature achieved during welding. Although the heat–treatment improves the toughness of the welded region, the increase is not as large as might be expected from the reduction in the scale of the microstructure. The purpose of the present work was to understand this insensitivity of the toughness to heat–treatment.

Experimental Procedures

The chemical composition of the steel is Fe–0.041C–1.1Mn–0.18Si wt% with micro–alloying of Nb and V. Details of the heat-treatment are proprietary, but it involves rapid heating to above a temperature at which austenite can form, and subsequently fast cooling.

Specimens were obtained from different stages of the manufacturing process: the unaffected base metal, the pipe just after welding, and finally, the pipe after welding and heat–treatment. Samples were cut normal to the welding direction which is parallel to the rolling direction of the steel and to the length of the pipe. Some were flattened to make non–standard cross–weld Charpy test specimens of size 55 × 6.7 × 10 mm. The tests were conducted according to the standard ISO 148-1.

Metallographic specimens were prepared in the usual way by grinding, polishing and etching (using 2% nital). Orientation imaging requires scratch–free surfaces so the metallographic samples were finished using colloidal silica. Scanning electron microscopy was conducted on a Camscan

Cloud-Based Solar Panel Cleaning System using Texas Instruments

Dr.K.Evangili Supriya
Academic Consultant
Department of Physics
Sri Krishnadevraya University
Anantapur, AP, India.
evangilisupriya.k@gmail.com

Ch. Joseph Sundar
Assistant Professor
Department of Mechanical Engineering
Srinivasa Ramanujan Institute of Technology,(SRIT), *Anantapur,AP*
joseph.sundar27@gmail.com

Dr.P.Divya Vani
Assistant Professor
Department of Humanities
G.Pullaiah college of Engineering and Technology (GPCET), Kurnool, AP
Vani.divya63@gmail.com

2022 Second International Conference on Computer Science, Engineering and Applications (ICCSEA) | 978-1-6654-5834-4/22/$31.00 ©2022 IEEE | DOI: 10.1109/ICCSEA54677.2022.9936157

Abstract— **Solar energy in recent decades gained high demand as it produces green and sustainable energy sources. Most countries with semi-arid areas choose solar energy as a possible way to generate clean energy for rural and urban households. The dominant obstacle for solar energy is a dense accumulation of atmospheric contaminants such as debris, solid dirt, and, dwelt particles causing the shadow that decreases its working performance. This constraint routed for the necessity of intermittent cleaning of the surface of Solar panels. Currently, cleaning techniques of the photovoltaic panels through labor are extravagant in time. To overcome this problem, a fully automated IoT-Based solar panel cleaning system is proposed. The developed system includes the CC3200 first on-chip Wi-Fi Texas instruments microcontroller, and sensors to sense the respective parameters. A servo motor and relay system is used to control the wiper speed and rotations. The collected data is uploaded to the ThingSpeak cloud and can be monitored in real-time time. GeoTagging approach is utilized to track the location of solar panels with debris and the alert is generated to the user using the GSM module. The result shows that the developed IoT-based kit effectively cleans the solar panel surface and enhances the output of current and maximum power by 50% after the panel is cleaned.**

Keywords— Solar Energy, CC3200, Cloud computing, Internet of Things (IoT), Geo Tagging

I. Introduction

The recent era is marked by an increase in photovoltaics usage in both research and industrial upturn. Renewable sources of energy, in particular photovoltaics, are considered a prime contribution to the decarbonization of the environment. However, areas with a heavy degree of irradiation and sun-blet region usually endure more dust and deficient water resources. The degradation of debris, and birds dropping pollen, onto the solar panel mirror surface leads to the loss of power as it minimizes the solar energy obtained from the collector by consuming (or) dissipating the sunlight[1].In addition to these factors, the working competence of solar panels subsides along with time, and many external factors like fallen leaves, heavy snow, solid dust, and water patches. Hence, several attempts have been carried out to minimize the panel cleansing strategies consisting of wet and dry cleaning techniques, automatic (or) manual cleanse mechanisms, distinct brushes and fabrics, and also definite chemical additives[2]. Apart from all the cleaning mechanisms, another dust reduction strategy is the usage of natural cleaning techniques such as wind and rain. In regions having less rainfall and more humidity like dry and semi-desert areas, dust eviction by which considered a natural cleaning mechanism[3]. Alternatively, various works have been carried out to develop anti-soiling coating.

A.Methods of Dust removal from PV: Various techniques[4] have been suggested and utilized for automatic self-cleaning for photovoltaic panels like motor brushing, using electric wipers, sprayers, robots, electrostatic cleaning, and piezoelectric methods.

Rainfall Cleaning methods:

This technique does not cost anything as it is unable seasonally. The reliability of this method is less especially in the countries having less intensity of rain like Iraq.

Manual cleaning method:

Laborers should clean the surface of solar panels as it is like cleaning windows of the building with separately designed brushes to avoid surface scratching.

Mobile cleaners' method:

This method includes machinery and also requires a storage container to supply water to the cleaning system.

Keeping the facts above in view, the article focuses on cleaning solar panels using IoT and Cloud computing. The designed intelligent system includes four components sensory module, a Microcontroller system, a Motor and cleaning module, and d user interface as shown in "Fig. 1".

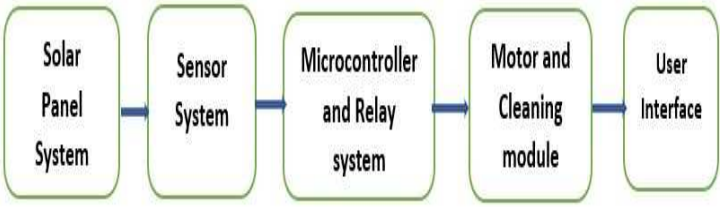

Fig. 1. Block Diagram of the developed System

. II. Literature review

Various Automatic self-cleaning methods have been developed to reduce the problems rises from manual and traditional cleaning procedures to prohibit the lack in productivity of solar energy due to dust. Numerous works have been presented across the globe for automatic self-cleaning for Photovoltaic cells.

Article[5] presented an Automated robot machine for cleaning the surface of the solar panel. It includes an Arduino microcontroller to detect the robot moment while cleaning. A water pump system equipped with a rough sponge is used. Paper[6] presented a method that controls photovoltaic surface cleaning and its power generation. Arduino UNO is used to monitor the cleansing task along with the windscreen wiper tool. In [7] an economical, automatic, and waterless solar panel cleaning system using an Arduino microcontroller that includes a two-step mechanism composed of an exhaust fan that acts as a blower and an automatic wiper to wipe the debris from the surface of a panel. Article [8] presented an IoT-based Robot for solar panel cleaning that systematically cleans PV. The automated robot is controlled and monitored and also the developed robot is auto-powered it enhancing the maximum power generation. A preliminary design [9] of a water sprayer solar cleaning device is designed and to rotate

the wiper system a DC motor is used. The motor direction and its rotation are controlled by the switch buttons. Scheduled Automatic cleaning device then enhances the efficiency and credibility beneath dusty and clean constraints. Paper [10] evaluated dust deposition on solar panels and parabolic trough collectors. The work mainly focuses on dust deposition accounting for the experimental data using distinct air pollutants, while changing the pollutant density. The resulting thermal and visible spectrum are analyzed, calculated, and compared. In [11] presented an Arduino solar panel cleaning system including an engine and an electric device for it. It includes a software environment for reliable working and cleaning of the solar panel. As the system is classified by minimum power consumption, the probability of solar panel shading is eliminated. The above survey says that existing researchers have designed Solar panel cleaning systems with distinct sensors and techniques such as ultrasonic sensor, DSM501A dust sensor, rain sensor, LDR, Motor driver, Blynk, Fuzzy logic, and Arduino microcontroller. Furthermore, an IoT-based solar panel cleaning system, Texas Instruments, and Geotagging are sporadically seen. So, developing a real-time Cloud IoT-based Solar panel cleaning system will be a competent solution for power generation.

Merits and Demerits of the existing and developed systems are listed in Table I.

TABLE I. Merit and Demerits of the Existing and Developed systems

Developed System	Existing Systems
1. System Installation can be done once.	System Installation cannot be done at once.
2. Less Maintenance and Operation expense	More Maintenance and operation expense
3. Less production in charge.	More Production charges.
4. Ease of components replacements	Difficult to components replacement.
5. Heavy machinery is not required	Heavy machinery is required
6. System can be monitored using IoT technology	The system can be monitored using Technologies like Zigbee, and Bluetooth.
7. Data can be accessed remotely through the ThingSpeak cloud.	Data cannot be accessed remotely.
8. Manual assistance is eliminated.	Manual assistance is not eliminated.

II. Hardware Description

A. CC3200-XL Launchpad:

It is the industry's first Wi-fi microcontroller from Texas Instruments including a Wi-Fi network processor, ARM cortex at 80MHz, RAM up to 256KB, 2UART, SPI, 1I2C, 4-16-bit General Purpose Timers, and 27 GPIOs. It works with 802.11 b/g/n Radio, Wi-Fi, Internet Protocol, and Integrated DC-DC providing a maximum range of supply voltage four-channel ADC, 64-Pin QFN packages. For debugging it has a built-in USB-to-JTAG for debugging. Multiple protocols like TCP/IP HTTP server, and TL/SSL server. It has two on-chip sensors Accelerometer BMA222, Thermopile Sensor[12].

B. GP2Y1010AUOF Optical Dust Sensor:

This sensor works on the principle of the optical sensing method. In this device, both the Infrared emitting diode along with the phototransistor are arranged diagonally. The reflected light of dust in the air is easily detected. It is more effective to detect extremely minute particles and is generally used in systems like Air conditioners, purifiers, etc. Also, it can easily detect the bird's dropping pollen, small sand particles, snow, and shadows using a pulse pattern of output voltage. The output voltage is calculated by the voltage without dust and the output volts age proportional to the dust density. It works with 5 volts. The device is lead-free and compliant with the ROHS device [13].

C. Rain Sensor YL-63:

This device is an easy device for rain detection. It has the characteristics of anti-oxidation, and anti-conductivity, to use for an extended period. The entire board works with 3V3 voltage and adopts high-quality two-sided nickel-coated material to collect the rain as it creates a path of parallel resistance. If the collected resistance is high, the Analog output voltage is high and vice-versa[14].

D. Servo Motor:

SG90 Servo motor is utilized to rotate the wiper to clean the surface of the panel[15]. It works like a DC Motor integrated with a Gear train along with a shaft encoder as shown in "Fig 2". It is a 3-pin interface with 5V input, ground, and control signal connected to GPIO-09 of CC3200. Once the debris is detected, the servomotor starts the wiper to rotate from 0^0 to 180^0 with a 50 HZ control signal as it is abided with a meso adjustment potentiometer. When the high level is 1ms~1.5ms and 1.5ms~ 2ms servo rotates forward and backward.

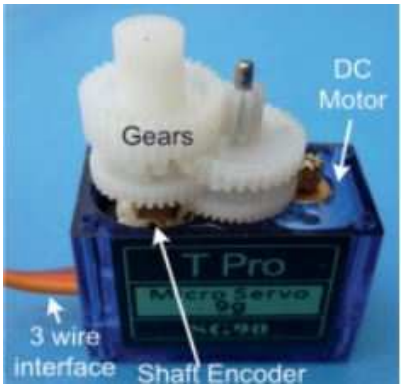

Fig.2. SG90 Servo motor

E. Solar panel:

a) Types of Solar Panel:

Solar cells are of two types namely mono-crystalline and poly-crystalline made up of silicon crystals. All the solar cells are arranged in series for a PV module[16].

b) Specifications of selected Solar panel:

The monocrystalline solar panel is of A+ Grade SBB cell technology built with a Heavy-duty silver anodized aluminum frame with pre-drilled holes for easy and fast installation. It performs well in low light and cloudy sky conditions as shown in "Fig. 3".

- The total length of PV cell = 100cm and
- width = 50cm
- The length of the wiper is almost = 50cm

Fig. 3. Tested Solar Panel

F. GSM SIM900A Module:

GSM(Global System for mobile communication) module works like a phone, its functions include sending the message, calling a phone number, and using GPRS with AT commands to send data. It works with frequencies ranging from 900 to 1800 MHz. The baud rate ranges from 9000 to 115200 MHz. the modem can be easily interfaced with external devices using serial communication. It includes built-in external devices using serial communication. It includes a built-in sim card holder, Network LED, Power Led, and L-Type Antenna. To work with an unregulated power supply Linear drop voltage regulator is available[17].

G. ThingSpeak cloud:

ThingSpeak is an advanced open data cloud platform with MATLAB software. Signing in to the cloud involves three steps.

- Collect: Privately sends the data to the cloud.
- Analyze: Visualize the collected data using MATLAB.
- Act: It triggers by data.

a) Steps to access the cloud:

- Create an account and sign in to the website with created ID.
- Create a channel with a name and it generates an ID and mentions it as a Public (or) Private channel.
- Once the channel is created, Read and Write API Keys will be generated.

The data can be viewed on an Android phone[18]. The screenshots of two-channel creations and their API keys are shown in "Fig.4".

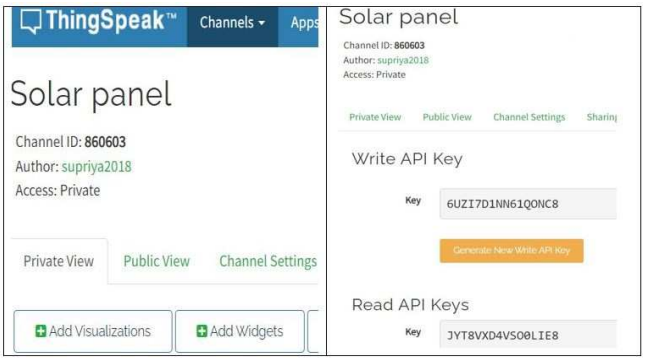

Fig.4. Solar Channel Id and its API Keys

IV. Working Principle

The Present work involves two sensors Rain sensor YL-63 and the GP2Y1010AU0F Dust sensor to detect the dust and rain on the solar panel surface. The entire schematics are shown in "Fig 5". Two Analog outputs of these two sensors are connected to the two ADC channels of GPIO5 and GPIO5, channels ADC-CH2, and ADC-CH3 of CC3200. As the selected microcontroller has an on-chip Wi-Fi feature it continuously collects the data to the Thing Speak cloud from the interfaced sensors and uploads the data to the Thing Speak cloud as shown in "Fig.6". Depending on the concentration of dust and rain on the solar panel surface, the servo motor attached to the relay system will be controlled and is interconnected to CC3200 using the pulse width modulation technique by connecting to the GPIO9 of CC3200.12V DC pumping motor sprays the water during the cleaning process. The selected panel is mounted at 30^0 angle tilt to enhance the panel effectiveness. Once the intensity reaches the threshold value it activates and the entire setup cleans the solar panel surface to work effectively. Sensor data can be graphically viewed and also on mobile through the Thing view app. If the dust is detected on the photovoltaic panel surface, GSM which is connected to CC3200 through serial communication (Tx, Rx pins of CC3200) activates and sends an alert and call to the registered mobile number and location tracking can be done in the cloud as shown in "Fig.7.".

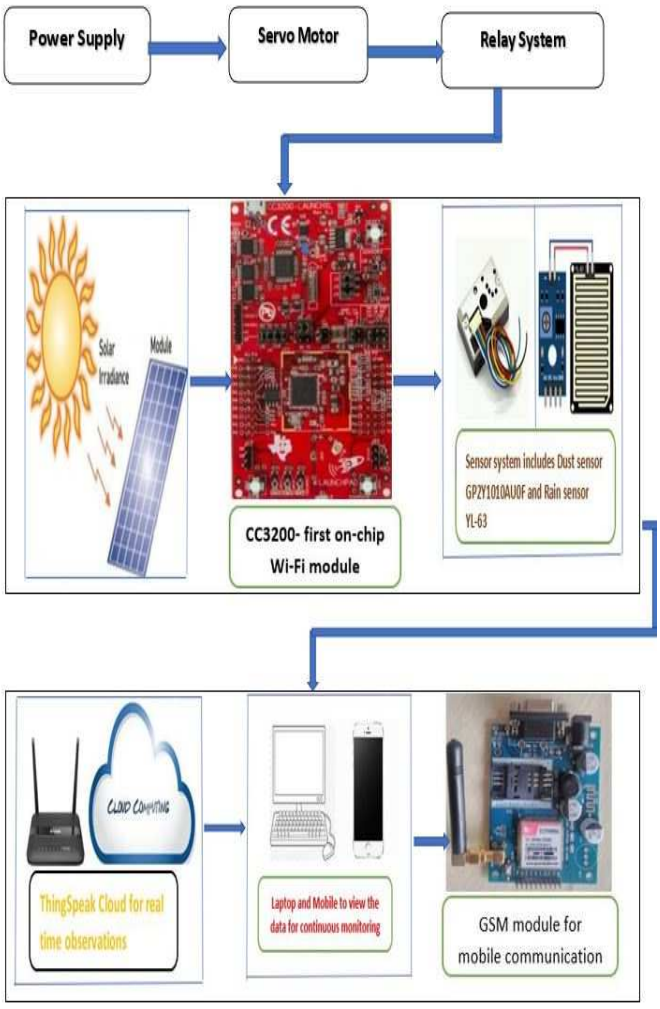

Fig.5. Schematics of the developed System

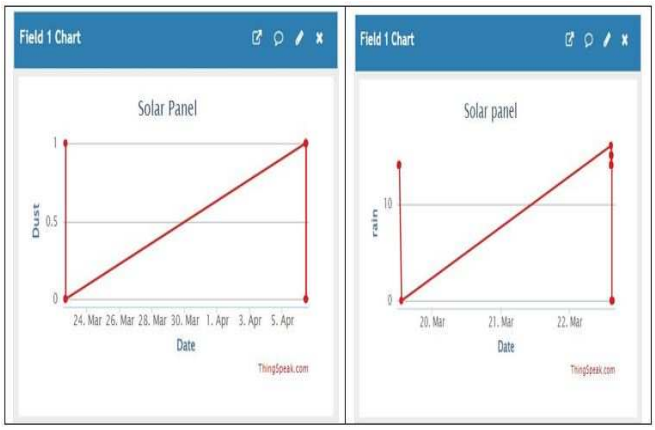

Fig.6. Graphical Representation of Sensors data in the ThingSpeak Cloud

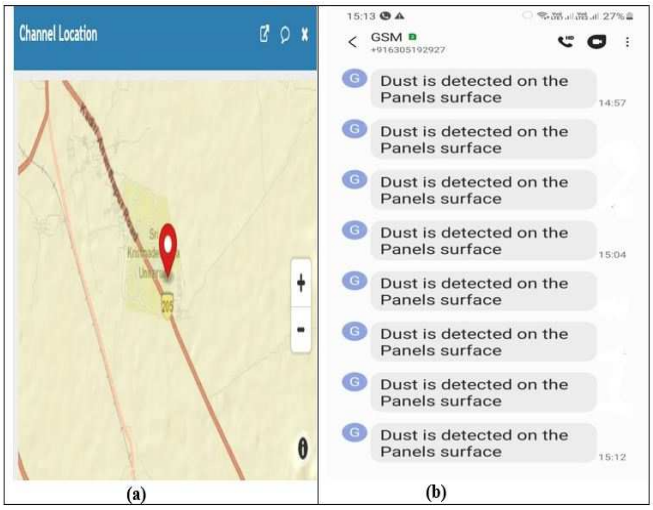

Fig.7. Location tracking using Thing Speak Cloud and Alert to the observer using GSM

V. Software Description

Energia is used to develop the software for the present work. This programming language is an open-source platform that works with the Mac OS, Windows, Unix, and Linux. It uses an mspgcc compiler using Energia Wireless modules that can be added to various types of RF modules like Wi-Fi, Bluetooth, Zigbee, cellular, etc[19]. The developed sketch for the experiment and flowchart is shown in "Fig.8" and "Fig.9."

Solar_panel- | Energia 0101E0015

File Edit Sketch Tools Help

Solar_panel- §

```
#include <stdlib.h>
#include <WiFi.h>
#include <Wire.h>
#define LED 6
int Solar pin = 24;
int rain pin = 25:
// you can adjust the threshold value
int thresholdValue = 2690;
// ThingSpeak Settings
char thingSpeakAddress[] = "api.thingspeak.com";
String writeAPIKey = "6UZI7D1NN61Q0NC8";
const int updateThingSpeakInterval = 16 * 1000;
//buffer for float to string
char buffer[25];
// your network name also called SSID
char ssid[] = "dlink";
// your network password
char password[] = "skuphy1234";
// initialize the library instance:
WiFiClient client;
```

Fig.8. Developed Sketch in Energia

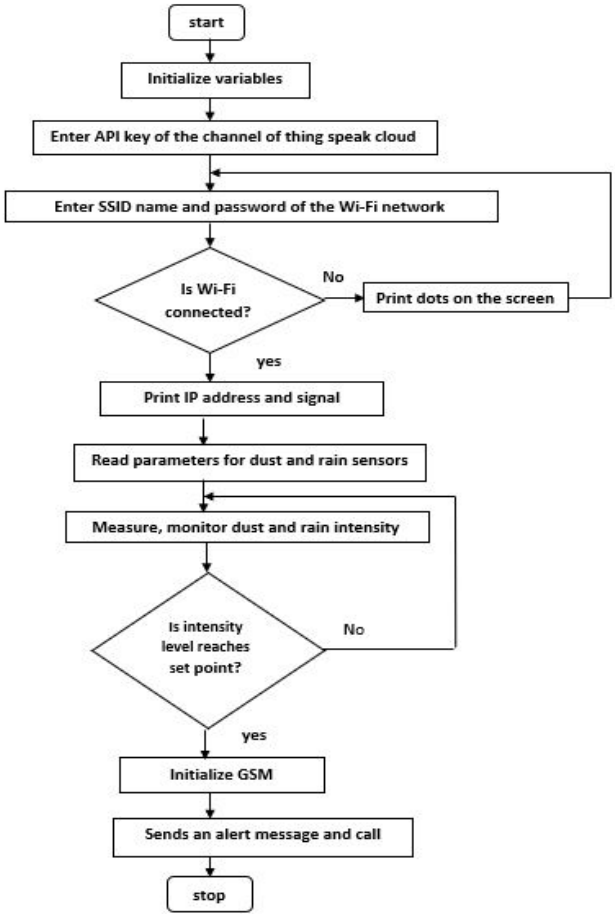

Fig.9. Flowchart for the present developed work

VI. I-V Characteristics of Solar Panel

Various experiments were conducted on a solar panel with dirt and without dirt to test the solar panel. In all these conducted experiments powder was used to emulate the debris/dust on the PV panel surface, the entire tests were conducted by measuring both voltage and current characteristics of the chosen solar panel with dust and without dust and also after cleaning the dust. The below figures illustrate the tested solar panel experimental setup. The total power of the solar panel was obtained by calculating the values of output current and voltage from the dusty, undusted, and cleaned surface of the selected solar panel for every one hour as indicated in the table using Equation (1)

$$P=VxI \quad (1)$$

VII. Results and Analysis

"Fig.10", shows the I-V characteristics of the surface with dust, with no dust, and cleaned surfaces of the solar panel using Origin software. Table II shows that the current dropped nearly 50% when the panel surface was dusty. The total power generated by the solar panel linearly decreased with the current reduction as shown in Table III. Then the surface cleaning was done by using the wiper. After cleaning, the current increased almost by 50%.

TABLE II: Measured Output Voltage and Current of the selected Solar Panel

Time	No Dust V(v) I(mA)		With Dust		After Cleaning	
			V(v)	*I(mA)*	*V(v)*	*I(mA)*
11:30 am	18.03	124.35	18.03	60.84	18.03	122.67
12:30 pm	18.09	132.13	18.09	66.78	18.09	139.33
1:30 pm	19.13	138.77	19.13	66.91	19.13	140.42
2:30 pm	19.01	130.24	19.01	59.89	19.01	129.32

TABLE III: Calculated total output Power in different conditions of tested Solar Panel

Time	P(W)		
	No Dust	*With Dust*	*After Cleaning*
11:30 am	2242.0305	1096.9452	2211.7401
12:30 pm	2390.2317	1208.0502	2520.4797
13:30 pm	2654.6701	1279.9883	2686.2346
14:30 pm	2475.8624	1138.5089	2458.3732

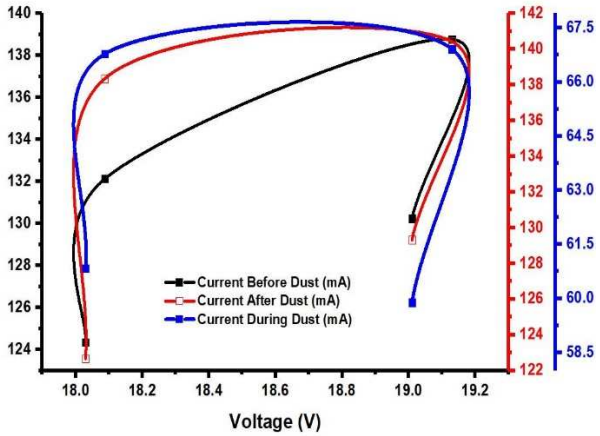

Fig.10. Voltage(V) versus Current(mA) Characteristics

VIII. Conclusion

A Low-cost, continual monitoring of solar panel cleaning system with GeoTagging approach was developed. The present system has a good capability to monitor continuously dust and rain on the Photovoltaic panel surface using the respective sensor and the data is uploaded to the ThingSpeak cloud and Thing view application on mobile for real-time observations and also an alert and call goes to the user using GSM the entire system can be composed of with very fewer hardware components with minimum power utilization as it becomes robust and affordable.

ACKNOWLEDGMENT

K. Evangili supriya and the Authors are extremely grateful to the Department of Science and Technology (DST), New Delhi, for sanctioning the INSPIRE fellowship and also thankful to DST for approving the FIST program in establishing the VLSI Lab in the Department of Physics.

REFERENCES

1. K.Abdul Khadar, K.Sai Ganesh, E.Sai Preetham, S.Chandra Shekar, Dr.PB.Venkateswara Rao, "Automatic Cleaning System Using IoT: IJCRT 2021, Vol .9, No.6, pp.337-339, June 2021.
2. Abhiraj Dumanwal, Adithya Ghangare, Akash Mithe, Shubum Parashar, "Solar Panel Cleaning Model Using Internet of Things", Vol.4, No.3, pp:17-20, March 2019.
3. Rajesh Gawai, Raghav Baheti, Apar Shambharkar, Devesh Patil, "Automatic Cleaning of Solar Panel and online monitoring the efficiency using IoT, Vol.17, No.10, October 2020, ISSN: 2395-0072, pp: 1446-1451.
4. Prathiba SR, Anupama Hongal, Jyothi MP, "IoT based Monitoring system in smart agriculture", 2017 International Conference on Recent Advances in Electronics and Communication Technology, Bangalore, India, pp:81-84, March, 2017.
5. .Faridah Hanim Mond Noh, Mohamad Faizal Yaakub, Ili Najaa, Aimi Muhd Nordin, Norain Sahari, Nor Aira Zambari, Sim Sy Yi Muhammad Syukri Mohd Saigon, "Development of Solar Panel Cleaning robot using Arduino", Indonesian Journal of Electrical Engineering and Computer Science, Vol.19, No.3, pp:1245-1250, September 2020.
6. Hussein A.Mohammed, Bahia A.M.Al-Hilli, Intisar Shaded Al-Mejibli, "Smart system for dust detecting and removing solar cells", The sixth scientific conference "Renewable Energy and its Applications, IOP conference series: Journal of Physics: Conference Series, Karabala, Iraq, Vol.1032, pp:1-8, February 2018.
7. Md.Rawshan Habib, Md Shahnewaz Tanvir, Ahmed Yusuf Suhan, Abhishek Vadher, Sanim Alam, Tahsirna Tashrif Shawnee, Kowshik Ahmed, Abdelrahman Alrashed, "Automatic Solar Panel Cleaning System based on Arduino for dust removal", Proceedings of the International Conference on Artificial Intelligence and Smart Systems (ICAIS-2021),IEEE Xplore,Coimbatore, India, March 2021, pp:1555-1558.
8. Santhosh Kumar S, Shivasahankar, Keshava Murthy, "Solar Powered PV Panel Cleaning Robot", 2020 5th International Conference on Recent trends on Electronics, Information, Communication, and Technology (RTEICT-2020), Bangalore, India, pp:169-172, November 2020.
9. N.Sugiartha, IGN Ardana, IM Sugina, IBG Widiantara, In Suprata, IK Adi, "Preliminary Design and Test of a Water Spray Solar Panel Cleaning system", International Conference on Applied Science and Technology , Journal of Physics: Conference Series, Bali, Indonesia,, Vol.1450, pp:1-7. October 2019.
10. Ruben Usamentiaga, Alberto Fernadez, Juan Luis Carus, "Evaluation of dust deposition on parabolic Trough collectors in the Visible and Infrared Spectrum," Sensors, Vol 20,No.21, pp: 1-20, November 2021.
11. Yuliya Zatsarinmaya, Denis Amiror, Maksim Elaev, "Solar Panel Cleaning System based on the Arduino Microcontroller", 2020 Ural Smart Energy Conference (USEC), Russia, pp.17-20, Nov 2020,
12. CC3200 Simple LinkTM Wi-Fi and Internet-of-Things Solution, a Single-Chip Wireless MCU. http://www.ti.com/lit/ds/symlink/CC3200.pdf. Accessed January 2022.
13. GP2Y1010AUOF Optical Dust Sensor. Accessed February 2022. https://www.sparkfun.com/datasheets/Sensors/gp2y1010au_e.pdf.
14. RainsensorYL63.https://www.openhacks.com/uploadproductos/rain_sensor_module.pdf. Accessed 15 Sept 2019.
15. Servo motor Datasheet http://www.ee.ic.ac.uk/pcheung/teaching/DE1_EE/stores/sg90_datasheet.pdf. Accessed February 2022.
16. Javad Farrokhi Derakhshandeh, Rand AlLuqman, Shahad Mohammad, Haya AlHussain, Ghanima AlHendi, Dalal AlEid, Zainab Ahmad "A comprehensive review of automatic cleaning systems of solar panels", sustainable Energy Technologies and Assessments, Vol 47, pp:1-15, October 2021.
17. SIM900A GSM module datasheet. https://www.rhydolabz.com/documents/gps_gsm/sim900_rs232_gsm_modem_opn.pdf. Accessed February 2022.
18. Thing Speak. https://thingspeak.com/. Accessed January 2022.
19. Energia. https://energia.nu/. Accessed January 2022.

AC Publications
Research English Journal (REJ)
Vol-8, Issue-4, 2022

Colonialism and its Impact on Indian Novels

G.Sashi kumar.,Professor of English, Humanities and Sciences,

G. Pullaiah College of Engineering and Technology (Autonomous), Nandikotkur Road Kurnool, Andhra Pradesh.

Paper Received on 02-11-2022, Accepted on 29-12-2022,
Published on 30-12-22; DOI: 10.36993/ RJOE.2023.7.4.39

Abstract: The literature landscape in India during the pre- and post-independence periods showcased a significant evolution in both content and style. Writers like Mulk Raj Anand, R.K. Narayan, and Raja Rao were pioneers in addressing the social and national issues prevalent in their times, especially during the pre-independence era. Their novels reflected the changing socio- political dynamics of India under colonial rule. In the pre-independence phase, theseauthors delved into themes related to social injustices, the caste system, rural life, and the struggle for independence. Mulk Raj Anand, for instance, wrote extensively about the exploitation faced by various marginalized groups such as untouchables, landless peasants, and industrial laborers. Novels like "Untouchable," "Coolie," "Two Leaves and A Bud," and "The Village" shed light on these societal issues and served as catalysts for social reform. The post- independence period witnessed a paradigm shift in the themes and styles of Indian English fiction. Authors like Mulk Raj Anand continued their focus on social reform, emphasizing the need for addressing prevailing social evils. Additionally, writers like G.V. Desai and Bhavani Bhattacharya contributed works that explored the realms of social realism and the socio-economic impacts of events like the Bengal famine. The postcolonial era saw the emergence of many female novelists in Indian English fiction who made significant contributions to the literary landscape. Writers such as Anita Desai, Arundhati Roy, Jhumpa Lahiri, Shobha De, Kamala Markandaya, Nayantara Sahgal, and Kiran Desai became known for their unique storytelling, exploring diversethemes ranging from familial relationships to societal changes and cultural complexities. These women novelists carved their niches by depicting varied facets of Indian society, their narratives often reflecting the struggles, aspirations, and identities of individuals within the context of a changing, post-independence India. Their works contributed immensely to the rich tapestry of Indian literature, showcasing the diverse voices and perspectives within the nation's literary canon.

Keywords: Postcolonial, oppression, nation, genre, novelists etc.

Postcolonial literature indeed encapsulates a significant phase in the history of nations that were formerly colonized. It represents a distinct body of literary work that shares commonalities despite emerging from various decolonized countries. This genre of literature examines the aftermath of colonialism, exploring

Postcolonial literature, through its narratives,

aims to reconstruct and re-envision history, offering alternative perspectives and reclaiming the dignity of nations and cultures that were previously subjugated. It highlights the cultural differences between native cultures and those of the imperial powers, aiming to restore pride, celebrate indigenous values, and address the complexities of cultural assimilation and resistance. Ultimately, it serves as a means to assert and preserve the distinct identities and narratives of formerly colonized nations. The issue of language and its connection to cultural expression and identity is a fundamental aspect of postcolonial literature. Raja Rao's insightful observation underscores the challenge faced by writers from colonized nations when using a foreign language, particularly English, to articulate their cultural and social heritage. Rao emphasizes the dilemma of expressing one's cultural essence authentically within the constraints of a language that belongs to the colonizers. Rao's statement reflects a sentiment shared by many postcolonial writers who grappled with the idea of writingin English, a language imposed by the colonizers. Rao

Rushdie's notion of "decolonizing" the language aligns with the endeavor of many postcolonial writers who strive to reshape English to represent their own identities and cultural landscapes authentically. This pursuit adds vitality and excitement to the literature of regions like Africa, the Caribbean, and India, infusing their narratives with a fresh, diverse, and inclusive perspective that breaks away from the colonial past and asserts their unique cultural identities.

In the realm of postcolonial literature in India, writers grappled with and portrayed numerous societal issues deeply entrenched in the fabric of Indian society. These issues included social evils such as Sati (thepractice of widow burning), the caste system, restrictions on widow remarriage, religious and social hegemony, among others. The focus of many writers during thisperiod, across various Indian vernaculars, was to raise awareness among the populace about the detrimental consequences of these entrenched evils.

INTERNATIONAL JOURNAL OF ENGLISH LANGUAGE, LITERATURE AND TRANSLATION STUDIES (IJELR)
A QUARTERLY, INDEXED, REFEREED AND PEER REVIEWED OPEN ACCESS INTERNATIONAL JOURNAL
http://www.ijelr.in (Impact Factor: 5.9735) (ICI)

RESEARCH ARTICLE

Vol. 10. Issue.1. 2022(Jan-March)

INTERNATIONAL STANDARD SERIAL NUMBER INDIA
2395-2628(Print):2349-9451(online)

TRACING THE INTRICACIES OF DISPLACEMENT IN ABDULRAZAK GURNAH'S NOVEL *BY THE SEA*

G. Sashi kumar.

Professor of English, Humanities and Sciences, G. Pullaiah College of Engineering and Technology (Autonomous), Nandikotkur Road Kurnool, Andhra Pradesh.

Article information
Article Received:13/1/2022
Article Accepted:15/02/2022
Published online:21/02/2022

ABSTRACT

This study enquires into Abdulrazak Gurnah's "*By The Sea*," which unearths the profound impact of post-colonial displacement on human life. Gurnah is a well-respected contemporary author, and his sixth novel portrays the devastating effects of colonialism on native people. The story is set in Zanzibar Island, where the British exerted their dominance, leading to conflicts with the local inhabitants. Through the first-person narratives of Saleh Omer and Latif Mahmud, two characters who were forced to leave their homeland and settle in new countries, the novel depicts their struggles with identity crisis, lack of physical and mental security, and existentialism. Despite their different backgrounds, Omer and Latif form a new relationship and seek friendship and camaraderie with each other. This novel serves as a powerful reminder of the brutalities of imperialism and the struggles faced by those who have been displaced from their homes.

Keywords: conflict, colonialism, displacement, home, language.

The depiction of inner conflict in literary works is a complex interweaving of various elements. Inner conflict is a universal human concern that cannot be ignored. As Robert Frost said, "Yet knowing how way leads on to way, I doubted if I should ever come back" (Frost, 93), which shows how Frost was uncertain about the right path to choose. Similarly, Gurnah's characters demonstrate a central conflict in their actions. Displacement is a central issue in postcolonial literature, and Gurnah's depiction of these concerns and his realistic portrayal of his fiction are highly commendable. In his novels, he writes, "In the darkness, I lose a sense of space, and in this nowhere, I feel myself more solidly" (*By the Sea*, 1).

The concept of 'home' seems simple at first glance. It represents a sense of security and familiarity that is important to humans. This idea has been reinforced by humanitarian efforts emphasizing the importance of having a stable home for individuals. However, in postcolonial theory, the idea of 'home' has problematic implications because it has become associated with exclusionary nationalism. This is evident in the rhetoric surrounding anti-immigration sentiments and postcolonial nation-building. The use of the idea of home in such contexts can be hegemonic or essentializing. Partha Chatterjee asserts in Scripting *The Nation and its Fragments*, that home is “not a complimentary but rather the original site on which the hegemonic project of nationalism

Available online at www.jilile.in

OF INDIAN LANGUAGESAND INDIAN LITERATURE IN ENGLISH

Journal of Indian languages and Indian literature in English, 01(08), 58-63; 2021 ISSN 2178-9229

CUSTOMS OF THE PAST AND CULTURAL PRACTICES OF THE PRESENT IN THE SELECT NOVELS OF MANJU KAPUR

M. Sridevi.

.Assistant Professor of English, Humanities and Sciences, G. Pullaiah College of Engineering and Technology (Autonomous), Nandikotkur Road Kurnool, Andhra Pradesh.

Submission Date: 15/01/2021
Acceptance Date: 25/01/2021

Abstract

Tradition refers to the customs, beliefs and cultural practices that are passed down from one generation to the next generation. The word 'tradition' itself derives from the Latin 'traditio', the noun from the verb 'tradere' literally meaning to transmit, to hand over or to give for safekeeping.It has its origin in the past. Modernity refers to the contemporary behavior or the way of doing things. It is fresh, new and modern. Tradition and Modernity both prevail together in India. Indianculture is a blend of traditional values and the modern spirit. Tradition and modernity are two terms used to express an entire range of differences between distant development stages in a society. Tradition will always refer to the ways of the past and modernity to what is happening now or will soon happen. Hence, it is quite natural for elders to lean towards tradition whereas young people usually propagate modernity as the better option. The question is though - do we really have to choose? Traditional approach represents ethics, religion, widely acceptable behavioral patterns which for many, means a lot. Young people tend to stray from this path praising the modern - liberal ways above the traditional approach. On the other hand, religion and tradition is full of ideas which are not applicable to modern societies and they cannot be fully transferred. Why? Because people live in a completely unique way nowadays, they are more conscious and well-educated. At the same time, some of the modernists go so far in their struggle for 'the new' that they produce ridiculous ideas. They might seem interesting but they are not valuable nor viable.

Keywords: AMITAV GHOSH, women, oppression, equality of rights, democracy, society and changes

ISSN 2178-9529
Galaxy: International Multidisciplinary Research Journal
www.galaxyimrj.com

Empowerment of Women in Shani Mootoo's *Valmiki's Daughter*

M. Sridevi.

.Assistant Professor of English, Humanities and Sciences, G. Pullaiah College of Engineering and Technology (Autonomous), Nandikotkur Road Kurnool, Andhra Pradesh.

Article History: Submitted-03/03/2021, Revised-30/11/2021, Accepted-25/12/2021, Published-31/12/2021.

Abstract:

The present paper "Predicament of Women in Shani Mootoo"s *Valmiki's Daughter*" will try to understand the different standpoints of feminism in Indian diaspora. Shani Mooto is very much vocal to women issues and their predicament in diasporic society. She has given very strong voice to her women characters to challenge the long rooted inequalities and marginalisation of women. In Indian diaspora, many Hindu families follow their culture and traditions but sometime it affect the women who have modern views. Mootoo's character Vasti in *Valmiki's Daughter* never follow traditional path like her sister. She also shows her feminist attitude to her family. Thus, predicament and marginalisation of women and their strong voices to fight against unjust activities will be critically discussed in this paper

Keywords: Indian Diaspora, Women Predicament, Marginalisation, Oppression, Feminism.

Introduction

South Asian diasporic writer Shani Mootoo was born in Dublin 1958, Ireland, spent most of the early time in Trinidad and later move to Canada, settled there, and started her career as visual artist and also enjoying a gifted career as a writer. Most of the fictional work of Mootoo has portrayed the lives immigrants and especially women immigrants in Caribbean Island and Canada who have been oppressed by the cultural and traditional norms in the society. Shani Mootoo also went through such kind of oppression and abuse in her life. The central themes of the works of Mootoo are gender, race, culture and sexual orientations among the migrant communities. She has individually double and by community triple, diasporic experiences that clearly visible in her writing. Her *Out on Main Street* is first collection of short

INTERNATIONAL JOURNAL OF ENGLISH LANGUAGE, LITERATURE AND TRANSLATION STUDIES (IJELR)
A QUARTERLY, INDEXED, REFEREED AND PEER REVIEWED OPEN ACCESS INTERNATIONAL JOURNAL
http://www.ijelr.in

RESEARCH ARTICLE

ISSN-2349-9451

Vol.2.Issue.1.,2021

CRITICAL STUDY IN MAINLAND CHINA OVER THE PAST DECADE ON CORRELATIONS WITH ENGLISH LEARNING STRATEGIES OF CHINESE EFL LEARNERS

Syeda Ayesha Jahan.

Assistant Professor of English, Humanities and Sciences, G. Pullaiah College of Engineering and Technology (Autonomous), Nandikotkur Road Kurnool, Andhra Pradesh.

Article Info:
Article Received:09/02/2021
Revised on: 18/02/2021
Accepted on: 23/02/2021

ABSTRACT

This article reviews the empirical studies (investigations by means of questionnaire or experiment) in mainland China over the past decade on correlations with English learning strategies employed by Chinese EFL learners. The correlations in this review mainly include the correlations between the learners' strategies and their gender differences, between their strategies and their English achievement or proficiency, and between their strategies and strategies-based instruction.

Key Words: English learning strategy; empirical study; correlation; Chinese EFL learner.

.

INTRODUCTION :

The past 30 years has seen in China a gradual shift within the field of foreign language learning and teaching with great emphasis being put on EFL learners and learning rather than teachers and teaching. With this gradual shift of interest in EFL learning and teaching, EFL researchers have showed great interest in how EFL learners process new information in their input materials (i.e. how they understand, learn, remember and use what they have learned from their reading and listening materials), and how they approach the tasks or problems they encounter in their EFL learning (i.e. what strategies they employ).

It is Rubin (1975) that drew the public attention to the customary learning behavior of the "good language learner". With the movement in the field of education, where emphasis had been placed on the learner's autonomous or independent learning, the field of second language acquisition and foreign language learning has seen a thriving branch of research on language learning strategies. Oxford (1990), O'Malley and Chamot

DOI: https://doi.org/11.52131/pjhss.2023.1102.0481

Pakistan Journal of Humanities and Social Sciences

Volume 10, Number 02, 2023, Pages 1786–1791
Journal Homepage:
https://journals.internationalrasd.org/index.php/pjhss

A Feminist Analysis of Virginia Woolf's A Room of One's Own

Syeda Ayesha Jahan

Assistant Professor of English, Humanities and Sciences, G. Pullaiah College of Engineering and Technology (Autonomous), Nandikotkur Road Kurnool, Andhra Pradesh.

ARTICLE INFO

Article History:
Received: May 09, 2021
Revised: June 19, 2021
Accepted: June 20, 2021
Available Online: June 21, 2021

Keywords:
Feminist Style
Gender-Specific
Perspective
Characteristics
Word
Sentence
Discourse

Funding:
This research received no specific grant from any funding agency in the public, commercial, or not-for-profit sectors.

ABSTRACT

This research paper explores the application of feminist stylistic analysis to Virginia Woolf's novel, A Room of One's Own. Using the theoretical framework of feminist literary criticism, this study examines the ways in which Woolf uses language and style to convey her feminist message. The research draws on close reading and textual analysis of selected passages from the novel, and employs feminist theories of language, gender, and power to interpret the meaning and significance of these stylistic choices. The findings of this study suggest that Woolf's use of language and style is crucial to her feminist message, and that it serves to challenge traditional gender roles and patriarchal power structures. Overall, this research contributes to our understanding of the intersection between feminist theory and literary analysis, and demonstrates the value of applying feminist stylistic analysis to works of literature.

1. Introduction

A Room of One's Own is a novel written by Virginia Woolf in 1929. In the essay, Woolf explores the societal and institutional barriers that have prevented women from achieving their full potential as writers and artists. The title itself is a metaphor for the physical and psychological space that women need in order to create and develop their artistic talents. Woolf argues that women have been historically excluded from the literary canon, and that this exclusion has been due to a lack of economic and social opportunities. She suggests that in order for women to succeed as writers, they must have access to education, financial independence, and a room of their own in which to work.

Woolf uses her characteristic stream-of-consciousness style to explore the ways in which societal expectations and gender roles have limited women's artistic expression. She argues that women have been forced to conform to male standards of writing, and that this has resulted in a lack of diversity and creativity in literature. Woolf suggests that in order to achieve gender equality in literature, women must be allowed to write in their own voices and explore their own experiences.

A Room of One's Own has become a seminal work in feminist literary criticism and has had a lasting impact on the way that literature is studied and taught. The essay's message about the importance of women's voices and experiences has been taken up by generations of feminist writers and scholars, and it continues to inspire women to pursue their artistic passions and ambitions. The study of feminist stylistic analysis of A Room of One's Own by Virginia Woolf is situated within the broader field of feminist literary criticism. This field emerged in the 1960s and 1970s as a response to the lack of attention given to women writers in traditional literary criticism. Feminist literary critics sought to uncover the ways in which literary works reflect and perpetuate gender stereotypes, and to promote the study of women's literature.

Research Journal of English Language and Literature (RJELAL)
A Peer Reviewed (Refereed) International Journal
Impact Factor 6.8992 (ICI) http://www.rjelal.com;
Email:editorrjelal@gmail.com; ISSN:2295-2636 (P); 2321-3108(O)

Vol.11.Issue 1. 2021 (Jan-March)

RESEARCH ARTICLE

INTERNATIONAL STANDARD SERIAL NUMBER INDIA
2395-2636 (Print):2321-3108 (online)

CONTRASTIVE PORTRAYAL OF GLOBAL SOUTH IN THE FICTIONS OF ARUNDHATI ROY AND ARAVIND ADIGA

Dr.T.Sujatha

Sr.Assistant Professor of English, Humanities and Sciences, G. Pullaiah College of Engineering and Technology (Autonomous), Nandikotkur Road Kurnool, Andhra Pradesh.

DOI: 10.33329/rjelal.12.2.44

Article info
Article Received:03/01/2024
Article Accepted: 20/01/2024
Published online:26/01/2024

Abstract

The East-West binary, once seemingly defined by the Cold War's stark opposition, now manifests in a fragmented landscape of proxy conflicts like Syria, Ukraine, and Israel. Amidst this pro-West and anti-West narrative, the Global South remains largely unheard, its diverse voices silenced and its struggles obscured by the clash of superpowers. This paper argues that Arundhati Roy and Aravind Adiga, through their literary works, provide a crucial counterpoint to this simplified narrative, offering a platform for subaltern voices from the Global South to be heard and understood. For instance, Roy's *The God of Small Things* exposes the devastating impact of neo-colonial development projects on Kerala's marginalized communities, mirroring real-life conflicts. Parallelly, Adiga's *The White Tiger* offers a scathing critique of economic inequality and the exploitation of India's underclass, influenced by the neoliberal economic model, highlighting their struggles for upward mobility within a rigged system. This paper is not just only about portraying marginalized narratives but it attempts to analyze and understand the impact of the hegemonic discourse of counter-narrative of the East-West conflict of the superpowers on the suppressed entities of Global southern communities. Applying Dependency theory in contrast with Post Development theory to the literary works of these two authors, it is to be verified here that the way Global South is exploited, oppressed, and remains unheard in the conflict of capitalist and autocratic superpowers. Focusing on two authors and a limited selection of works inherently limits this analysis of the vast and diverse Global South. While insightful, their narratives cannot encompass all voices and experiences within this region.

Keywords: - Global South, Subaltern Voices, Dependency Theory, Post-development Theory, Core, Periphery, Modernity, Local Knowledge, Ecology, Westernization, Neoliberalism, Marxism, Neocolonialism.

Introduction

Literature on the Global South encompasses diverse voices, narratives, and perspectives emerging from regions historically marginalized in the global discourse. Writers from Africa, Latin America, Asia, and the Middle East have produced

ISSN Online : 2709-4030
ISSN Print : 2709-4022
Vol.7 No.1 2021

Guilt along with Transgression-Inner Suffering of Transgenders in Arundhati Roy's *The Ministry of Utmost* Happiness

Dr.T.Sujatha

Sr.Assistant Professor of English, Humanities and Sciences, G. Pullaiah College of Engineering and Technology (Autonomous), Nandikotkur Road Kurnool, Andhra Pradesh.

Abstract

The present study centers on the life of transgender which is full of distress experiences throughout her life in Arundhati Roy‟s novel, *The Ministry of Utmost Happiness*. The novel explores many narratives that focus on the exploitation and pain experienced by transgender individuals, particularly with reference to Guilt and Transgression-Inner Suffering. In South Asian civilization, transgender individuals are classified as a distinct third gender. Specifically, in Indian society, transgender individuals are deprived of their rights and subjected to exploitation and the perpetuation of many stereotypical portrayals led the characters to guilt and transgression-inner suffering. Therefore, they are subjected to ridicule and mockery, with people using various derogatory terms to simplify and categorize them. An identical representation has been given and undertaken in the present study to examine the mistreatment and anguish experiences of transgender individuals in Arundhati Roy‟s novel, *The Ministry of Utmost Happiness*. Close textual analysis has been employed as a methodology to examine the primary text in order to investigate the exploitation and anguish experienced by transgender individuals leading to guilt and transgress-inner suffering. The researcher has determined that the suffering and exploitation of transgender individuals are the result of societal causes, as well as the strong presence of inner distress. The research indicates that transgender individuals are marginalized in Indian

INTERNATIONAL JOURNAL OF ENGLISH LANGUAGE, LITERATURE AND TRANSLATION STUDIES (IJELR)
A QUARTERLY, INDEXED, REFEREED AND PEER REVIEWED OPEN ACCESS INTERNATIONAL JOURNAL
http://www.ijelr.in

RESEARCH ARTICLE

ISSN-2 3 4 9 - 9 4 5 1

Vol.2.Issue.1.,2021

AN ECOCRITICAL STUDY OF *CAPTAIN OF THE SLEEPERS* BY MAYRA MONTERO

K.Santhosh Reddy.

Assistant Professor of English, Humanities and Sciences, G. Pullaiah College of Engineering and Technology (Autonomous), Nandikotkur Road Kurnool, Andhra Pradesh.

ABSTRACT

Captain of the sleepers (CS) by Mayra Montero is a tale about Andres yasin and his family. The island inhabited by the natives is later occupied by the navy, who cause innumerable troubles to the islanders in the name of military exercise. Accompanying the main plot is the story line of Estela's affair with a man which disturbs the mind of her son, Andres immensely as it leads him to meet J.T.Bunker after fifty years to know the truth of the affair. This paper brings to the forefront the complex problems of expropriation, the devastation done to the ecology, including the turbulences the human inhabitants of the island faces. And focus vividly on the degradation of the natural resources in the Vieques Island by the Marines, in the name of military exercises.

Keywords: Ecocriticism, Anthropocentricism, Pacifist Feminism and Environmental degradation.

Article Info:
Article Received:12/02/2015
Revised on: 18/02/2015
Accepted on: 22/02/2015

Captain of the sleepers has been published in 2002 and translated, then published in U.S. in the year 2005. It is story which revolves around Andres Yasin and his family members in the Island of Vieques during the nationalist movement in Puerto Rico in 1950's, and later in the year 2000 when the boy is portrayed as an adult, who goes to meet the captain to know the mysterious around his mother's life and death because of the affairs. The chapters keep on alternating between the past and the present. In his sixty two years oldness Andres Yasin comes to the island called St. Croix. This particular island and the hotel where he stays act as a medium in retrieving his memory about the incident that has happened in this island, and the island of Vieques inhabited by his family, in his childhood days. The novel shifts to the past. In doing so, he narrates each and every scene that revives back in his mind in full form - his past life in Vieques Island with his mother Estela, father Frank and J.T.Bunker - friend of Frank also known as captain are recollected.

©KYcPUBLICATIONS
http:www.ijelr.in
A Peer Reviewed & Refereed Journal

Vol.1. Issue.1:2021
Research Article
Open Access Journal

INTERNATIONAL JOURNAL OF ENGLISH LANGUAGE, LITERATURE AND TRANSLATION STUDIES (IJELR)

INDIRA GOSWAMI'S *THE UNFINISHED AUTOBIOGRAPHY:* MELANCHOLIC DOOM OF WIDOWS IN THE TRAP OF CREDENDA

K.Santhosh Redddy

Assistant Professor of English, Humanities and Sciences, G. Pullaiah College of Engineering and Technology (Autonomous), Nandikotkur Road Kurnool, Andhra Pradesh.

Article Received on:16-06-2021
Article revised on: 18-07-2021
Accepted on:20-07-2021

ABSTRACT: Goswami's works focuses on several facets of women's empowerment in India. Her stories deal with the lives of women and their problems. Her book *Neelkantha Braja* was one of the earliest works of Indian literature to highlight the exploitation of destitute widows in Brindavan. The plight of widows in Hindu society, oppression, suppression and exploitation of girls were main themes of her novels. The paper seriously attempt to bring out the melancholic doom of widows in the trap of credenda of Indira Goswamy's autobiography.

Key words: Love, marriage, sex and widow

Indira Goswami was known as Mamoni Raisom Goswami and popularly as Mamoni Baideo. She was an Assamese editor, poet, teacher, scholar, professor, writer and peace adorer. Her works are published in Assamese and English. She was encouraged by Kirti Nath Hazarika who published her first short stories. Her work *The Moth Eaten Howdah of a Tusker* is considered as one of the best works in Indian literature. It is a classic in Assamese literature and about the plight of Brahmin widows in Sattras of Assam. Amrita Pritam regarding *The Moth Eaten Howdah of a Tusker* says that "Indira Goswami is one of those rare souls who have been able to get an insight into the great power which is working behind this universe. In turn the endeavor to grapple with that finds reflection in this book and lends strength to it…This power that this metamorphosis has bestowed upon her has now became a matter of pride for every Assamese women" (vi). Goswami got the Sahitya Akademi Award in 1983 for the novel *The Rusted Sword*. Her novel *Pages Stained with Blood* is about the bloody anti-Sikh riots in Delhi. She focuses on the problems of women from different aspect. Regarding Indira Goswami, Preeti Gill says, "… to me she was very much a feminist writer stating her views strongly and effectively in story after story and engaging with the social injustices and the inequalities she encountered" (Goswami, 2012: 121).

There are a few Indian women auto-biographers who have given about their regional language. She is one among them. Her autobiography *Adhalekha Dastaveja* which was published in 1988 and later on it was translated into English as *The Unfinished Autobiography.* A journalist called Homen Borgohain invited her to write an autobiography of her in his weekly newspaper 'Nilachal.' She wrote under the pen name Mamoni Raisom Goswami. Many people think that autobiographies are only commercial but it is not true always. They are written to describe the writer's experiences in a sincere way. Sodhi (1999: 13) rightly says that "It is a revelation and a "re-creation of the self." It is very important for women writers, as they have faced uncountable problems from society such as gender discrimination, oppression and sexual exploitation. Women

©KS PUBLICATIONS
http:www.ijelr.in
A Peer Reviewed & Refereed Journal

Vol.1. Issue.1:2021
Research Article
Open Access Journal

INTERNATIONAL JOURNAL OF ENGLISH LANGUAGE, LITERATURE AND TRANSLATION STUDIES (IJELR)

ASHIANA – THE HOUSE OF PRIVACY
ATTIAHOSAIN'S SUNLIGHT ON A BROKEN COLUMN

Mubeen Taj

.Assistant Professor of English, Humanities and Sciences, G. Pullaiah College of Engineering and Technology (Autonomous), Nandikotkur Road Kurnool, Andhra Pradesh.

Article Received on:19-06-2021
Article revised on: 22-07-2021
Accepted on:24-07-2021

ABSTRACT: 'Ashiana' is the name of the house in the novel Sunlight on a Broken Column written by Attia Hosain.It is about the women who lives in the four walls and the outer world is away for the woman because they remain in purdah.In Ashiana, there is a special place for women named asZenana, where the girls have been brought up by Aunt Abida. She takes the whole responsibility of bringing up Laila, the orphan and protagonist of the novel. is like a modern nuclear home. The traditional household gives women very limited access to the outside world because of Babbajan.

Key words: purdah, ashiana, zenana, nuclear

INTRODUCTION:

The purdah brings out the values of duty and responsibility, but the new generation using it for their selfish ends. 'Ashiana' is not just a house it made of stones, but it consists of different women characters who lead a different way of life .In its four walls one could get the experience of a whole nation fighting its political and personal battles. Babbajan holds them to confine in their own quarters and survive and purdah to display infront of male members that fosters when characters of different temperaments are grouped under a common roof. Attia Hosain appointed some of the characters who effectively depicted some of the situations in their roles. The outer world is away for the woman because they remain in the purdah, but they could see everything by hiding themselves in purdah. Her experience are perhaps more intense and evocative than she cares to exhibit – so many lives snuffed out within the purdah.

Zenana, a place for women: Sunlight on a Broken Column is about feudal power. The household generally divided according to the distribution of power. The architecture is designed to live with different spaces for men and women and it shows the house has two portions and a common corridor. The doors leading to the woman's quarters or the zenana are locked every night to be opened only the next day. The zenana included a courtyard which has an extended kitchen by the women during the time of festivities. Outside the house, has quarters for the servants of the household.

The Zenana also implies purdah, which means curtain.Uma Parameshwaran says:

©KC PUBLICATIONS
http:www.ijelr.in
A Peer Reviewed & Refereed

Vol.1. Issue.1:2021
Research
ArticleOpen Access

INTERNATIONAL JOURNAL OF ENGLISH LANGUAGE, LITERATURE AND TRANSLATION STUDIES (IJELR)

PATHOS OF THE POOR AND THE WEAK IN A. PARTHASARATHY'S 'THE RIVER OF BLOOD' TRANSLATED BY KA. NAA. SUBRAMANYAN

Mubeen Taj

.Assistant Professor of English, Humanities and Sciences, G. Pullaiah College of Engineering and Technology (Autonomous), Nandikotkur Road Kurnool, Andhra Pradesh.

Article Received on:17-06-2021
Article revised on: 19-07-2021
Accepted on:22-07-2021

ABSTRACT: *The River of Blood* by A. Parthasarathy is a replica of the then society where rich politicians implement their draconian law by setting fire to the houses of down trodden people who are neither supported by law nor safe guarders of law and order (police force). This pathetic situation is picturesquely portrayed in the novel. It is the case of suppression of the oppressed where domination leads on to dehumanization and takes its ruthless stance when the well to do leader Naidu turned antagonistic towards the people of the weaker sections. He plotted against all people who are in one way or the other related to the communist group.

Down trodden people and widows of low caste people are the ones who suffered a lot and have become the scapegoats for no fault of theirs. It is a satire on existing law and order which seem to be supporting the whims and fancies of rich people like Naidu. It is an example of how uncouth are the ways of rich in dismantling and dismembering the poor and helpless. Thus, it is the demonstration of the dominance of the rich and destruction of the weak.

Parthasarathy was born in 1930 in Chennai. He published about thirty-five novels, plays, short stories and essays. He received the Sahitya Akademi prize for *Kurudhippunal* (Blood Stream, 1977), the Saraswati Sammam Prize (1999), and the Sangeeth Natak Academy Award (2004) for his play *Ramanujar* (*Ramanujar: The Life and Times of Ramanujan*). Parthasarathy is one of the most eminent and critically acclaimed playwrights in Tamil and his work resonates with contemporary world trends: he has infused modern Tamil drama with vitality and sensibility drawn from both the Native and outside sources. In *Nandan Kathai* (The Story of Nandan) Parthasarathy depicts the stigmatized world of the Scheduled Caste Dalit communities and it not only challenges existing forms of Tamil theater, but also questions the socio-political situation in Tamil Nadu. In *Kongai Thee* (Kongai Fire) he portrays two female protagonists of the Tamil epic, Kannagai and Madhavi, and attempts a psychological study of characters. *Eruthi Attam* (The Last Dance), on the other hand, is an adaptation of Shakespeare's *King Lear* in the fashion of Beckett's *Endgame* as done by Peter Brooks in the London RSC production, based on Antonin Artaud's theater of cruelty.

The Mathematical Educator 9 (1): 73-77, 2022
ISSN 0218-9100

Disjoint Sets and its Application to Electrical Networks

N. Janaki
Department of Mathematics , G. Pullaiah college of Engineering & Technology.
Kurnool, Andhra Pradesh, India.

Abstract: Problem statement: One of the well known problems in Telecommunication and Electrical Power System is how to put Electrical Sensor Unit (ESU) in some various selected locations in the system. **Approach:** This problem was modeled as the vertex covering problems in graphs. The graph modeling of this problem as the minimum vertex covering set problem. **Results:** The degree covering set of a graph for every vertex is covered by the set minimum cardinality. The minimu of a graph cardinality of a degree covering set of a graph G is the degree covering number γP(G). **Conclusion:** We show that Degree Covering Set (DCS) problem is NP-complete. In this study, we also give a linear algorithm to solve the DCS for trees. In addition, we investigate theoretical properties of γP (*T*) in trees T.

Key words: Electrical Sensor Unit (ESU), vertex covering, Degree Covering Set (DCS), degree covering number, electrical networks, electrical power system, graph modeling

INTRODUCTION

At this moment we are dependable with the electivity power. The consumption of electricity is increasing every year. The electric power industries have to monitor carefully their system's state periodically as defined by a set of state variables (Ramos and Tahan, 2009; Kumkratug, 2010; Osuwa and Igwiro, 2010). One method of monitoring these variables is to place Electrical Sensor Unit (ESU) in some various selected locations in the system (Ahmadia *et al*., 2010). Because of the high cost of a ESU, it is desirable to minimize their number while maintaining the ability to monitor (observe) the entire system (Ketabi and Hosseini, 2008). We define a system is to be observed if all of the state of the system can be decided from a set of measurements.

Approach: Let G = (V, E) be a graph that modeled as an electrical system, where a vertex represents an electrical point (such as a electrical point of bus) and an edge represents a electrical line. The objective is how can we locate a smallest set of ESU to monitor the entire system is a graph theory problem closely related to the well-known minimum vertex covering problems. Hence, Electrical Sensor Unit (ESU) is not only of interest in the electrical engineering but also as a challenge problem in graph theory. For more discussion about covering and related subset problems as well as terminology not defined here, we encourage the reader to two books (Ramos and Tahan, 2009).

A ESU measures the state variable (voltage and phase angle) for the vertex at which it is placed and its incident edges and their end vertices. The other finding rules are as follows:

- We observed the incidences of vertices to edges
- We observed joining any edges

MATERIALS AND METHOD

For a given set of vertices P representing the nodes where the ESU are placed, the following algorithm determines the collection of collection of vertices C and edges F.

Let $P \subseteq V$ be the set of vertices where the ESU are placed:

- Initialize C = P and F = {e ∈ E(G) | e is incident to a vertex in P}
- Add to C any vertex not already in C which is incident to an edge in F
- Add to F any edge not already in F such that
  - Both of its end vertices are in C or
  - It is incident to a vertex v of degree greater than one for which all the other edges incident to v are in F
- If steps 2 and 3 fail to locate any new edges or vertices for inclusion, stop. Otherwise, go to step 2

The objective of the problem is to solve the electrical system, we want C = V(G) and F = E(G) and we want to minimize |P|. This monitoring problem was introduced and studied in (Pask *et al*., 2005; Katrenic and Semanisin, 2010).

Computational Methods for Differential Equations
http://cme.tabrizu.ac.ir
Vol. 11, No. 2, 2021, pp. 108-119

Solving Systems of Integro-Differential Equations

N. Janaki
G. Pullaiah College of Engineering & Technology.
Kurnool.
Andhra Pradesh.
India.

Abstract This paper has been devoted to apply the Reconstruction of Variational Iteration Method (RVIM) to handle the systems of integro-differential equations. RVIM has been induced with Laplace transform from the variational iteration method (VIM) which was developed from the Inokuti method. Actually, RVIM overcome to shortcoming of VIM method to determine the Lagrange multiplier. So that, RVIM method provides rapidly convergent successive approximations to the exact solution. The advantage of the RVIM in comparison with other methods is the simplicity of the computation without any restrictive assumptions. Numerical examples are presented to illustrate the procedure. Comparison with the homotopy perturbation method has also been pointed out.

Keywords. System of integro-differential equations, Volterra equation, Reconstruction of variational iteration method, Homotopy perturbation method.

2010 Mathematics Subject Classification. 34K30, 34A12, 45G15.

1. Introduction

Systems of integral equations, linear or nonlinear, appear in scientific applications in engineering, physics, chemistry and populations growth models[4-6, 14, 17]. Studies of systems of integral equations have attracted much concern in applied sciences. Volterra studied the hereditary influences when he was examining a population growth model. The research resulted in a specific topic, where both differential and integral operators appeared together in the same equation. This new type of equation is named as Volterra integro-differential equation, given in the form:

$$y^{(i)}(x) = f(x) + \int_0^x k(x,t)u(t)dt,$$

Generation for Two Dimensional Cutting Stock Problem

S. N. Chandrika , N. Janaki

G. Pullaiah College of Engineering and Technology, Kurnool, Andhra Pradesh, India

***Abstract* —— Selection of feasible cutting patterns in order to minimize the raw material wastage which is known as cutting stock problem has become a key factor of the success in today's competitive manufacturing industries. In this paper, solving a two-dimensional cutting stock problem is discussed. Our study is restricted to raw material (main sheet) in a rectangular shape, and cutting items are also considered as rectangular shape with known dimensions. The *Branch and Bound* approach in solving integer programming problems is used to solve the problem.**

***Keywords*— Two-Dimensional cutting stock problem, Cutting patterns, Branch and Bound algorithm**

I. INTRODUCTION

Minimizing wastage is a key factor in improving productivity of a manufacturing plant. Wastage can occur in many ways and cutting stock problem can be described under the raw material wastage. An optimum cutting stock problem can be defined as cutting a main sheet into smaller pieces while minimizing total wastage of the raw material or maximizing overall profit obtained by cutting smaller pieces from the main sheet. Many researchers have worked on the cutting stock problem and developed different algorithms to solve the problem. Among them, Hifi et al (2000) and Coromoto et al (2007) have made an approach to cut a large rectangular stock of known dimensions to *n* types of smaller rectangles of known dimensions. Hifi has made assumptions that all pieces have fixed orientation (i.e a piece of length *l* and width *w* is different from a piece of length *w* and width *l*, for all $l\ (\neq w)$, and all applied cuts are of guillotine type (a cut from one edge of the rectangle to the opposite edge which is parallel to the two remaining edges). Hifi developed a mathematical model to maximize overall profit by cutting smaller rectangular pieces from the large rectangular stock[1].

Also, Coromoto has used a *Parallel Algorithm* and *Sequential Algorithm* to solve the mathematical model which maximizes the total profit incurred by cutting *n* number of rectangular items from a large rectangular main sheet. Coromoto has made an observation that all cutting patterns can be obtained by means of horizontal and vertical builds of meta-rectangles and used *Viswanathan and Bagchi Algorithm* to produce best horizontal and vertical builds[2].

In addition to above two studies, many researchers have introduced different approaches to maximize the utilization area of the main sheet or to minimize the waste area of the main sheet, and have assumed both main sheet and smaller pieces are in rectangular shape with known dimensions[3,4,5]. There are different arrangements to cut required pieces from the existing raw material to maximize the used area. Each arrangement is defined as a cutting pattern. In this study, modified *Branch and Bound Algorithm* is presented and a computer program using Matlab software package is developed to generate feasible cutting patterns for two-dimensional cutting stock problem.

Bimagic Labeling for Disconnected Graphs

S. N. Chandrika, G. Siddesh Babu

Department of Mathematics, G. Pullaiah College of Engineering and Technology, Kurnool, Andhra Pradesh, India

*

Abstract— An edge magic total labeling of a graph $G(V,E)$ **with *p* vertices and *q* edges is a bijection *f* from the set of vertices and edges to** $1,2,...,$ p q **such that for every edge *uv* in *E*,** $f(u)+f(uv)+f(v)$ **is a constant *k*. If t here exist two constants** k_1 **and** k_2 **such that the above sum is either** k_1 **or** k_2**, it is said to be an edge bimagic total labeling. A total edge magic (edge bimagic) graph is called a super edge magic (super edge bimagic) if** $f(V(G))=\{1,2,...,\ p\}$**. A total edge magic (edge bimagic) graph is called a superior edge magic (superior edge bimagic) if** $f(E(G))=\{1,2,...,$ q$\}$**.In this paper we give magic and bimagic labelings for some class of disconnected graphs**

AMS Subject Classification: 05C78

Keyword- **graph, labeling, magic labeling, bimagic labeling, function.**

I. INTRODUCTION

A labeling of a graph *G* is an assignment *f* of labels to either the vertices or the edges or both subject to certain conditions. Labeled graphs are becoming an increasingly useful family of Mathematical Models from a broad range of applications. Graph labeling was first introduced in the late 1960's. A useful survey on graph labeling by J.A. Gallian (2011) can be found in [1]. All graphs considered here are finite, simple and undirected. We follow the notation and terminology of [2]. In most applications labels are positive (or nonnegative) integers, though in general real numbers could be used. A (*p, q*)-graph $G=(V,E)$ with *p* vertices and *q* edges is called total edge magic if there is a bijection $f:V\cup E\to\{1,2,...,p+q\}$ such that there exists a constant *k* for any edge *uv* in *E*, $f(u)+f(uv)+f(v)=k$. The original concept of total edge-magic graph is due to Kotzig and Rosa[3]. They called it magic graph. A total edge-magic graph is called a super edge-magic if $f(V(G))=\{1,2,...,\ p\}$. Wallis [4] called super edge-magic as strongly edge-magic.

It becomes interesting when we arrive with magic type labeling summing to exactly two distinct constants say k_1 or k_2. Edge bimagic totally labeling was introduced by J.Baskar Babujee [5] and studied in [6] as (1,1) edge bimagic labeling. A graph G p q(,) with p vertices and q edges is called total edge bimagic if there exists a bijection $f:V\cup E\to\{1,2,...,p+q\}$. such that for any edge $uv\in E$, we have two constants k_1 and k_2 with $f(u)+f(v)+f(uv)=k_1$ or k_2. A total edge-bimagic graph is called *super edge-bimagic* if $f(V(G))=\{1,2,...,\ p\}$. *S*uper edge-bimagic labeling for path, star- $K_{1,n}, K_{1,n,n}$ are proved in [7]. *S*uper edge-bimagic labeling for cycles, Wheel graph, Fan graph, Gear graph, Maximal Planar class-Pl_n: $n\geq 5$, $K_{1,\ m}\cup K_{1,\ n}(m,n\geq 1), P_n\cup P_{n+1}(n\geq 2)$, $C_3\cup K_{1,n}(n\geq 1), P_n+N_2(n\geq 3), P_2\cup mK_1+N_2)(m\geq 1)$, (3, *n*)-kite graph $(n\geq 2)$, are proved in [8, 9, 10].], In [11], defined the superior edge magic as "A graph *G* = (*V*,*E*) with *p* vertices and *q* edges has a superior edge magic total labeling if there is a bijection function *f*: $V\cup E\to\{1,\ 2,\ldots,\ p+q\}$ such that *f*(*u*)+*f*(*v*)+*f*(*uv*) are all constant for all $uv\in E(G)$, where $f(E(G))=\{1,2,\ldots,q\}$".In this paper we exhibit magic and bimagic labelings for some class of disconnected graphs.

II. MAIN RESULTS

In this section we will give magic and bimagic labelling for disconnected

Algorithm 2.1

Input : The number of vertices and edges of the graph nP_3.

Output : Superior edge bimagic labeling for nP_3.

begin

$V = \{ v_i^j : 1\leq i\leq 3;\ 1\leq j\leq n\}$ and

$E = \{ v_i^j v_{i+1}^j : 1\leq i\leq 2;\ 1\leq j\leq n\}$.

for j = 1 to n

{

if (j ≡ 1 (mod 2))

{

$$f(v_1^j) = 2n+\left(\frac{n}{2}\right)+\left(\frac{j+1}{2}\right);$$

$$f(v_3^j) = 3n+\left(\frac{j+1}{2}\right);$$

Design And Development Of 3-Phase Variable Drive

G. Harsha Vardhan Reddy , Archana Danappanavar

G. Pullaiah College of Engineering and Technology, Kurnool, India.

Abstract : With the change in scenario of continuous thrust for the improvement of efficiency of the overall system, motors are being coupled with variable frequency drives (VFD) to achieve energy savings, reduced wear and tear on motors, reduction of maintenance cost of mechanical flow controls etc. To meet the market requirements in the low voltage segment, 1MW, 690V ac drive has been developed. The system was successfully tested for V/f control, sensor-less vector control, power on ride through and catch on fly. Various issues related to testing of the machine with open loop v/f control and sensor less vector control were addressed successfully. Load testing of the 1MW VFD also completed with back to back test facility. This paper presents the development and testing of the developed 1MW VFD with the experimental results**.**

I. Introduction

The simple structure and robustness of the induction machine has made it the most preferred machine for industrial applications. However, when directly operated from the 50Hz AC grid this machine operates only at speeds near the synchronous speed. For applications requiring the variable speed, variable frequency drive is invariably required. It is also advantageous to use Variable Voltage Variable Frequency (VVVF) drives for greater efficiency, as compared to schemes which use mechanical gates and dampers for controlling the machine speed. Now a days a VVVF drive is commonly realized using IGBT based three-phase voltage source inverter (VSI) whose output voltage & frequency is controlled appropriately by controlling the switching pulses of IGBTs.To meet the market requirements in the low voltage segment, 1MW, 690V ac drive has been developed. The single line diagram of developed 1MW LV VFD is shown in Fig. 1. The power circuit comprises of input filter, three phase diode bridge rectifier, DC link, three phase inverter and output filter. System studies, design of IGBT based Voltage Source Inverter, input & out filter have been completed and verified with simulation studies using MATLAB / Simulink. Control algorithm for V/f control, sensor-less vector control, catch on fly and power on ride through have been developed and verified using simulation studies.

II. DEVELOPMENT OF 1MWVFD

Fig. 1: Single line Diagram of 1MW LV VFD

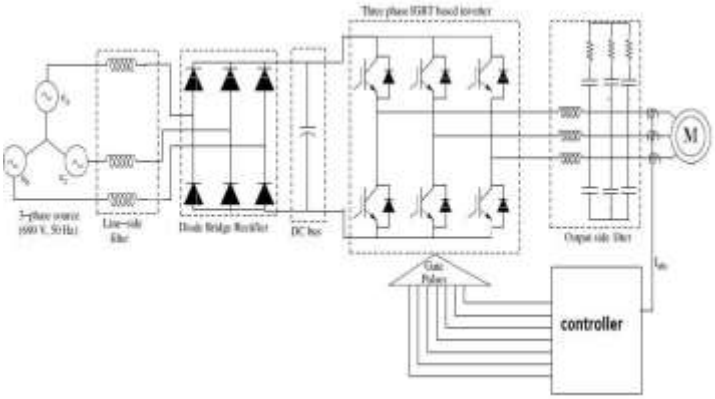

The power structure of the drive used is as shown in Fig. 1. The three phase balanced supply from the transformer is rectified by a three phase diode bridge rectifier to obtain the required DC bus voltage. A precharging circuit consisting of a resistor in parallel with a relay or contactor is used to prevent large inrush currents that may damage the DC bus capacitor. The relay bypasses the resistor from the circuit when the capacitor voltage has built up to a large enough value. The rectifier normally draws distorted and peaky currents from the supply and hence an inductance is used in series with the line to make the currents smoother. The rectified output is then given to the inverter whose switching signals are controlled suitably to obtain the required voltage. Wide bandwidth, high precision, Hall Effect sensors are used to sense the instantaneous line currents for feedback. The DC bus voltage is also sensed by using a precision Hall Effect sensor. The controller is a Digital Signal processer (DSP) from Texas Instruments. The control algorithm running on the processor senses the feedback signals through the built-in Analog-Digital Converter (ADC) on the controller and processes these information to generate the required switching pulses. The converter is switched at a frequency of 1.5 kHz. The inverter output voltage is again filtered by using an output LC filter with a split capacitor topology. Active damping technique is used to provide lossless damping to the resonant frequency oscillations [1]. Thermal design was carried out for 1MW

CREAT. MATH. INFORM.
21 (2021), No. 1, 27 - 33

Online version at http://creative-mathematics.ubm.ro/
ISSN 1584-286X

The processing of data for statistical tests of their basic parameters

G. Harasha Vardhan Reddy

G. Pullaiah college of Engineering and Technology, Kurnool, India.

ABSTRACT. This article focuses on the application of established data on flight delays at the airport Košice and its adaptation for further processing. These data were recorded for 36 months of 2006-2008. Modification of data is necessary for their further analysis in terms of time series analysis. Statistical tests of the basic parameters of the values of the flight delays at the airport Košice are made with their analysis.

1. The Description of Processed Data

The data, which we have obtained the Košice airport, is prepared in this article. These data cover the period of 36 months from January 2006 to December 2008. We have given large data sets, which have undergone initial processing of data. This initial processing of basic data and a formal modification of data to be able to continue working with them, is partly published in the works [1, 2, 3, 5]. In this work the adjustment process of the population was described to allow the stored data to obtain initial indicators delays at the airport Košice. Also from these data, their basic parameters of flights at Košice airport were published. This initial analysis also forms the basis of our research in this area. Assuming no fundamental processed and adjusted data and also from already published the basic parameters of these large data sets.

Based on this information, we had to decide which data will be analysed further. Thus, the selected data will be subjected to further processing treatment and subsequent analysis. This article will restrict itself only to the data selection, processing, presentation and analysis using basic statistical tests of hypotheses. This analysis tells us more about these data and because of their treatment will be possible to do a partial comparison between the years 2006 to 2008.

We build on the work [5] in which we have described the characteristics and parameters of the recorded data. There is described the whole process of modification of data and how to further processing. As regards the extensive information in our article we appointed only to those that we immediately need for our analysis.

Similarly, we will get the basic information from the articles [1, 2, 3], which are already published with the results of processing, which we refer in work [5]. These data are served as input for our decision on the selection of data for further processing and analysis. Also we can use them to compare with our obtained results.

In conclusion of this article we will attempt to indicate the direction of further work in this field. Space for research is relatively large because it is possible to examine whether the economic crisis has an impact on the development of monitored parameters and how it affected the predicted tendencies to the real trends of monitored parameters. This is

Journal of Mathematics and Statistics 9 (3): 225-233, 2021
ISSN 1549-3644

Nonlinear Growth Models for Modeling Oil Palm Yield Growth

G. Siddesh Babu and N. Janaki

Department of Mathematics.

G. Pullaiah College of Engineering and Technology, Kurnool, Andhra Pradesh, India

Abstract: This study provided the basic needs of parameters estimation for nonlinear growth model such as partial derivatives of each model, determination of initial values for each parameter and statistical tests of industrial usage. Twelve nonlinear growth models and its partial derivatives for oil palm yield growth are presented in this study. The parameters are estimated using the Marquardt iterative method of nonlinear regression relating oil palm yield growth data. The best model was selected based on the model performance and it can be used to estimate the oil palm yield at any age of oil palm. This study found that the Gompertz, logistic, log-logistic, Morgan-Mercer-Flodin and Chapman-Richard growth models have the ability for quantifying a growth phenomenon that exhibit a sigmoid pattern over time. Based on the statistical testing and goodness of fit, the best model is the Logistic model and followed by the Gompertz model, Morgan-Mercer-Flodin, Chapman-Richard (with initial stage) and Log-logistic growth models.

Key words: Nonlinear growth model, partial derivative, oil palm yield

INTRODUCTION

Growth model methodology has been widely used in the modeling of plant growth. Since growth of living things are normally nonlinear, it is reasonable to explore the use of nonlinear growth model to oil palm yield. In the oil palm industry, there are only a few theoretical model formulated specifically for oil palm industry applications. Modeling of the growth in other disciplines and application here a considerable potential for modeling of the Fresh Fruit Bunches (FFB) growth and oil palm yield. This is partly attributed to the fact that the statistical methodology used for fitting nonlinear models to oil palm growth data is closely related to the mathematics of the models and not explored yet. From our exploratory study on modeling practices, little work has been reported on modeling the oil palm yield growth. A nonlinear growth model was developed and proposed the used of partial derivatives of twelve nonlinear growth models. Growth studies in many branches of science have demonstrated that more complex nonlinear functions are justified and required if the range of the independent variable encompasses juvenile, adolescent, mature and senescent stages of growth[1]. Some of the application of the nonlinear model in agronomy was conducted by[2] is cocoa industry. While research in modeling tobacco growth data was done by[3-4].

The problem in modeling oil palm yield growth is that it does not follow a linear model. It normally follows a nonlinear growth curve. With the increase in the number of independent variables, modeling a nonlinear curve becomes more complex. This causes the model to be more inaccurate. The function of a growth curve has a sigmoid form ideally its origin is at (0,0), a point of inflection occurring early in the adolescent stage and either approaching a maximum value, an asymptote or peaking and falling in the senescent stage. Normally, oil palm will be harvested after four years of planting. The oil palm yield will increase vigorously until the tenth year of planting. The yield will then remains at a stable stage until the twenty-fifth year. The oil palm yield growth data are given in Table 1. The data used in this study are secondary data from research done by[5-6]. The research was conducted at Serting Hilir in Negeri Sembilan which normally annual rainfall in this location is had 1600mm to 1800 mm with two distinct droughts in January-March and June-August, however, the weather relatively wet. The data used here is the average of fresh fruit bunches and measured in tonnes/hectare/year from year 1979 to 1997.

Nonlinear models are more difficult to specify and estimate than linear models and the solutions are determined iteratively[7-8]. The iterative method used in the nonlinear regression model include the modified Gauss-Newton method (Taylor series), gradient or steepest-descent method, multivariate secant or false position and is the Marquardt method[7]. If a model, after reparameterization, does not behave in a near-linear fashion, the parameter estimates will not have desirable properties such as unbiasedness, normality and minimum variance and hence, complex estimation techniques (e.g[9]) may be necessary[8]. In such cases,

Journal of Algebra and Related Topics d Statistics 4 (1): 339-342, 2022
ISSN 2345-3931

On Some Stability Results for Fixed Point Iteration Method

G. Siddesh Babu
Department of Mathematics, G. Pullaiah College of Engineering and Technology, India.

Abstract: In this study, we establish that both the Mann and Ishikawa iteration processes are T-stable for the mappings T satisfying a more general contractive definition than that of Osilike[1] . The results obtained generalize some of the recent results of Osilike[1] which are themselves generalizations and extensions of some of the results of Harder and Hicks[2] and Rhoades[3,4].

Key words: Stability results, fixed point iteration procedure

INTRODUCTION

Let (E, d) be a complete metric space and $T : E \to E$ a selfmap of E and $F(T) = \{p \in E : T_p = p\}$, the set of fixed points of T. For $x_o \in E$, define sequence $\{x_x\}_{n=o}^{\infty}$ iteratively by

$$x_{n+1} = f(T, x_n), \quad n = 0, 1, 2, \ldots \qquad (1)$$

Suppose $\{x_n\}_{n=o}^{\infty}$ converges to a fixed point p of T and let $\varepsilon_n = d(y_{n+1}, f(T, y_n))$, where $\{y_n\}_{n=o}^{\infty} \subset E$. Then, the iteration procedure (I) is said to be T-stable or stable with respect to T if and only if $\lim_{n\to\infty} \varepsilon_n = 0$ implies $\lim_{n\to\infty} y_n = p$.

Harder and Hicks[2] established several stability results under various contractive conditions using the above concept. Rhoades[3,4] extended the results of Harder and Hicks[2] to other classes of contractive mappings. In Rhoades[4], the following contractive definition was considered : there exists a constant $c \in [0,1)$, such that for each $x, y \in E$,

$$d(Tx, Ty) \le c \max\{d(x, y), \frac{1}{2}[d(x, Tx) + d(y, Ty)], d(x, Ty)], d(x, Ty), d(y, Tx)\} \qquad (2)$$

Using (2), Rhoades[4] established several stability results which are generalizations and extensions of most of the results of Harder and Hicks[2] and Rhoades[5]. It was shown in Rhoades[6] that if T satisfies (2) then,

$$d(Tx, Ty) \le \frac{c}{1-c} d(x, Ty) + c\, d(x, y)$$

Osilike[1] employed the following contractive definition: for each $x, y \in E$, there exist constants $a \in [0,1)$ and $L \ge 0$ such that

$$d(Tx, Ty) \le L d(x, Tx) + a\, d(x, y). \qquad (3)$$

Using (3), Osilike[1] proved several stability results which are generalizations and extensions of most of the results of Rhoades[4].

Employing the same contractive definitions as in Harder and Hicks[2], Berinde[7] proved the same stability results for the same iteration procedures by an alternative method.

In this study, we extend some of the recent results of Berinde[7], Osilike[1] and Rhoades[4] to a more general contractive definition.

Preliminaries: In the sequel, we shall employ the following contractive definition. For each $x, y \in E$, there exist a constant $b \in [0,1)$, and a continuous, monotone increasing function $\varphi : \Re_+ \to \Re_+$ with $\varphi(0) = 0$, such that

$$d(Tx, Ty) \le \varphi(d(x, Tx)) + bd(x, y). \qquad (4)$$

The contractive definition (4) is more general than those considered by Berinde[7], Harder and Hicks[2], Rhoades[3,4] and Osilike[1]. This is evident by specifying φ in (4) as follows. If $\varphi(u) = Lu$ in (4) above, where $L \ge 0$ is a constant, then we obtain the contractive mapping of Osilike[1] which is itself a generalization of those in Harder and Hicks[2], Berinde[7] and Rhoades[4]. Also, if $L = mb$, where $m = (1-b)^{-1}$, $b \in [0,1)$, we obtain the contractive mapping considered by Rhoades[4].

Also, if $L = 2\delta$, $b = \delta$, where $\delta = \max\left\{\alpha\frac{\beta}{1-\beta}, \frac{\gamma}{1-\gamma}\right\}$, $0 \le \alpha < 1$ $0 \le \beta < 0.5$, $0 \le \Upsilon \le 0.5$, then we obtain the Zamfirescu's contractive definition which was employed in Harder and Hicks[2] and Berinde[7]. Furthermore, if $\varphi(u) = 0$, then (4) reduces to $d(Tx, Ty) \le bd(x, y)$, $b \in [0,1)$ which is another contractive definition used by Harder and Hicks[2] and Berinde[7].

In the sequel, we shall establish stability results for the following iteration procedures:

The Forcing Monophonic Hull Number of a Graph

V. Narasimha Reddy
Department of Mathematics
G. Pulliaha College of Engineering and Technology , Kurnool.
Andhra Pradesh, India.

Abstract — For a connected graph G = (V, E), let a set M be a **minimum monophonic hull set of *G*. A subset $T \subseteq M$ is called a forcing subset for *M* if *M* is the unique minimum monophonic hull set containing *T*. A forcing subset for *M* of minimum cardinality is a minimum forcing subset of *M*. The forcing monophonic hull number of *M*, denoted by $f_{mh}(M)$, is the cardinality of a minimum forcing subset of *M*. The forcing monophonic hull number of *G*, denoted by $f_{mh}(G)$, is $f_{mh}(G)=\min\{f_{mh}(M)\}$, where the minimum is taken over all minimum monophonic hull sets in *G*. Some general properties satisfied by this concept are studied. The forcing monophonic hull numbers of certain classes of graphs are determined. It is shown that, for every pair *a, b* of integers with $0 \leq a \leq b$ and $b \geq 2$, there exists a connected graph *G* such that $f_{mh}(G) = a$ and $mh(G) = b$.**

Keywords: **hull number, monophonic hull number, forcing hull number, forcing monophonic hull number.**

AMS Subject Classification: 05C12, 05C05.

I. INTRODUCTION

By a graph $G = (V, E)$, we mean a finite undirected connected graph without loops or multiple edges. The order and size of G are denoted by p and q respectively. For basic graph theoretic terminology, we refer to Harary [1, 9]. A convexity on a finite set V is a family C of subsets of V, convex sets which is closed under intersection and which contains both V and the empty set. The pair (V, E) is called a convexity space. A finite graph convexity space is a pair (V, E), formed by a finite connected graph $G = (V, E)$ and a convexity C on V such that (V, E) is a convexity space satisfying that every member of C induces a connected sub graph of G. Thus, classical convexity can be extended to graphs in a natural way. We know that a set X of R^n is convex if every segment joining two points of X is entirely contained in it. Similarly a vertex set W of a finite connected graph is said to be convex set of G if it contains all the vertices lying in a certain kind of path connecting vertices of W[2,8]. The distance $d(u,v)$ between two vertices u and v in a connected graph G is the length of a shortest u–v path in G. An u–v path of length $d(u,v)$ is called an u–v geodesic. A vertex x is said to lie on a u-v geodesic P if x is a vertex of P including the vertices u and v. For two vertices u and v, let $I[u,v]$ denotes the set of all vertices which lie on $u - v$ geodesic. For a set S of vertices, let $I[S] = \cup_{u,v \in S} I[u, v]$. The set S is *convex* if $I[S] = S$. Clearly if $S = \{v\}$ or $S = V$, then S is convex. The *convexity* number, denoted by $C(G)$, is the cardinality of a maximum proper convex subset of V. The smallest convex set containing S is denoted by $I_h(S)$ and called the *convex hull* of S. Since the intersection of two convex sets is convex, the convex hull is well defined. Note that $S \subseteq I[S] \subseteq I_h(S) \subseteq V$. A subset $S \subseteq V$ is called a *geodetic set* if $I[S] = V$ and a *hull set* if $I_h(S) = V$. The *geodetic number* $g(G)$ of G is the minimum order of its geodetic sets and any geodetic set of order $g(G)$ is a *minimum geodetic set* or simply a *g- set* of G. Similarly, the *hull number* $h(G)$ of G is the minimum order of its hull sets and any hull set of order $h(G)$ is a *minimum hull set* or simply a *h- set* of G. The geodetic number of a graph is studied in [1,4,10] and the hull number of a graph is studied in [1,6]. A subset $T \subseteq S$ is called a *forcing subset* for S if S is the unique minimum hull set containing T. A forcing subset for S of minimum cardinality is a *minimum forcing subset of M*. The *forcing hull number* of S, denoted by $f_h(S)$, is the cardinality of a minimum forcing subset of S. The *forcing hull number* of G, denoted by $f_h(G)$, is $f_h(G) = \min\{f_h(S)\}$, where the minimum is taken over all minimum hull sets S in G. The forcing hull number of a graph is studied in[3,14]. A *chord* of a path $u_o, u_1, u_2, \ldots, u_n$ is an edge u_iu_j with $j \geq i + 2$. $(0 \leq i, j \leq n)$. A $u - v$ path P is called *monophonic path* if it is a chordless path. A vertex x is said to lie on a $u - v$ monophonic path P if x is a vertex of P including the vertices u and v. For two vertices u and v, let $J[u,v]$ denotes the set of all vertices which lie on $u - v$ monophonic path. For a set M of vertices, let $J[M] = \cup_{u,v \in M} J[u, v]$. The set M is *monophonic convex* or *m-convex* if $J[M] = M$. Clearly if $M = \{v\}$ or $M = V$, then M is m-convex. The *m-convexity* number, denoted by $C_m(G)$, is the cardinality of a maximum proper m-convex subset of V. The smallest m-convex set containing M is denoted by $J_h(M)$ and called the *monophonic convex hull or m-convex hull* of M. Since the intersection of two m-convex set is m-convex, the m-convex hull is well defined. Note that $M \subseteq J[M] \subseteq J_h(M) \subseteq V$. A subset $M \subseteq V$ is called a *monophonic set* if $J[M] = V$ and a *m-hull set* if $J_h(M) = V$. The *monophonic number* $m(G)$ of G is the minimum order of its monophonic sets and any monophonic set of order $m(G)$ is a *minimum monophonic set* or simply a *m- set* of G. Similarly, the *monophonic hull number* $mh(G)$ of G is the minimum order of its m-hull sets and any m-hull set of order $mh(G)$ is a *minimum monophonic set* or simply a *mh- set* of G. The monophonic number of a graph is studied in [5,7,11,13] and the monophonic hull number of a graph is studied in [12,13]. A vertex v of G is said to be a *monophonic vertex* of a graph G if v belongs to every minimum monophonic set of G. A vertex v is an *extreme vertex* of a graph G if the sub graph induced by its

Journal of Science and Sustainable Development 9(4): 351-353, 2021
ISSN 2070-1748

Discrete Optimization Description for the Solutions in the Matching Problem

V. Narasimha Reddy
Department of Mathematics, G. Pullaiah College of Engineering and Technology, Kurnool, Andhra Pradesh, India

Abstract: This study was concerned with the characterization of solutions in the matching problem. The general mixed-integer programming problem is given together with the definition of the convex hull of the integer solutions. In addition, the matching problem is defined as an integer problem and an algorithm is described to find the optimum matchings. Some illustrative examples are introduced to clarify the presented theory in the study.

Key words: Mixed-integer programming, convex hull, matching problem

INTRODUCTION

Shortly after the development of his simplex algorithm for linear programs, Dantzig[1] pointed out the significance of solving integer programming problems. Many problems involving nonconvex region or functions can be converted into integer programs, e.g. linear programs with separable, piecewise linear, but nonconvex objective functions. The challenge raised by Dantzig was to develop effective procedures, such as his simplex method was proving to be for linear programs, to handle these more difficult integer programs.

Today, there are codes, including commercial codes, which effectively solve a small, but important, class of integer programs. This class is not well defined but can be said to include integer programs with linear programming relaxations, i.e. up to several thousand rows and columns, but with a small number of integer variables x_j, $j \in J$, or a strong linear programming relaxation.

Mixed-integer programming problem: The general mixed-integer programming problem can be formulated mathematically as follows[2]:

Maximize $z = cx$,

Subject to

$Ax = b$, (1)

$x_j \geq 0$, $(j = 1, 2,\ldots,n)$ (2)

x_j integer, $j \in J \subseteq \{1, 2,\ldots,n\}$, $J \neq \phi$. (3)

An integer programming problem is a pure integer problem if $J = \{1, 2,\ldots,n\}$. The linear programming relaxation of the integer programming problem is the corresponding linear program with constraints (1) and (2) imposed, but not (3).

Strong linear programming relaxations: The considerations given here turn out to be very important practically. Any method that solves linear programs as part of a method to try to solve integer programs will profit from a better linear programming formulation.

Earlier, we defined the integer programming problem and its linear programming relaxation. Correspondingly, define the convex hull of integer solutions to be

$P_I = \text{conv}\{x \mid x_j \geq 0, j = 1, 2,\ldots,n;\ x_j \text{ integer}, j \in J;\ Ax = b\}$ (4)

and the linear programming polyhedron to be

$P_L = \{x \mid x_j \geq 0, j = 1, 2,\ldots,n;\ \text{and } Ax = b\}$ (5)

Clearly, $P_I \subseteq P_L$.

There are many linear programs giving the same P_I but different P_L's and this is illustrated in the following examples:

Example 1: Consider

$P_I = \text{conv}\{(x_1, x_2) \mid 2x_1 \leq 7, 4x_2 \leq 9, x_1 \geq 0, x_2 \geq 0 \text{ and integers}\}$,

and

$P_{L_1} = \{(x_1, x_2) \mid 2x_1 \leq 7, 4x_2 \leq 9, x_1 \geq 0, x_2 \geq 0\}$,

$P_{L_2} = \{(x_1, x_2) \mid x_1 \leq 3, x_2 \leq 2, x_1 \geq 0, x_2 \geq 0\}$.

The polyhedra P_I, P_{L_1} and P_{L_2} are shown in Fig. 1a and 1b.

It is clear that $P_I = P_{L_2}$, while $P_I \subset P_{L_1}$.

Example 2: Consider the constraints:

$x_1 + x_2 \leq 2y$, $0 \leq x_j \leq 1$, $j = 1, 2$ and $y = 0$ or 1.

The two polyhedra P_I and P_L are shown in Fig. 2a and 2b.

$P_I = \{(x_1, x_2, y) \mid 0 \leq x_1 \leq y, 0 \leq x_2 \leq y, 0 \leq y \leq 1\}$.

If we had originally stated the problem as having constraints

$0 \leq x_1 \leq y$, $0 \leq x_2 \leq y$, $y = 0$ or 1,

then the linear programming relaxation would have had $P_L = P_I$.

Journal of Acharya Narendra Dev Research Volume 68 Issue 10, 28-35, March 2022
ISSN: 0978-3287

Vertex-Transitive bi-Cayley Graphs over a Nonabelian Set

C. Venkateswaramma

Assistant Professor, Department of Mathematics, G. Pullaiah College of Engineering and Technology, Kurnool.

Received: 30 January 2022 Revised: 08 February 2022 Accepted: 18 March 2022 Published: 31 March 2022

Abstract *- The vertex-transitive graph is a graph with high symmetry. A graph Γ is said to be a bi-Cayley graph over a group H if it admits H as a semiregular automorphism group with two orbits of equal size. And Γ is normal with respect to H if $R(H)$ is normal subgroup of $Aut(\Gamma)$. In this paper, we complete the classification of the cubic vertex-transitive normal bi-Cayley graphs over a group of order pq^2, where p and q be two primes with $p>q$. Furthermore, these cubic vertex-transitive bi-Cayley graphs are also a Cayley graph.*

Keywords *- Bi-Cayley graph, Normal, Cayley graph, Vertex-transitive, Isomorphism.*

1. Introduction

The vertex-transitive graph is a graph with high symmetry, and the symmetry of a graph is described by some transitivity properties of the graph. Cayley graph is a famous symmetric graph, which has important significance in many fields such as mathematical models, computer networks and communication technology. As a natural generalization of the Cayley graph, the bi-Cayley graph was proposed by Resmini and Jungnickel [1] when they studied the normality of Cayley graphs, and bi-Cayley graph is also important research tool for vertex-transitive graph, edge-transitive graph, semisymmetric graph and even symmetric graph. The symmetry of the bi-Cayley graph has been a hot topic, and the research focus being on classifying bi-Cayley graphs with specific symmetry properties over a given finite group H.

For a graph Γ, we denote by $V(\Gamma), E(\Gamma), \mathrm{Aut}(\Gamma)$ the vertex set, edge set and full automorphism group of Γ, respectively. The graph Γ is said to be *vertex-transitive* or *edge-transitive* if $\mathrm{Aut}(\Gamma)$ acts transitively on $V(\Gamma)$ or $E(\Gamma)$, respectively. Initially, bi-Cayley graph over the cyclic group and abelian group were studied (see[2,3,4,5,6,7,8]). In recent years, the research focus being on classifying bi-Cayley graphs over finite nonabelian groups. For example, in [9], cubic symmetric bi-Cayley graphs on non abelian simple groups were classified and the full automorphism groups of these graphs were determined; trivalent vertex-transitive bi-Cayley graphs over dihedral groups were classified and Cayley property of trivalent vertex-transitive bi-dihedrants was presented in [10]. And for more results about it, we refer the reader to [11,12,13,14,15,16].

The normality of the bi-Cayley graph is an important property in the study of transitivity and full automorphism group of bi-Cayley graphs (see[17,18,19,20]). Much work has also been done on normal bi-Cayley graph. For example, it was shown that every finite group has a normal bi-Cayley graph in [21]. For a bi-Cayley graph Γ over a group H, the normalizer of group H in the full automorphism group of bi-Cayley graph Γ was determined in [22].

In this paper, we will apply the normality of bi-Cayley graph to study the bi-Cayley graph with respect to the vertex-transitive property and its full automorphism group. We present a classification of the vertex-transitive property of cubic normal bi-Cayley graphs Γ over a group of order pq^2, and it is shown that if Γ is vertex-transitive, it is also a Cayley graph.

Theorem 1.1 *Let* $\boldsymbol{H = \langle a, b | a^p = b^{q^2} = 1, b^{-1}ab = a^{r^{\frac{p-1}{q}}}, q | p-1 \rangle}$, where p and q be two primes with q<p, and r is a primitive root of modulo p. Let $\boldsymbol{\Gamma}$ = BiCay (H, R, L, S) be a connected normal cubic bi-Cayley graph over group H, it is vertex-transitive if and only if the (R, L, S) is equivalent to the one of the triples in Table 1. Furthermore, all the graphs in Table 1 are both Cayley graph.

Table 1. Cubic vertex-transitive normal bi-Cayley graphs over group *H*.

No	(R,L,S)	conditions	Cayley
1	$(\emptyset, \emptyset, \{1, ab^{-s}, b^s\})$	$1 \le s \le q-1$	Yes
2	$(\emptyset, \emptyset, \{1, ab^{2s}, b^s\})$	$1 \le s \le q-1$	Yes
3	$(\emptyset, \emptyset, \{1, ab^k, b^{2k}\})$	$k = nq + t(t \ne 0), 0 \le n, t \le q-1$	Yes
4	$(\{ab^s, (ab^s)^{-1}\}, \{b^s, b^{-s}\}, \{1\})$	$1 \le s \le q-1$	Yes

)

Increasing the motivation of the students to learn mathematics

C. Venkateswaramma, N. Janaki

Assistant Professor, G. Pullaiah College of Engineering and Technology, Kurnool, Andhra Pradesh.

Abstract *– The students use computers, smartphones and other electronic devices everyday for their own needs. The success in Mathematics is getting lower and lower, both on local level in Macedonia and on global level also [6]. A lot of the students are having difficulties with learning Mathematics, and with that also the motivation for learning Mathematics decreases. The difficulties are shown in both, mastering the material in school and solving the exercises at home. Also, when the students solve real-life problems, they are not connecting what was learned on Mathematics classes with those problems. They almost don't use the Mathematics and the electronic devices at all for solving the real-life problems. If we succeed in encouraging the students in using these electronical devices and softwares for: examining, investigating, visualizing and solving real-life problems, we will get students that are motivated for learning mathematics, and with that also we will get increased level of knowledge of mathematics.*

In this project, for increasing the motivation for learning mathematics and increasing the level of knowledge, we made a web application http://mathlabyrinth.azurewebsites.net

The problems that are put on the web application are connected with real-life problems the students have, who need knowledge from secondary education mathematics to solve them.

Keywords - *mathematics, motivation, web application, exercise, IT.*

I. INTRODUCTION

In several latest researches that have been done in our country, and wider, it has been established that the knowledge in mathematics and the pupils` motivation for studying mathematics are reduced and they are below the minimum level of knowledge. Thus, one of the priorities of our country and wider in the field of education is to motivate the pupils to study mathematics and to increase the level of knowledge in the same subject with the pupils of all ages.

How to increase the level of knowledge in mathematics and how to increase the motivation for studying mathematics?

Because the pupils use computers, smart phones and other electronic devices for their needs more and more, there is a need to incorporate them in the education and in the studying of mathematics. The free software (GeoGebra) is used in the teaching, which is used to solve and visualize the constructive exercises [1], exercises with functions, exercises from plane geometry and solid geometry, exercises with probability [7] and others. Using the software class marker there have been made electronic tests to test the pupils` knowledge [2], which are quite positively accepted by them. However, IT is not used enough in the teaching and it is still necessary to work on raising the pupils` motivation and their level of knowledge.

In order to establish the benefits of the use of the web application in teaching mathematics and increasing the motivation, and by doing that increasing the knowledge in mathematics too, two surveys have been made with the pupils of the Gymnasium "Kocho Racin" from Veles. One before beginning with the use of the web application in the teaching of mathematics, and the other after one year usage of the web application.

146 pupils participated in the first survey. The accent of this survey is put on solving textual exercises in which the problems of the real life are elaborated, using the IT while solving them, solving the exercises in domestic conditions (home work) and motivation for studying mathematics [3].

Some of the questions from the first survey, before beginning with the use of the project and given answers:

- To the question "Do you think that you can increase the motivation for studying mathematics by solving practical exercises" 67% of the pupils asked answered that always or often they are motivated to study mathematics.

Do you think that you can increase the motivation for studying mathematics by solving practical exercises.

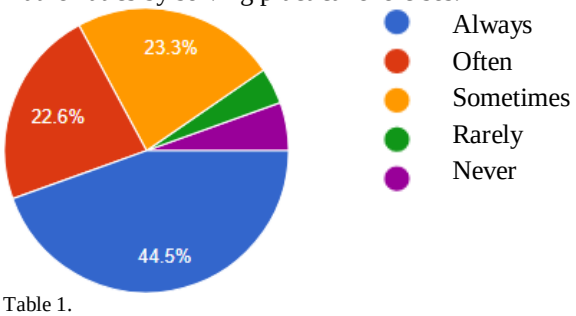

Table 1.

To the question "When you have problems while doing your homework, would you like to have a web site which will give you the steps and help for problems solving" 86% of the asked pupils said that

Journal of Science and Sustainable Development Volume 66 Issue 12, 1-9, December, 2021
ISSN: 2070-1748

Mathematical Analysis of Hymns for Meditation

A. G. Gopinath
Assistant Professor, Department of Mathematics,
G. Pullaiah College of Engineering and Technology, Kurnool,
Andhra Pradesh, India

Abstract *— In this work we study the mantra and Vedic chants used for meditation and convert them to time series with the frequency of 44100 Hertz. We then perform the mathematical and statistical analysis of these chants and compare these results with few of the popular known songs in Hindi, Kannada and Spanish/English. We also consider the Tirumala temple bell sound for our analysis and study. We conclude that the meditation songs are lyapunov stable and in fact they are asumptotically stable. And hence are perfect for meditation.*

Keywords — *Correlation, Entropy, Lyapunov Spectrum, Power Spectrum, Time Series*

I. INTRODUCTION

India is a very mysterious country. We find its mystery in its diversity, not just in the flora and fauna, but also in the tradition of the people and more importantly the influences on them and the cultural diversity. Yet some things have never changed. The Chanting of Vedic hymns and mantras are one such example. Today most of the yoga gurus and people use many of the Vedic chants as powerful form of meditation. Youtube has popularized them extensively. Thus many questions arise. Are these connected in any way as many of them are used for the similar purpose? Can we study their patterns?

With the invention of nonlinear time series analysis tools by Hegger Kantz and Shcrieber [1] in late decades of the previous century, I felt that such a study is possible. Thanks to them that there is a freely available codes on internet as TISEAN 3.0.0 which executes these studies on any time series fed as data.

Here we first describe the Vedic chants amd other songs which have been used for the study in the first section. In the next section about how the data have been extracted and what are the different studies and analysis done on the data. The third section discusses the analysis and interpretation and finally the fourth is the conclusion.

II. MATERIALS AND METHODS

1. THE DATA

For this study I considered the following mantras and downloaded them from the websites which provide them freely.

1. Maha Mryuthyunjaya Mantra chanted 108 times by Adi Yoga guru
2. Om Mantra chanting
3. Shivastuti for meditation freely available from a website
4. Maha Mrythyunjaya Mantra fewer times available freely from a website.
5. Tirumala temple bell sounds
6. “Sonide nakhare” a Hindi film song.
7. “Ee sanje yakagide” a Kannada film song
8. “Bailamos” a Spanish song

One can argue that these songs or chants have to be understood first and then the music should suit in such a way that they can be useful for meditation. Hence I have chosen these from the websites which provide them for meditation. The temple bell for its sound resembling the Om mantra and other songs from films and pop music only for the sake of comparison. Also though Mathematically I will not be able to say anything regarding the meaning of the chants, the rendering and the chant when converted in the form of numbers would give out some patterns which is explained in this paper.

I first downloaded the mp3 files from the websites. Then converted the mp3 to .wav format using audacity. Audacity converts the file into left and right stereo audio files with the frequency of 44100 Hz. Then the audioread of OCTAVE was used to convert the .wav to data points.

Though the number of data points generated for these mantras were different from each other, the analysis is made in such a way that there is uniformity in them.

Stability of Stratified Compressible Shear Flow

Dr. ManjuBala and A. G. Gopinath

Assistant Professor, Department of Mathematics, S.V. College, Aligarh

Assistant Professor, Department of Mathematics , G. Pullaiah College of Engineering and Technology, Kurnool.

Abstract

In the present chapter we have studied the effect of a magnetic field on linear stability of stratified horizontal flows of an in viscid compressible fluid by the generalized progressing wave expansion method. Here we have discussed the different cases and have established the conditions for the stability. It is found that the magnetic field stabilizes the system.

Keywords: *Linear stability, Inviscid compressible fluid shear flows.*

Introduction:-

In the present chapter we have studied the effect of a magnetic field on linear stability of stratified horizontal flows of an inviscid compressible fluid by the generalized progressing wave expansion method. Here we have discussed the different cases and have established the conditions for the stability. It is found that the magnetic field stabilizes the system.

[11] and [12] has studied the linear stability of stratified horizontal flows of an inviscid compressible fluid. He has shown that a shear in the horizontal directions always gives rise to instabilities and also that all shear flows are unstable if the external force field vanishes. The same results are also obtained for homogeneous incompressible fluid in [2] and [8]. Previously this problem was discussed by [7] for incompressible fluid, and also by [6], [4] and [19] under various restrictions. Stability in the rotating Bfenard problem with Newton-Robin and fixed heat flux boundary conditions was studied by [3]. Straughan, B. also discussed the problem of Stability and wave motion in porous media [15].

2. Formulation of the problem:-

The basic equations for governing the motion of an ideally conducting inviscid, compressible and adiabatic fluid in the presence of a magnetic field [13, 15] are

$$\frac{\partial \nu}{\partial t} + \nu.\nabla\nu = -\frac{1}{\rho}\nabla p + \nabla v + (\nabla \times B)\times B \qquad (2.1)$$

$$\frac{\partial B}{\partial t} = \nabla \times (\nu \times B) \qquad (2.2)$$

$$\frac{\partial \rho}{\partial t} + \nabla.(\rho v) = 0 \qquad (2.3)$$

$$\frac{\partial}{\partial t}(p\rho^{-\gamma}) + \nu.\nabla(p\rho^{-\gamma}) = 0 \qquad (2.4)$$

Where ν denotes the velocity, ρ, the density; B, the magnetic field; V, the external potential force; p, the pressure; and γ a constant.

The Application of Minimum Polynomial

G. Ramakrishna

G. Pullaiah College of Engineering and Technology, Kurnool, Andhra Pradesh.

Abstract *- Matrix theory plays an important role in algebra research and linear control, and the minimum polynomial plays an important role in matrix. Therefore, it is necessary to study the application of minimal polynomials. In this paper, six applications of minimum polynomial include solving matrix function and its inverse function by using minimum polynomial, determining singularity of matrix polynomial, solving matrix equation, determining whether matrix can be diagonalized, solving basis and dimension of linear space, and solving differential equation with constant coefficient.*

Keywords *- The matrix function and its inverse, The singularity of matrix polynomials, Diagonalizable, The basis and dimension.*

1. Introduction

In the development of society and the development of mathematics, algebra is always very important. At the same time, the minimum polynomial plays an important role in algebra. Not only the theoretical research, the practical application of the minimum polynomial also solves many problems. For example, matrix polynomials can judge whether a matrix can be diagonalized, solve matrix functions and linear equations, etc., which are also very important in the study of automation control. Therefore, if you want to do new research in the field of algebra and engineering control, you must be very familiar with the minimum polynomial, but also grasp how the minimum polynomial can help us solve practical problems.

The concept of minimal polynomial is first given in the Hamilton-Cayley theorem. Therefore, [1-3] describes the origin and development of the Hamilton-Cayley theorem, as well as the rationality proof and other related properties of the theorem. Before proposing the minimum polynomials, we mainly study the characteristic polynomials of matrices. The minimum polynomial is a special case of the characteristic polynomial, so to understand the minimum polynomial we should start with the characteristic polynomial. Literature [4-10] has analyzed the impulse condition that the characteristic polynomial is equivalent to the minimum polynomial, and the method of solving the minimum polynomial. If you want to solve practical problems by minimal polynomials, you need to have a good understanding of their properties and particularity. Literature [11-20] introduces various properties of minimal multinomial and gives corresponding proofs. The application of minimum polynomial in control system and linear multivariable system is briefly introduced in literature [21-25]. Therefore, the main contents of this paper are as follows: Section 2: Using the minimum polynomial to solve the matrix function and its inverse function; Section 3: Judge whether the matrix polynomial has singularity; Section 4: Using minimal polynomial to solve matrix equation; Section 5: How to judge whether the matrix can be diagonalized by using the minimum polynomial; Section 6: Solving the basis and dimension of linear space according to the minimum polynomial; Section 7: Solving differential equations with constant coefficients by means of minimum polynomials; Finally, the eighth section summarizes the full text.

2. Solving the Matrix Function and its Inverse

For polynomials of high degree, it is very troublesome to solve the matrix function. If we want to do it directly, the minimum polynomial here makes it easy and fast.

Example 1. Setting $A=\begin{pmatrix}2 & 0 & 0\\ 1 & 1 & 1\\ 1 & -1 & 3\end{pmatrix}$, $f(\lambda)=\lambda^6+2\lambda^5-\lambda^4+3\lambda^2-2\lambda+1$, try to solve$f(A)$.

Solution: First find the minimum polynomial: $f_A(\lambda)=|\lambda E-A|=(\lambda-2)^3$, the minimum polynomial of matrix A possible:$m_1=(\lambda-2)^3$， $m_2=(\lambda-2)^2$， $m_3=(\lambda-2)$.

Because $m_3(A)=(A-2E)\neq 0$,$m_2(A)=(A-2E)^2=0$, so $m_A(\lambda)=(\lambda-2)^2$.

Optimal Solution of a Degenerate Transportation Problem

G. Ramakrishna, V. Narasimha Reddy
Assistant professor, Department of science and Humanities,
G. Pullaiah College of Engineering and Technology, Kurnool.

ABSTRACT: *The Transportation Problem is criticaltool for real life problem. Mathematically it is an application of Linear Programming problem. At the point when the analysts are doing some work on Transportation problem has a typical inquiry that, how we can way to deal with the optimality of Transportation problem. Optimality gives us the optimal route that prompts the either most extreme benefit or least aggregate cost whichever is required. Since last numerous years, there was so much research has been improved the situation for Non-Degenerate Transportation problem, however here we are acquainting the new approach to get the optimality when the Transportation problem facing the degeneracy.so , here in this paper, the algorithm tries to clarify the optimal solution of Degenerate Transportation Problem, or close to the optimal solution.*

KEY WORDS: *IBFS, Degeneracy, optimality, L-Shape of Transportation problem, Degrees of freedom for optimality.*

INTRODUCTION: Transportation problem is exceptionally powerful crucial part of linear programming problem which can be connected for required sources of supply to corresponding destination of demand, with the end goal that the aggregate transportation cost ought to be limited. The essential phase of any transportation problem as Initial Basic Feasible Solution is gotten by any of the techniques as North West Corner strategy, Least Cost Method, Vogel's Approximation technique, and the remaining and most vital work is to be for optimality of the Transportation problem is Verified by MODI.

The Transportation Problem was first settled by F.L. Hitchcock. At that point after T. C. Koopmans worked again on the hypothesis of F.L. Hitchcock in the following paper-(2).These two research work are extremely useful in the development of transportation techniques. The linear programming with fuzzy numbers and its optimal solution presented by Bazarra, Jarvis and Sherali in 1990. On the other hand Lai and Huang in 1992, accepted the circumstances in which all the parameters are fuzzy number. Additionally they have utilized the triangular possibility distribution on fuzzy numbers. Since most recent couple of years prior, in 2006, Swarup, Gupta and Mohan disclosed the strategy to reach up to the sensitivity analysis or post optimality analysis of the different parameters in the linear programming problems. In corporate division so many producers took after the Optimization basics as often as possible in the linear programming problem for any kind of real world problem. For this imperative reason, it is exceptionally pivotal to build up the new methodologies that can prompt the model to "best fit" in to the real world as much as possible.

Here we have built up another way to deal with the optimal solution or close to the optimal solution. Additionally, the new calculation depicted here gives the best way for the optimality with stepwise methodology with numerical cases for the justification.

MATHEMATICAL ASPECTS RELATED TO TRANSPORTATION PROBLEM:

Balanced Transportation Problem:
A Transportation Problem is said to be balanced transportation problem if total number of supply is same as total number of demand.

Unbalanced Transportation Problem:
A Transportation Problem is said to be unbalanced transportation problem if total number of supply is not same as total number of demand.

Objective Function: It is a linear function of decision variables expressing the objective of the decision maker.

Feasible solution: Any solution $X_{ij} \geq 0$ is said to be a feasible solution of a transportation problem if it satisfies the constraints.

Analysis of Sugarcane Production in India using Mathematical Model

S. Nikhath

Assistant Professor, Department of Mathematics, G. Pullaiah College of Engineering and Technology, Kurnool.

Received Date: 11 February 2022
Revised Date: 23 March 2022
Accepted Date: 25 March 2022

Abstract *- Agriculture plays a vital role in the Indian economy. Over seventy percent of the rural households depend on agriculture. Agriculture is an important sector of Indian economy as it contributes about 17% to the total GDP and provides employment to over two third of the population. Agriculture derives its importance from the fact that it has vital supply and demand links with the manufacturing sector and is a source of employment generation for the rural population in India. Sugar industry is the second largest agro-based industry in the country. Uttar Pradesh is the largest State of India and is pre-dominant in agricultural crops and has faster endowment in sugarcane crop. Sugar industry in India has been focal point for socio-economic development in rural areas by mobilizing rural resources, generating employment and higher income etc. In the present paper, an attempt has been made to study the production trend and growth rate for Sugarcane by using three years moving average for area sown, productivity and production. It is observed that area sown has constantly increased from 2.05 M hectare in 1958-59 to 4.79 M hectare during 2018-19. The production has also increased from 74.11 M tones in 1958-59 to 380.34 in 2018-19. The growth rate has been highest at the level of 5.98 % per annum during 1958-59 to 1968-69 and lowest i.e. 0.67% during 1998-99 to 2008-09. The productivity level has been 36132.33 kg/ha during 1958-59 which has gone up to 79398.67 kg/ha during 2018-19. The productivity level has shown positive growth rates per annum during all the periods except 1998-99 to 2008-09. State-wise analysis has also been carried out for Sugarcane producing States and it is concluded that government may take appropriate measures to provide necessary infra-structure and technology, as these states have suitable Agro-climate condition for sugarcane.*

Keywords *- Area Sown, Growth Rate, Productivity, Production, Sugarcane.*

I. INTRODUCTION

Agriculture in India is one of the most prominent sectors to its economy and about 70% of the population depends on Agriculture. The sugarcane and potato are the main cash crops and providing huge employment opportunities in rural and urban areas. India has emerged as the largest sugar producing country in the world with a 18.7% share of the world's sugarcane production. India is the second-largest producer of sugarcane in the world. India is known as the homeland of Sugar. Brazil is the largest sugarcane producing country in the world followed by India, China and Thailand. Sugar industry is the second largest agro-based industry in the country. Sugar industry in India has been focal point for socio-economic development in rural areas by mobilizing rural resources, generating employment and higher income etc. Uttar Pradesh is the largest State of India and is pre-dominant in agricultural crops and has faster endowment in sugarcane crop. While agriculture in India has achieved grain self-sufficiency but the production is, resource intensive, cereal centric and regionally biased. India also needs to improve its management of agricultural practices on multiple fronts. The total food grain production is estimated to be 305 million tones during 2020-21 and the production of sugarcane has been 356 millions tones in the same year.

II. REVIEW OF WORK DONE

A lot of work has been attempted for enhancing the productivity, quality and generation of employment in sugarcane crop. Some of the findings are: Yadav (2008) has studied the mechanization of sugarcane in India and found the positive impact of technology and mechanization in India. Singhals (2008) have suggested implementation of computer based decision support system for sugarcane producers in order to get higher return. Hirudayanathan and Krishanan Murthi (2007) have studied sugarcane crops in small farms in Southern India and suggested strategy to earn high return to sugarcane grower in small farms. Thorbum, Webster, et al (2007) have studied the sugarcane production in Australia and found balanced production and environmental goals of nitrogen and fertilizers. H.Swain and R.R. Bhakur (2006)- have studied the trends and variability of commercial crops in Rajasthan and found the bumper rise in the production of potato crops and obtained growth rate @ 2.95% per annum and sugar production declined @ 1.15% per annum. M.S. Swaminathan (2006) – highlighted four pillars for agricultural development mainly productivity, quality, profitability and sustainability. Kumar Kishore and Agrawal P.C. (2004) have studied the impact of water resource management on production. They have developed a linear model and found that one percent increase in irrigated area, the production increase @ 52.5 kg per hectare.

Bring a Nonempty Set, Get a Ring

S Nikhath , N. Janaki

Assistant Professor, Department of Mathematics, G. Pullaiah College of Engineering and Technology, Kurnool.

Andhra Pradesh, India.

Abstract— A nonempty set equipped with two binary operations which satisfy certain well known properties is called ring. Now a question may arise that 'Is it possible to define binary operations on any nonempty set so that the corresponding algebraic structure becomes a ring?'. This article answers the question in affirmative sense and establishes some results in this context. Bijection between two sets having same cardinality plays the main role in this article.

Keywords — *Binary operation, Ring, Cardinality.*

Mathematics subject classification 2010: 97H20

Main results:

Let's begin with two lemmas which will be used as the main tools to reveal the answer of the aforementioned question.

Lemma 1. There exists commutative ring of any pre-assigned order (except singular and limit cardinals) with identity.

Proof. The rings $(\{0\},+,\cdot)$, $\mathbb{Z}_n$ $(n \geq 2)$, $\mathbb{Z}$, $\mathbb{Q}$, $\mathbb{R}$ and $\mathbb{C}$ ensure the existence of commutative ring of order upto $\mathfrak{c}$ other than 1. Now for any $X \neq \Phi$ consider the set $\{\mathbb{Z}_2\}^X$ of all functions having domain X and codomain $\mathbb{Z}_2$ and define binary operations $\oplus$ and $\odot$ on it by

$(f \oplus g)(x) = f(x) + g(x),\ \forall\ x \in X$ and

$(f \odot g)(x) = f(x).g(x),\ \forall\ x \in X.$

Then $(\{\mathbb{Z}_2\}^X, \oplus, \odot)$ is a commutative ring of order $2^{|X|}$ with identity $I(x) = \bar{1} \in \mathbb{Z}_2\ \forall\ x \in X$, where $|X|$ denotes the cardinality of X.

Now generalized continuum hypotheses completes the proof.

Lemma 2. There exists commutative ring of any preassigned order.

Proof. Let X be any infinite set and R be the collection of all elements of $\{\mathbb{Z}_2\}^X$ with finite support. Then $(R, @, *)$ is a commutative ring of order $|X|$ where,

$(f@g)(x) = f(x) + g(x),\ \forall\ x \in X$ and

$(f * g)(x) = f(x).g(x),\ \forall\ x \in X.$

Theorem 1. Any nonempty set can be made a commutative ring.

Proof. Suppose X be any nonempty set and consider a commutative ring $(R,+,.)$ so that $|X| = |R|$ (by **Lemma 2**). Let us choose a bijection $f: X \to R$ and define binary operations $\textcircled{S}$ and $\star$ in X as follows

$x \textcircled{S} y = f^{-1}(f(x) + f(y)),\ \forall\ x, y \in X$ and

$x \star y = f^{-1}(f(x).f(x)),\ \forall\ x, y \in X.$

Then $(X, \textcircled{S}, \star)$ is a commutative ring.

Example 1. Consider the bijection $f: \mathbb{N} \to \mathbb{Z}$ defined by

$$f(n) = \frac{n}{2},\ \text{if } n \text{ is even},$$
$$= \frac{1-n}{2},\ \text{if } n \text{ is odd}.$$

Define a binary operation $\diamond$ on the set $\mathbb{N}$ by

$m \diamond n = f^{-1}(f(m) + f(n)),\ \forall\ m,\ n \in \mathbb{N};$ that is,

$m \diamond n = m + n - 1,$ if m and n are odd,

$= m + n,$ if m and n are even,

$= o - e$, if $o > e$ and
$= 1 - (o - e)$, if $o < e$,

where o =Odd$\{m, n\}$ and e =Even$\{m, n\}$. It can be verified that $(\mathbb{N}, \diamond)$ is a cyclic group generated by 2 or 3. The identity element of this group is 1 and the inverse of one member of every pair $\{2n, 2n+1\}$ is the other, $n \in \mathbb{N}$.

Again define a binary operation $\square$ on $\mathbb{N}$ by

$m \square n = f^{-1}(f(m).f(n)),\ \forall\ n \in \mathbb{N};$ that is,
$m \square n = 1,$ if at least one of m and n is 1,

$$= \frac{(m-1).(n-1)}{2},\ \text{if both are odd and } m \neq 1,\ n \neq 1$$

$$= \frac{m.n}{2},\ \text{if } m \text{ and } n \text{ both are even,}$$

$$= 1 + \frac{(o-1).e}{2},\ \text{if one of } m \text{ and } n \text{ is odd and other is even,}$$

where o =Odd$\{m, n\}$ and e =Even$\{m, n\}$. Then $(\mathbb{N}, \diamond, \square)$ is a commutative ring with identity 2.

Some results that can be worked out in similar fashion are listed in the following.

Theorem 2. (1) For any nonempty set X and any element e of it there is a binary operation o so that (X, o) forms a group with identity element$e$. If $|X| \leq a$ then o can be defined on X in such a way that (X, o) forms a cyclic group generated by g with identity element e where g and e are any preassigned distinct (if there) elements of X.

(2) Let Y be a nonempty subset of a finite set X so that $|Y|/|X|$. Then there is a binary operation $*$ on X such that Y becomes a subgroup of the group $(X, *)$; if $|X| = a$ or c then replacement of the condition $|Y|/|X|$ by $|X - Y| = a$ or c respectively will not make an exception.

(3) Any set X such that $|X| = p^n$, a or c, where p is a prime and n is any natural number, can be achieved the designation of a field.

Proof. Proofs of (1) and (3) intuitionally follow from the above discussion, rather, let's prove (2). For the first part consider the additive cyclic group $\mathbb{Z}_{|X|}$ and a subgroup H of it so that $|H| = |Y|$. Choose bijections $g: Y \to H$, $h: X - Y \to \mathbb{Z}_{|X|} - H$ and define desired binary operation $*$ on X as follows

$x * y = f^{-1}(f(x) + f(y)),\ \forall\ x, y \in X,$

where the bijection $f: X \to \mathbb{Z}_{|X|}$ is defined by

$f(x) = g(x),$ whenever $x \in Y$
$= h(x),$ whenever $x \in X - Y$

To prove the next part let's begin with the case when $|X| = a$ and Y is a nonempty finite subset of X with $|Y| = n$. Consider the group $(G, .)$ and its subgroup $C_n = \{z; z^n - 1 = 0\}$ where $G = \bigcup_{n \in \mathbb{N}} C_n$ and ' . ' denotes the complex multiplication. Choose bijections $i: Y \to C_n$, $j: X - Y \to G - C_n$, then, construct a bijection $f: X \to G$ defined by

$f(x) = i(x),$ whenever $x \in Y$
$= j(x),$ otherwise.

Then $(X, *)$ is a group and Y is a subgroup of it where

$x * y = f^{-1}(f(x).f(y)),\ \forall\ x, y \in X.$

If $|X| = a = |Y|$ where Y is a subset of X satisfying $|X - Y| = a$ then replace G by the additive group $\mathbb{Q}$ of rational numbers and C_n by the additive group $\mathbb{Z}$ of integers. If $|X| = c$ and Y is nonempty finite then replace G by the multiplicative group $\mathbb{C}^*$ of nonzero complex numbers. If $|X| = c$ and $|Y| = a$ then replace G by the multiplicative group $\mathbb{C}^*$ or $\mathbb{R}^*$ and C_n by $\mathbb{Q}^*$. At the end, if $|X| = c = |Y|$ where Y is a subset of X so that $|X - Y| = c$ then replace G by the multiplicative group $\mathbb{C}^*$ and C_n by $\mathbb{R}^*$.

I conclude proposing the following.

Problem 1: Let X be an infinite set of cardinality greater than c and Y be any nonempty subset of it. Is it possible to define a binary operation o on X so that Y becomes a subgroup of the group (X, o) ?

Problem 2: Is it possible to define binary operations on any infinite set of cardinality greater than c to make it a field ?

Acknowledgement: I am grateful to Professor Alan Dow for suggesting the technique for the proofs of **Lemma 1** and **Lemma 2**.

References

[1] Hewitt, E. and K. Stromberg, Real and Abstract Analysis, Berlin: Springer-Verlag, 1969.

[2] Baumgartner J. E. and Prikry K., Singular cardinals and the generalized continuum hypothesis, Amer. Math. Monthly, 84 (1977), 108-113.

[3] W. B. Easton, Powers of regular cardinals, Ann. Math. Logic 1 (1970), 139-178.